# The Institute of Paper Chemistry

Appleton, Wisconsin

Doctor's Dissertation

**An Investigation of the Retention of Titanium Dioxide on Wood Pulp Fibers**

**Jonathan R. Miller, Jr.**

**June, 1972**

# AN INVESTIGATION OF THE RETENTION OF TITANIUM DIOXIDE ON WOOD PULP FIBERS

A thesis submitted by

Jonathan R. Miller, Jr.

B.Ch.E. 1966, Georgia Institute of Technology

M.S. 1968, Lawrence University

in partial fulfillment of the requirements
of The Institute of Paper Chemistry
for the degree of Doctor of Philosophy
from Lawrence University,
Appleton, Wisconsin



June, 1972

TABLE OF CONTENTS

## SUMMARY

The purpose of this investigation was to provide a better understanding of particle retention in fiber mats by speaking to particular aspects of the problem. The major objectives of this work were:

1. To obtain quantitative data on the extent of particle removal and its relationship to the overall retention process.
2. To explore the interrelationships of colloidal and hydrodynamic variables on the attachment process and the extent of interactions.
3. To examine in some detail the variables occurring within a pad and the effects on retention rate.

This study was concerned with the specific system composed of titanium dioxide particles and wood pulp fibers. Colloidal environment was controlled by pH adjustment only. The study was essentially divided into two phases. The first phase consisted of particle removal studies, and the second phase was concerned with particle attachment. Visual observations and constant-rate filtration experiments were utilized in both phases of the study.

For this system at constant colloidal conditions and over the shear ranges employed, no significant amounts of removal of bound particles were observed. Microscopic observations showed that individual particle removal was insignificant. These observations also showed that the major removal mechanism was the loss of fiber fragments with particles attached. It was concluded that the titanium dioxide-fiber bond was strong enough to withstand the shear forces encountered in this study. These bonds appear to be stronger than the bonds in certain sections of the fiber wall. Filtration experiments were used to quantitatively test for particle removal. No significant loss or

redistribution of titanium dioxide could be determined in the experiments. Over this limited range of experimental variables, the retention process can be considered irreversible at constant colloidal conditions. The removal of bound particles, however, was found to be sensitive to colloidal environment. By restoring the repulsive potentials of the system, the particles were readily removed from the fiber surface. This effect was attributed to the repeptization phenomenon.

Visual observations of wood pulp fibers being permeated by suspensions of titanium dioxide have also shown the complexity of the attachment process. The fibrillar nature of the wood pulp fiber makes the flow patterns about it very complex. These fibrils, which extend from the fiber surface, act as excellent collectors of particles.

The collection of particles by fiber mats is normally described in terms of a dimensionless parameter called the collection efficiency. Physically, the collection efficiency is the fraction of particles which are retained in passing through a given fiber layer. The previous concept of a collection efficiency composed of a separable collision probability and adhesion probability was found to be inadequate in describing the attachment process for this system. The conversion of free particles to bound particles involves interactions between the colloidal and hydrodynamic variables. The interrelationship between these variables was visualized as occurring through the kinetic energy of the particles.

Variations of the collection efficiency within individual pads were attributed to compressibility effects. Depending on the colloidal conditions, the collection efficiency increased with increasing compression at low states of compression and decreased when the pad was highly compressed. These results could be qualitatively explained by changes in local values of pore size, velocity, and retention area.

# INTRODUCTION

Loading, a traditional papermaker's term, means the incorporation of inorganic materials called fillers into the fibrous web to improve the quality of certain papers or boards. Fillers improve the smoothness of papers. Uncoated, supercalendered papers with high filler content display a high surface smoothness. Ink receptivity is also improved in filled papers as the fillers have a better wettability than the cellulose fibers. Opacity control in low basis weight papers is achieved by filler addition. Fillers may also be added to filter paper to adjust porosity. High brightness fillers are used to improve whiteness in some papers. Thus, fillers perform a variety of useful functions in papermaking and an understanding of the mechanism of their incorporation into the sheet is essential for efficient usage.

Common materials used as fillers in the paper industry are clays, synthetic silica pigment, natural silicates such as talc, calcium sulfite, calcium carbonate, calcium sulfate, barium sulfate, zinc sulfide, and titanium dioxide. Fillers vary in particle size over a fairly wide range, but most are very small compared to fiber lengths. They are added to pulp slurries at the wet end of the paper machine. Some of the filler may become attached to fibers prior to sheet formation, during the period between the point of addition of the filler and the arrival of the stock at the wire. Additional filler may be incorporated into the sheet during drainage. Conclusive evidence on the relative importance of loading prior to and during sheet formation has not yet been obtained.

## COLLOIDAL EFFECTS

Early studies revealed the importance of the colloidal environment of the system on the total amount of filler in the sheet. It was found that pH and the presence of salts had pronounced effects, indicating that electrokinetic factors play a role in filler retention (1). Brill (2) has shown that the presence of some polymers such as oxidized (chlorinated) starch decreases the amount of filler in the sheet. Other polymers such as Sveen glue, locust bean and guar gums, cationic starches, and more recently polyelectrolytes have been shown to increase filler content (3). The amount of polymer and the point of addition in the papermaking system influence its effectiveness. The exact mechanism of how these polymers work is not fully understood. Under certain conditions they have little or even adverse effects on the amount of filler in the sheet.

## FORMING EFFECTS

Many studies have been conducted which show that the distribution of filler in sheets is also dependent on the method of sheet formation. The most extensive study in the actual papermaking system was made by Groen (4). He found that on fourdrinier-made paper the top side of the sheet was richer in particles than the wire side. This confirmed the results of most earlier investigations. The general form of the distribution was as follows:

Filler concentration was lowest in the extreme wire-side layer. Proceeding toward the top side, the filler concentration increased rapidly at first and then more slowly. A relatively constant pigment concentration could exist through much of the mat. A slight increase sometimes occurred on the top side.

The location in the mat where the sharp decrease in concentration toward the wire side commenced was found to be a function of paper machine speed. Use of a wet dandy roll led to a slight enrichment of the top section of the sheet, while a dry dandy roll had no effect.

Groen's explanation of this observed distribution was based on variation in mat structure during formation. He gave the following qualitative explanation for the distribution of particles: "In the first stage of drainage, the filter mat is formed only by the wire, with coarse openings compared with the particle size. Consequently, the first hypothetical layer will be relatively poor in filler particles. The next layer contains somewhat more filler, because now an open layer of fibers takes the place of the wire as the filter medium. During continued drainage, subsequent layers will be built up, steadily increasing in filler content. The loading material acts as a filter aid in plugging the pores, as do small particles when filtering on filter paper. The top layer will contain less loading, however, because the filler particles are retained not by this layer but by the next one. The resulting theoretical filler distribution will show a maximum, with a decrease toward the top side and a somewhat larger decrease toward the wire side."

Paper from a cylinder mold machine shows a distribution of filler opposite that of paper made on a fourdrinier machine. The filler content on the top side is always less than that of the wire side. Starting from the top side, a gradual increase in filler content is observed, followed by a horizontal section, and then a slight decrease near the wire side.

Steenberg (5) felt that the differences in these distributions were due to the intermittent drainage on the fourdrinier and the continuous drainage on

the cylinder mold machine. He felt that as the sheet passed over a table roll it was compressed elastically. In the compressed state, the particles would become trapped, but released when the pressure drop decreased. As the sheet passed over another table roll, some of the particles would pass into the white water as the sheet was again compressed.

Both Steenberg's and Groen's explanations treat loading as essentially a mechanical process. This may be contrasted with the work that has shown the importance of colloidal factors. Considerations such as these show the complexity in treating loading in the papermaking process itself. Laboratory studies provide an opportunity to simplify the system to the point where the effects of colloidal variables and forming variables can be studied in detail. The continued study of the effects of selected variables under laboratory conditions must result in an improvement in the understanding of loading.

## REVIEW OF RETENTION CONCEPTS

Particle retention is a general term used to describe the process by which small particles are removed from a suspending medium and collected by a solid substrate. When the substrate is a fibrous sheet and the collection occurs as part of the sheet-forming process, retention is synonymous with the traditional term "loading."

## MECHANISMS OF PARTICLE RETENTION

The starting point in considering the retention process is to determine how the particles are incorporated into the final sheet. Haslam and Steele (6) have suggested three different mechanisms by which this may be accomplished. These mechanisms are filtration, entrapment, and coflocculation. Filtration and entrapment are both physical processes, and may be grouped under the general term "sieving." Coflocculation is a physicochemical process.

### SIEVING

Sieving is a term used to describe the mechanical trapping of particles. Sieving by entrapment implies the mechanical attachment of particles to individual fibers. This could possibly take place in the hollow lumens of fibers or by the wedging of particles in the fiber wall. Sieving by filtration implies the mechanical trapping of particles in the three-dimensional network formed by the fibers in a sheet. This action depends almost entirely on the particle size and the internal pore structure of the sheet. Sieving by filtration occurs when the particles are too large to pass through the pores of the fiber mat. It would be expected that retention by this mechanism would be completely reversible if the mat were redispersed.

COFLOCCULATION

Retention by coflocculation is concerned with the interaction of the same interfacial forces which are involved in ordinary colloidal flocculation. By proper manipulation of these interfacial forces, the particles may become attached to the fiber surface by physicochemical bonds. These forces are usually divided into an attractive force and a repulsive force. The magnitude of each depends on the particular system being considered.

All particles of matter attract one another with a finite force. This attractive effect is caused by the residual valence forces present on all surfaces. These forces are sometimes grouped together under the term "Van der Waals-London forces." The attractive force between particles of colloidal size varies approximately with $\underline{r}^{-9}$, where $\underline{r}$ is the distance of separation, at small distances of a few angstroms, and with $\underline{r}^{-7}$ at larger separations up to several hundred angstroms. Attractive forces are essentially independent of the colloidal environment and are unique to each system. These attractive forces are always present, and the particles will become bound to the fiber if they are the predominant forces acting.

Normally, the particles will have to overcome a repulsive barrier before they can get sufficiently close to the fiber surface to be held by the attractive forces. The repulsive forces are electrostatic in nature, and are proportional to an exponential power of distance. They are due to the formation of an electrically charged layer on the particle and on the fiber surface. Inorganic particles normally acquire their electric double layer by preferential adsorption of ions from solution (7). The origin of the charge on the cellulose fiber is somewhat more obscure (8). It is probably due to both direct ionization of ionizable groups and preferential adsorption of ions. The magnitude and

sometimes the sign of those charges is dependent on the ionic environment. If the charges on the particles and fiber are alike in sign and sufficient in magnitude, the particles cannot become bound. If the charges on the particle and fiber are unlike in sign or low in magnitude, the particles may become bound through the Van der Waals-London forces.

Most fillers used in the paper industry and the cellulose fibers themselves acquire negative charges in distilled water (8). This is the reason for the repulsive force, as the charges on the particles and fibers are normally alike in sign. Adjustment of the colloidal environment, however, can change the magnitude and sometimes the sign of this electrostatic force.

## RELATIVE IMPORTANCE OF SIEVING AND COFLOCCULATION

The controlling mechanism of particle retention is determined by a number of factors. In many of the retention systems encountered in the paper industry, the particle size of the filler is too small to be retained solely by a sieving mechanism. There is a growing awareness in the industry that coflocculation between pigment and fiber is the dominant mechanism in many systems of commercial importance. Among these is the retention of titanium dioxide on wood pulp. Studies of retention of titanium dioxide particles on pulp fibers have been carried out by Williams and Swanson (9). They conclude on the basis of the strong influence of ionic environment as well as visual evidence that coflocculation is the predominant retention mechanism for this system.

The treatment of retention as a coflocculation process is a relatively recent development. It involves considerations which are significantly different from those relevant to sieving. This thesis is concerned with retention by coflocculation, and is restricted to the specific system of titanium dioxide particles and wood pulp fibers.

## PREVIOUS STUDIES

The retention of titanium dioxide in fiber mats has been studied rather extensively in recent years. This is due not only to the importance of titanium dioxide as a filler in the paper industry, but also to the fact that it is a chemically stable, easily characterized, small particle system. Despite the large amount of work done, the retention behavior of this filler is by no means well understood. This is due to the many hydrodynamic and colloidal variables involved.

Past studies of retention have tended to proceed along two rather distinct paths, hydrodynamic and colloidal, depending on the variables being investigated. Han (10) and Johnson (11) attempted the first quantitative treatment of retention in a fiber-fluid system by introducing the concept of a collection efficiency from the field of aerosol filtration. To a first-degree approximation, this was successful and the collection efficiency proved to be a useful means for characterizing retention in a fiber mat. The work of both Johnson and Han was directed mainly at the understanding of hydrodynamic variables. They sought correlations of the collection efficiency with variables such as velocity and fiber diameter at fixed colloidal conditions.

Williams and Swanson (9) undertook an extensive study of the effects of colloidal variables on retention in the titanium dioxide-pulp fiber system. They determined collection efficiency as a function of colloidal variables and introduced the concept of a proportionality factor, $\alpha$, multiplying the collection efficiency predicted from hydrodynamic variables to determine the effective collection efficiency. They were able to achieve a correlation between the amount of retention obtained in a stirred tank prior to pad formation and the collection efficiency obtained by pad formation. They established that the

effects of colloidal variables on retention of titanium dioxide on pulp fibers were similar to a typical hydrophobic colloid system.

All of the above studies found that the collection efficiency was not a constant in the pads. Subsequent work by Grace (12) demonstrated that the simple concept of collection efficiency seemed inadequate to completely describe retention during mat formation. In order to understand this, it is necessary to examine the retention process in a more quantitative manner.

## NATURE OF THE RETENTION PROCESS

A quantitative description of the retention process must begin with the distinction between free and bound particles. This allows the introduction of the concept of particle concentrations. Free particles are associated with the suspending fluid. They are free to move in the fluid and can be transported by the bulk motion of the fluid. Bound particles are associated with the fibers. They are not free to move in the suspension, and may be considered to have no independent motion at all.

Bound particles are, of course, particles which have been retained, and so the retention process can be considered the process by which free particles are converted to bound particles. The relative magnitude of the free and bound particle concentrations measures the extent of retention. The rate at which retention proceeds can be measured by the time derivatives of these particle concentrations. An understanding of the variables affecting this rate is the starting point for any comprehensive theory of the retention process.

RETENTION EQUATIONS

Nelson (13), Han (10), and Grace (12) have considered the retention of small particles in a fibrous mat. Using continuity considerations, they have developed partial differential equations which relate free and bound particle concentrations to the retention rate. Grace's method of presentation will be followed here.

A derivation of these retention equations is given in Appendix I. The derivation consists basically of four different mass balances made on the water, the fiber, the free particles, and the bound particles. Combining these four mass balances yields a pair of retention equations for free and bound particles, respectively.

$$-\rho_w A \left[ U_o - \frac{U_f}{(1-\varepsilon)} + \frac{\varepsilon}{1-\varepsilon} \frac{s\rho_w U_o}{\rho_f + s\rho_w} \right] \frac{\partial P}{\partial m} = \frac{\rho_w \varepsilon}{\rho_f (1-\varepsilon)} \frac{\partial P}{\partial t} + \phi \qquad (1)$$

$$\frac{s\rho_w \rho_f A U_o}{\rho_f + s\rho_w} \frac{\partial P'}{\partial m} + \frac{\partial P'}{\partial t} = \phi \qquad (2)$$

where

$P'$ = bound particle concentration, mass bound particles per unit mass of fiber,

$P$ = free particle concentration, mass free particles per unit mass of fluid,

$\rho_w$ = fluid density,

$\rho_f$ = fiber density,

$s$ = consistency, mass fibers per unit mass of fluid,

$A$ = area of mat,

$m$ = fiber mass-mat coordinate, from top of mat,

$t$ = time,

$U_o$ = forming velocity or filtrate velocity, and

$\phi$ = retention rate, time$^{-1}$.

There are very few restrictions on these equations in their general form. However, it should be noted that these equations in the ($\underline{m}$, $\underline{t}$) form do not describe any retention which might occur during a mixing period prior to mat formation. The most serious assumption is the treatment of a mat of discrete fibers as a continuum without distinct boundaries. It is a valid approach if the area of the mat under consideration is large enough that a great many fibers are involved. The distinction of free and bound particles as the only allowable particle states and the treatment of retention as a kinetic process are very reasonable assumptions.

These retention equations are coupled partial differential equations, first order in each of two independent variables. Boundary conditions on these equations (and on the retention process) would normally be set at $\underline{m} = 0$ (the mat surface) and $\underline{t} = 0$ (start of process). The coupling between the two equations occurs through the retention rate ($\phi$).

The retention rate, as defined by Equations (1) and (2), is the net mass rate of free particles becoming bound per unit mass of fibers. In general, it must be assumed that particles can be removed as well as retained. Overall retention is, then, a net effect and the retention rate is a net rate. The following definitions will be made in this thesis in order to emphasize that overall retention is the net result of competing processes. The absolute process by which particles become bound will be called attachment, and the rate at which it occurs will be called the attachment rate. The absolute process by which bound particles become free will be called removal, and the rate at which it occurs will be called the removal rate. Thus, $\phi$ is composed of two parts — an attachment rate and a removal rate.

APPLICATION OF THE RETENTION EQUATIONS

The retention equations in their general form are quite complex. Exact solutions can be obtained only in certain special cases. These special cases involve two factors: the specification of a prescribed manner for carrying out the process and an assumption about the retention rate. No assumptions will be made about the retention rate at this point. However, the simplifications resulting from the application of the equations to a constant-rate filtration will be considered.

In a filtration, a mat is formed from a suspension of particles and fibers. The retention process occurs simultaneously with the sheet-forming process. In a constant-rate filtration, the mat is formed at a constant rate; that is, the suspension flows toward the forming wire at a constant velocity. With certain assumptions, presented in Appendix II, the retention equations simplify to:

$$s\rho_w AU_o \frac{dP'}{dm} = \phi, \tag{3}$$

$$-\rho_w AU_o \frac{dP}{dm} = \phi. \tag{4}$$

The time independence of these equations is unique to a constant-rate filtration. The reasons for this are discussed in Appendix II. This time independence makes the constant-rate filtration an especially desirable method of carrying out retention rate studies. The relationship between free and bound particle concentrations may be obtained by combining Equations (3) and (4), giving

$$\frac{d}{dm}(P + sP') = 0 \tag{5}$$

or

$$P + sP' = sP_{oo} \qquad (6)$$

where $P_{oo}$ = initial particle concentration, mass particles per mass fibers. Equation (6) provides a means for determining the free particle concentration from the bound particle concentration.

THE RETENTION RATE

The collection efficiency concept requires $\emptyset$ to have the form

$$\emptyset = Ks(P_{oo} - P') \qquad (7)$$

where K is the rate constant proportional to the collection efficiency. This form states mathematically that the rate at which free particles become bound particles is proportional to the free particle concentrations. Thus, the collection efficiency approach assumes that retention is first order in free particles.

Physically, the collection efficiency is the fraction of particles which are retained in passing through a given fiber layer. For a homogeneous particle system, the collection efficiency is then the probability that a given particle will not pass through a fiber layer. The attractiveness of the collection efficiency is that it permits the construction of ideal models for mathematical predictions of collection efficiency and logical development of variable correlations. The classical way that this is done is to assume a separability of colloidal and hydrodynamic variables. Particle trajectories are calculated from hydrodynamic considerations to determine the collision probabilities, and colloidal variables are assumed to govern the probability that a given collision will be effective.

The rate constant in Equation (7) is related to the collection efficiency in the following equation:

$$K = ES\rho_w U_o \tag{8}$$

where

$\underline{E}$ = the collection efficiency and

$\underline{S}$ = fiber specific surface, area of fiber per unit mass of fiber.

If the rate constant or collection efficiency is constant, Equations (3) and (4) can be readily solved. The solution for bound particles, Equation (3), is given by Equation (9):

$$P_{oo} - P' = (P_{oo} - P_o')e^{-Km/\rho_w AU_o}. \tag{9}$$

In terms of the collection efficiency, this becomes

$$P_{oo} - P' = (P_{oo} - P_o')e^{-ESm/A}. \tag{10}$$

$\underline{P_o}'$ is the bound particle concentration (mass particles per unit mass fiber) at $\underline{m} = 0$, the top of the pad. This term is known as the prepad retention. It accounts for any particles that may become bound during the mixing period prior to the start of a filtration. Equations (9) and (10) imply a bound particle distribution which starts at $\underline{P_o}'$ at the top of the pad ($\underline{m} = 0$) and asymptotically approaches $\underline{P_{oo}}$ at sufficiently large $\underline{m}$. Plots of ln ($\underline{P_{oo}} - \underline{P}'$) versus $\underline{m}$ should yield a straight line. The collection efficiency or rate constant can be determined from the slopes of such plots. Deviations of the plots from linearity reflect a nonconstant collection efficiency during the filtration. Depending on conditions, the collection efficiency has been found to increase or decrease through the pad (sometimes both). Many reasons have been advanced for the observed changes in collection efficiency (or rate constant). They include such things as particle removal, saturation of the fiber surface with particles, changes in local porosity and velocity affecting hydrodynamics, and others. The resolution of the factors involved in nonconstant collection efficiencies would certainly provide a deeper understanding of the retention process.

In summary, although beginnings have been made at understanding the fundamentals of retention, a good deal more remains to be done. Continuity considerations provide an insight into the particle distributions obtained, but demonstrate clearly that the collection efficiency (or retention rate) is not a simple function. It has been amply shown that colloidal variables have a profound influence on retention, but they have been treated only in a semi-quantitative or qualitative manner. There is a particular need to understand the factors giving rise to the complexity of the retention rate and to resolve apparently conflicting results from superficially similar experiments.

## PRESENTATION OF PROBLEM

The purpose of this investigation was to provide a better understanding of retention by speaking to particular aspects of the problem. The major objectives of this work were:

1. To obtain quantitative data on the extent of particle removal and its relationship to the overall retention process,
2. To explore the interrelationships of colloidal and hydrodynamic variables on the attachment process and the extent of interactions. This would help eliminate confusion and conflicts between data,
3. To examine in some detail the variables occurring within a pad and the effects on retention rate.

# EXPERIMENTAL PROCEDURES

## GENERAL APPROACH

This study was restricted to the specific system composed of titanium dioxide particles and wood pulp fibers. Although wood pulp fibers constitute a complex porous medium which is very difficult to describe quantitatively, it was felt that the results obtained with this system would be more applicable to papermaking systems than results obtained with smooth cylindrical fibers. Titanium dioxide particles were selected because previous investigators had already determined that its retention on pulp fibers was primarily a coflocculation mechanism. Stable suspensions of small particle size ranges could be prepared, and analytical techniques for determining the amount retained in pads had also been developed.

In carrying out this work, reliance was placed on retention during constant-rate filtrations. This method was selected because it led to reproducible methods of contacting particles and fiber, was easily controlled, and lent itself to theoretical treatment.

The interpretation of the experimental data obtained from constant-rate filtrations was aided by microscopic observations of the retention process. Details of the experimental program are given in the remainder of this section.

## FIBERS

The primary fibers used in this study were commercial bleached sulfite fibers. They were obtained in dry sheet form of approximately 400 g. per sheet. Microscopic analysis showed the pulp to be composed of the following amounts of wood species: 60-80% spruce, 10-20% hemlock, 10-20% balsam fir,

and 5-10% larch. The sheets were shredded by hand and dispersed in distilled water. After soaking for approximately 24 hours, the pulp was stored at 40°F. at about 30% solids.

The pulp was treated in various ways and designated as Pulps 1, 2, and 3. Description of the treatment process follows.

Pulp 1. Twenty-gram o.d. whole pulp charges were placed in the Bauer-McNett classifier. Only the fiber retained on the 14-mesh screen after 30 minutes of classification with distilled water was kept for retention experiments.

Pulp 2. Using the same procedure as above, the fines passing through a 60-mesh screen were removed from the whole pulp. This pulp minus the fines was used in retention experiments.

Pulp 3. Fifty grams of o.d. whole pulp were stirred in a British disintegrator for 3 hours. This beaten pulp received no classification. It was used in this form in retention experiments.

In addition to the sulfite pulp fibers, both rayon fibers and laboratory-prepared holopulp fibers were used for some filtration experiments. The rayon fibers were manufactured by FMC Corporation, American Viscose Division. They were conventional viscose rayon fibers which were 1.5 denier and 1/4 inch in length.

The holopulp fibers were prepared in the laboratory from noble fir wood. A complete description of the pulping procedures and the fibers can be found in Lapinoja's dissertation (24). These fibers were found to be unsuitable for the purpose of this work due to their high hemicellulose content. The results of filtration experiments performed on these fibers can be found in Appendix VIII.

## TITANIUM DIOXIDE PARTICLES

The titanium dioxide particles used in this work were a pigment grade of the anatase form manufactured by the Glidden Company. The particles had been characterized by Williams (14) and Webb (15) using a centrifugal sedimentation analysis. The results of an analysis on the entire pigment is shown in Fig. 1. As seen in this figure, the particle diameters ranged from approximately 0.1 to 1.0 μm. with 80% of the particles less than 0.3 μm.

The titanium dioxide was dispersed by means of a Hamilton Beach mixer, Model No. 25, in distilled water at 73% solids, a concentration near the point where the slurry becomes a thick paste. This slurry was mixed for 30 min. while water cooling the container. It had been found in previous investigations (15) that the best dispersed suspensions, as indicated by minimum viscosity, are prepared by initially dispersing at 73% solids as described, and then diluting to the desired concentration. This slurry was then diluted to a 0.0193-g. titanium dioxide/ml. slurry which was kept on a continuously rotating drum to prevent settling. For a given filtration run, the desired amount of pigment was added by volume measurement.

## ELECTROLYTE SELECTION

Investigations by Williams and Swanson (9) had resolved that the titanium dioxide-wood system could be coflocculated by the presence of various electrolytes. Their work also showed the system was likewise sensitive to changes in hydrogen ion concentration. Briefly, at low pH's, the system coflocculated readily and, at high pH's, the system was stable.

Hydrogen chloride and sodium hydroxide were the only electrolytes selected to control the colloidal environment. The primary reason was the ease in

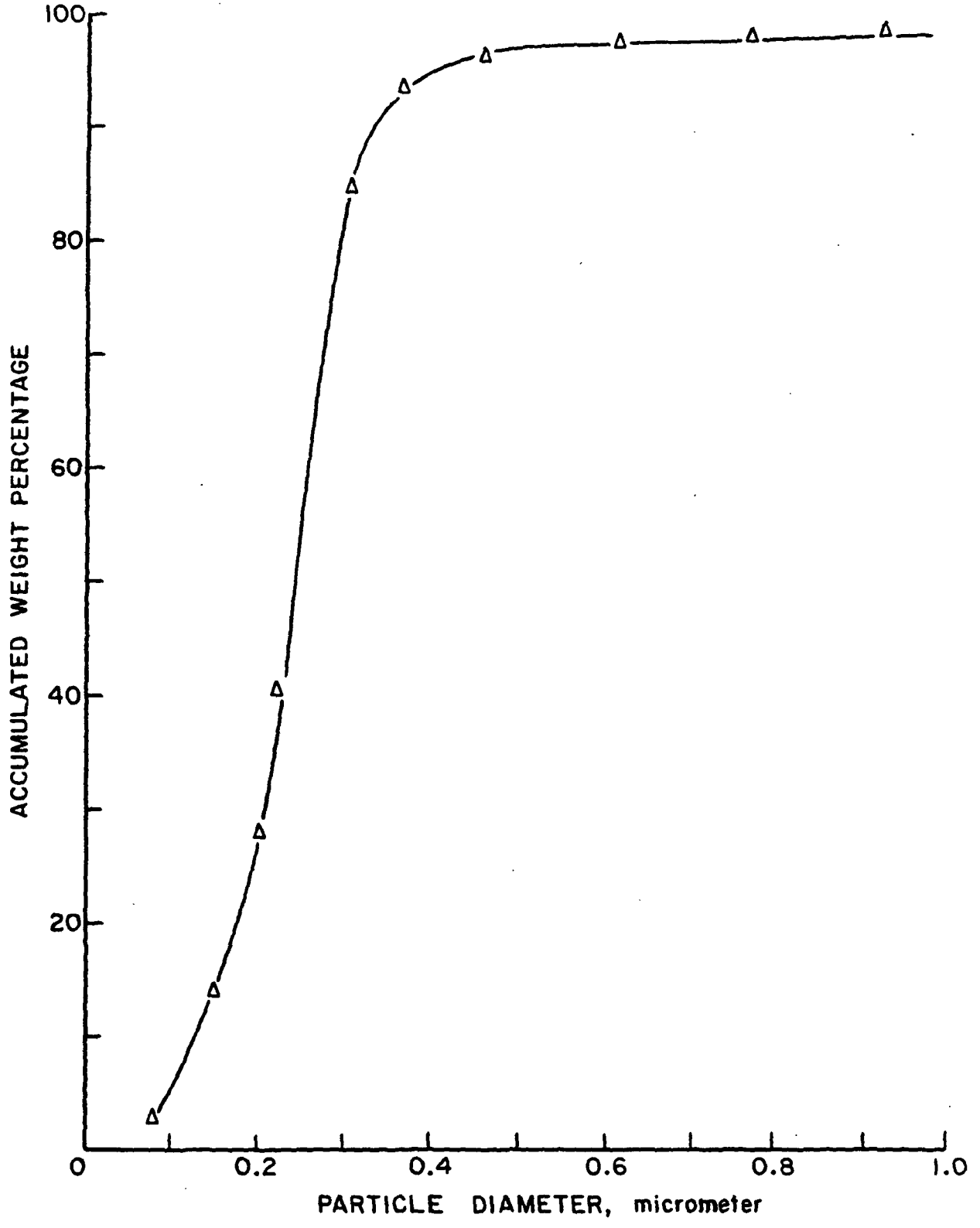


Figure 1. Particle Size Distribution of Titanium Dioxide

determining the colloidal state of the system by merely measuring and adjusting the pH of the suspension.

## APPARATUS

A piping diagram of the constant-rate filtration apparatus is shown in Fig. 2. The apparatus includes a 50-gallon storage tank (A) for boiling and cooling the distilled water to deaerate it. One hundred liters of this water would then be filtered through a Millipore filter (J) (pore size 1.2 μm.) and pumped to a 30-gallon teflon lined tank (B) where the fibers and titanium dioxide were added. The slurry was then gravity-fed to the forming tube (C) where the filtration was carried out.

The forming tube is made of Lucite, 3-in. inside diameter, 1/4-in. wall thickness. The area available for flow is 45.3 square centimeters. The backing plate for the septum (I) on which the pulp pad is formed is also made of Lucite, 1/2-in. thick. Three-sixteenth-inch holes were drilled in the septum in an equilateral triangular pattern. Additional smaller holes were drilled where this pattern did not come close to the edge of the area available for flow. The septum was a plastic screen made of 0.02-inch diameter wires woven in a 36 x 28 wires-per-inch pattern.

Flow through the forming tube was controlled by a variable-speed gear pump (H) which was capable of flow rates corresponding to velocities from approximately 0.5 to 5.0 cm./sec. The liquid passing through the pump was sent to either of two rotameters (E, F), depending on flow rate. Pressure drop across the pad was monitored by a Pace pressure transducer (D). This signal was sent to a strip-chart recorder, giving a continuous recording of the pressure.

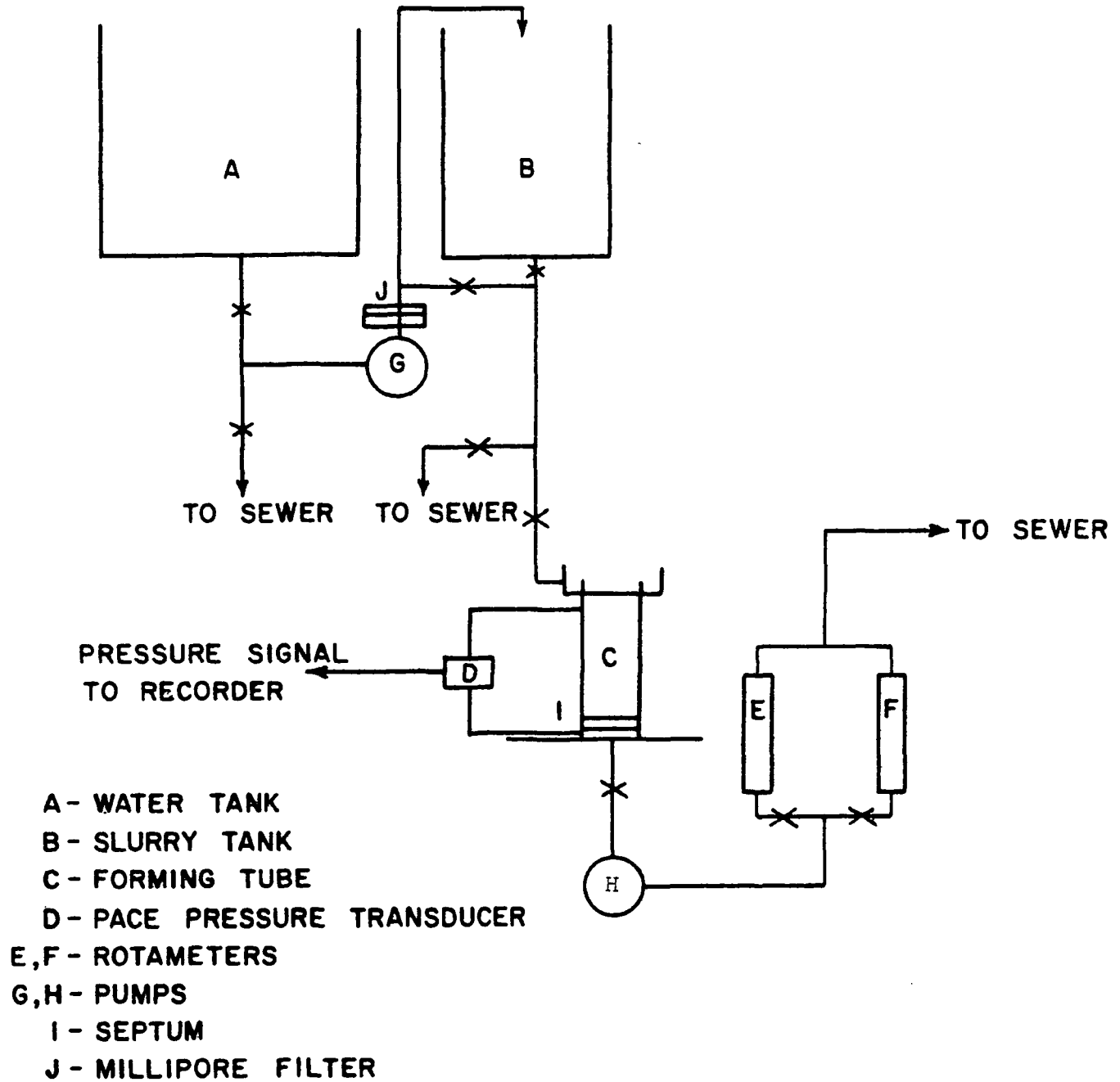


Figure 2. Simplified Piping Diagram of Constant-Rate Filtration Apparatus

The Pace unit was calibrated by the use of a mercury manometer. All piping used in the system was 1/2-inch polypropylene tubing.

## DESCRIPTION OF A CONSTANT-RATE FILTRATION

Ten grams of dispersed, deaerated pulp were added to 100 liters of the deaerated water. The pH of the pulp suspension was then adjusted to the desired level. The desired quantity of pigment was added to the pulp slurry (0.5 g.). The pigment-pulp suspension was mixed for 15 minutes before filtration was initiated. The pad was then carefully formed at the desired flow rate. At the end of the run, the suspension remaining in the tube above the pad was siphoned off and the remaining water was drained carefully through the pad. The pad was then removed from the filtration tube. Two or more pads could be made from one batch of suspension.

## ANALYSIS OF PARTICLE DISTRIBUTION IN THE PADS

The analysis of the pads was carried out as follows. After removing the pad from the filtration tube, it was split into layers using dissecting needles. The layers of pulp were dried overnight in an oven at 100°C. The weight of the pulp plus titanium dioxide of each layer was determined by weighing the dried samples. The layers were then ashed in a muffle furnace according to the following schedule: 600°F. for 30 minutes, 700°F. for 20 minutes, 800°F. for 20 minutes, 1000°F. for 25 minutes, and 1400°F. for 60 minutes. This ashing procedure was used to minimize loss of titanium dioxide by entrainment in the gases. The titanium dioxide content of each layer was then determined by dissolving the ash in concentrated sulfuric acid and ammonium sulfate and measuring the UV absorbance of the solution after addition of hydrogen peroxide. The reference for the absorbance measurement was a titanium sulfate solution to which no

hydrogen peroxide was added. The absorbance was converted to titanium dioxide mass by use of a calibration curve. The ratio of titanium dioxide to pulp mass for each layer could be determined in this manner. Details of the procedure are given in Appendix III. The procedure for converting the titanium dioxide-to-pulp ratio into the bound particle distribution is given in Appendix IV.

## APPARATUS FOR VISUAL OBSERVATIONS

Early in the investigation it was felt that visual observations of the retention process occurring on a single fiber would aid in the interpretation experiments. An apparatus for viewing the process was constructed. Figure 3 shows a diagram of the apparatus. It was constructed from a 1/4-inch thick Plexiglas slide. Two 1/4-inch holes were drilled approximately 1/2-inch apart and small stainless steel capillary tubes were inserted from the ends of the slides into these reservoirs. The area between the reservoirs was turned down 0.010 inch and constitutes the viewing area. Small clumps of fibers could be placed on this area or single fibers pinned at the ends by pieces of modeling clay. A standard microscope slide cover glass was then placed over this area. A 1/4-inch thick rubber gasket and a stainless steel plate were used to hold the cover glass in place. Flow of the titanium dioxide suspension was achieved by a hypodermic needle or from a pressurized buret. Observations were made using a standard microscope at various magnifications from 10 to 400X. A movie camera was later incorporated into the system for filming the process directly through the microscope. Dark field illumination was used as the lighting technique. Under this lighting technique, the titanium dioxide particles appeared as small white particles. The fibers were transparent except for their interfaces which scattered the light and appeared white.

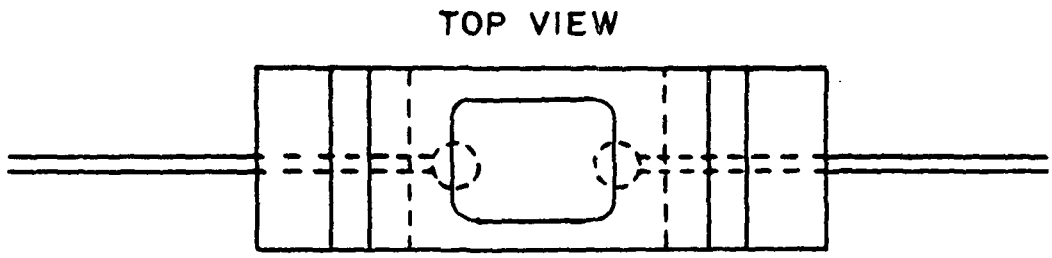


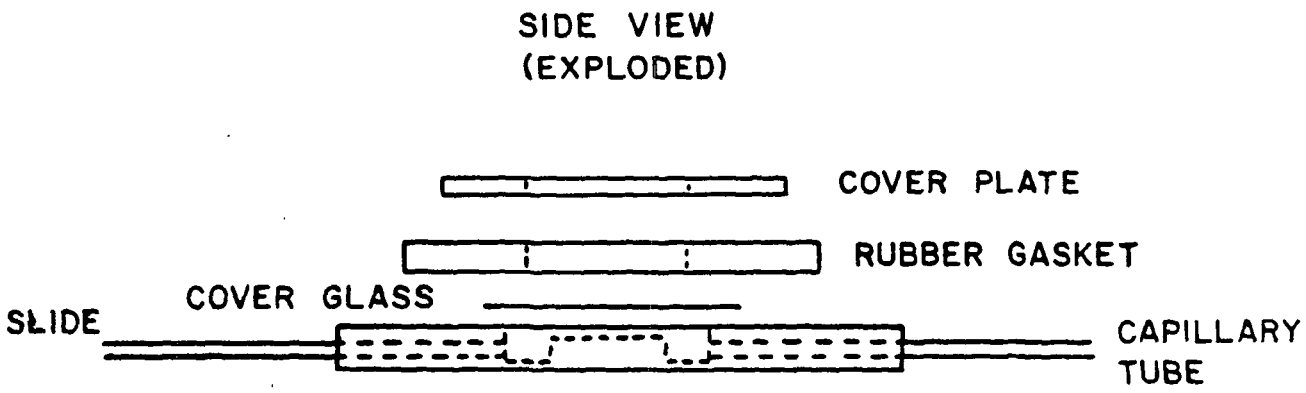


Figure 3. Diagram of Flow Cell Used in Visual Observations

# PARTICLE REMOVAL

## CONCEPTS OF REMOVAL

### BACKGROUND

The collection efficiency concept does not account for the removal of bound particles. Implicit in this concept is that once a particle becomes bound it cannot be removed. It has been established by Han and Chang (16) that removal does occur in the retention system composed of wood pulp fibers and pulp fines. They prepared fines by dry and wet grinding of fibers to a size range of 0.05-0.50 μm. These fines were tagged with radioactive silver -110 and used in retention experiments. A pad was loaded with these fines and then removal was studied by passing fluid (without particles) through the pad at a fixed rate. The permeation fluid was at the same colloidal conditions as pad formation. The particles remaining in the pad were measured as a function of time by continuously monitoring the radioactivity of the pad. They found the removal of fines to be both time and velocity dependent. For a uniformly loaded pad, fines removal was found to increase with increases in velocity. Permeation of a pad at a given velocity resulted in large amounts of removal initially. The amount decreased with time. The amount removed was found to fit an exponential decay function with time.

Nelson (13) further considered the removal of bound particles in the retention process. He represented removal by a detachment coefficient times the bound particle concentration. The detachment process was supposed to compete with the attachment process which is described by the collection efficiency.

Walkush (17) has found fines retention in a stirred tank to be by the coflocculation mechanism. He also found fines retention to be readily reversible. However, the fines system is not necessarily analogous to the titanium dioxide-fiber system. The attractive forces should not be the same and the fines probably do not react to fluid drag forces in the same manner as titanium dioxide. For these reasons, it could be misleading to apply the results of one retention system to another.

Studies of the retention of titanium dioxide on wood pulp by Williams and Swanson (9) and Grace (12) have led to the postulation of removal in this system. In some of their experiments, the retention rate was found to be zero while the free particle concentration was not zero. Grace found that Nelson's method of quantitatively describing removal with a constant detachment coefficient times the bound particle concentration did not adequately describe his experimental observations. This method predicted a removal rate that was too gradual in its onset. The existence of a critical bound particle concentration was postulated and removal was assumed negligible below this concentration.

Experimentally, the removal process is difficult to separate from the attachment process. In the previous work with titanium dioxide, only the final bound particle distributions were obtained. These distributions were the net result of both processes. A need existed to study removal independently of attachment. The initial objective in the present study was to investigate the role of removal in the titanium dioxide-wood pulp system.

## REMOVAL PROCESS

Bound particles are held to fiber surfaces by Van der Waals-London attractive forces. In order for a bound particle to be removed, an additional force or

forces of sufficient magnitude to overcome this attractive force must be applied. Possible removal forces encountered by bound particles in the papermaking process are fluid drag forces, changes in repulsive force due to changes in ionic environment, forces due to surface tension effects when an air-water interface is drawn through the sheet, and possible shear forces due to relative fiber motion during mat compression. Removal by surface tension was not investigated in this study. Care was taken to minimize any removal effects it may have. Removal due to relative fiber motion was also not studied explicitly. Increases in fluid drag forces are accompanied by mat compression where small amounts of relative fiber motion may occur. Any removal effects due to this mechanism were lumped under the effects of fluid drag forces.

Changes in colloidal environment can result in changes in the magnitude of the repulsive force experienced by a bound particle. However, a fluid drag force is usually additionally required to redisperse a flocculated system. This would lead to a removal rate with the contribution from the repulsive force being a significant part of the total removal force.

## REMOVAL STUDIES

### VISUAL OBSERVATIONS

Microscopic observations were made on wood pulp fibers being permeated with a titanium dioxide suspension. It was observed and recorded on film[1] that once a single particle became attached to the fiber it was rarely removed. Little individual particle removal was observed when the flow past a fiber was increased by as much as an order of magnitude (i.e., 0.3 to 3.0 cm./sec.). The major

[1]Available at The Institute of Paper Chemistry.

type of removal observed was that of pieces of the fiber with its titanium dioxide attached sloughing off. This removal occurred at fibrils and on sections of the fiber wall. Some sections of a fiber could become heavily laden with retained particles and experience no removal, while other sections would lose several areas of fibril or fiber wall and its attached titanium dioxide. A step change in the permeation velocity would normally result in the loss of a few fiber fragments and continued permeation at a given velocity resulted in very little additional removal. The fiber fragments which were removed varied in size, but all were quite large compared to an individual titanium dioxide particle.

Based on these visual observations, the weakest link in the system appeared to be the fiber itself. The individual titanium dioxide-fiber bond seemed to be strong enough to withstand the shear levels present. From the observed particle size, it would be expected that a large portion of the fiber fragments which were removed would be recaptured by a sieving mechanism in the fiber layers below the layer at which the removal occurred. The net result in a continuous forming process such as a constant-rate filtration would be a shift in the bound particle distribution toward the septum.

## FILTRATION EXPERIMENTS

The visual observations suggested that removal was a relatively minor effect in the titanium dioxide-wood pulp system. However, it was difficult to make quantitative statements concerning removal from the visual data alone. Accordingly, additional experiments were performed to obtain quantitative data. These essentially followed the method of Han and Chang by permeating a loaded pad with a particle-free fluid.

In order to study the effects of hydrodynamic and colloidal variables on the removal process, a reproducible method of obtaining pads with a known bound particle distribution was needed. The analytical techniques for determining bound particle distribution required destruction of the pads. Hence, a comparative method of studying removal had to be used as there was no way to determine bound particle distributions before and after treatment on a single pad. It was found (see Fig. 4) that two pads formed from the same suspension had bound particle distributions which were identical within experimental error. This fact allowed the removal process to be investigated independently of the attachment process. One pad could be formed and used as the control. A second pad would then be formed from the same suspension under identical conditions and then treated in various ways to try to remove the bound particles. Both pads could then be analyzed for titanium dioxide content. The difference in the amount of titanium dioxide between the two pads would be the amount removed. The data for the removal experiments are given in Appendix V.

With the major mechanism of removal clarified by the visual observations, constant-rate filtrations as described above were performed to determine to what extent this mechanism operated. The first removal experiment consisted of forming two pads using the highly classified Type 1 pulp. The experiment was carried out at pH 2.8, which was previously shown to provide good flocculating conditions. The forming velocity was 1 cm. per sec. The first pad was formed and removed from the system. The second pad was formed, and without interruption of the flow it was permeated an additional 10 minutes at 1 cm. per sec. with water. The water used during the permeation was at the same pH as the original suspension. The changing of the flow was accomplished by simply switching to a tank containing the permeating fluid. The results are shown in Fig. 5. As can be seen, there is no significant difference between the two distribution curves.

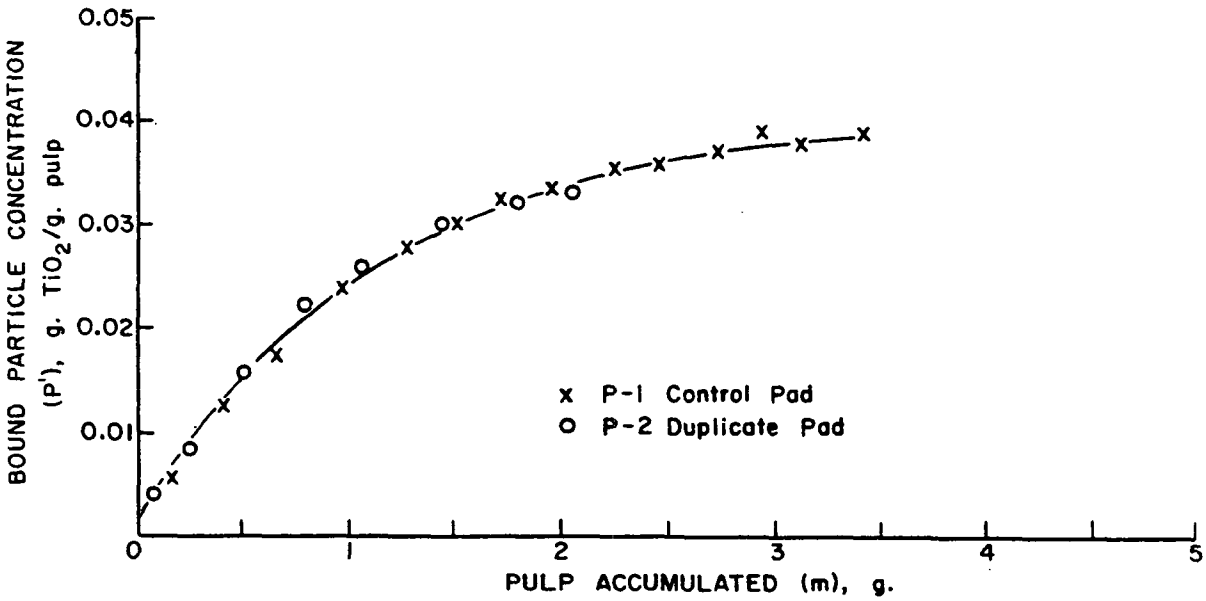


Figure 4. Bound Particle Distributions for Consecutively Formed Pulp Pads. P-2 Received no Treatment

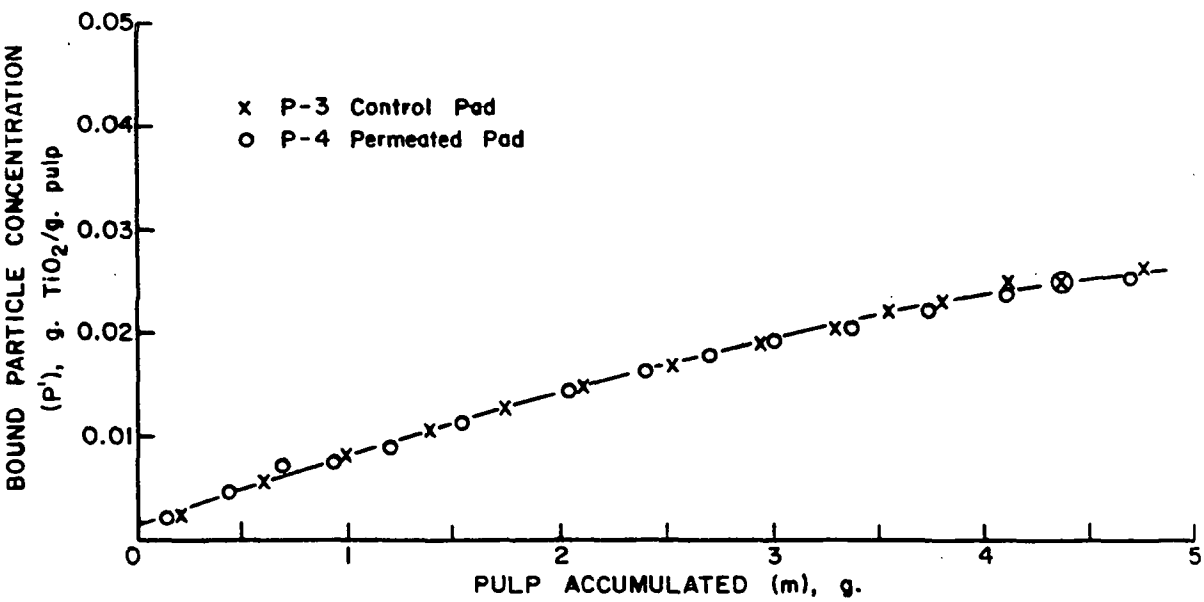


Figure 5. Bound Particle Distributions for Pulp Pads. P-4 was Additionally Permeated at the Same Velocity as Formation

By permeating at the same velocity as formation, the fluid drag forces in the pad were not raised appreciably over the shear levels present during formation. The pressure drop over the pad did not increase significantly during the permeation; therefore, the particles did not experience any large increase in drag forces. The forces were approximately the same as when the particles were originally retained. Hence, no removal was observed.

The visual observations had shown that the major loss mechanism was due to the loss of fiber fragments with the titanium dioxide attached. Based on the results of the above experiment, it appeared that very few fiber fragments were generated during the permeation of the Type 1 pulp. The next experiment was designed to see if removal occurred in a pad that had fiber fragments present. A Type 3 pulp which was not classified was used. Williams (14) had shown in stirred tank experiments that titanium dioxide became attached to fines as well as to fibers. Therefore, the fines present in the Type 3 pulp could retain titanium dioxide during the mixing period prior to pad formation and during pad formation itself.

This second experiment was performed, using the Type 3 pulp, with the conditions the same as in Experiment 1. The results are shown in Fig. 6. A comparison of Fig. 6 with Fig. 5 shows that the bound particle distribution rises much more rapidly with the Type 3 pulp. This is due to the higher surface area of the Type 3 pulp. Williams (14) has investigated the effects of surface area on retention. He found an approximately linear relationship between the amount of retention and the hydrodynamic surface area of the pulp. An increase in retention would therefore be expected for this pulp.

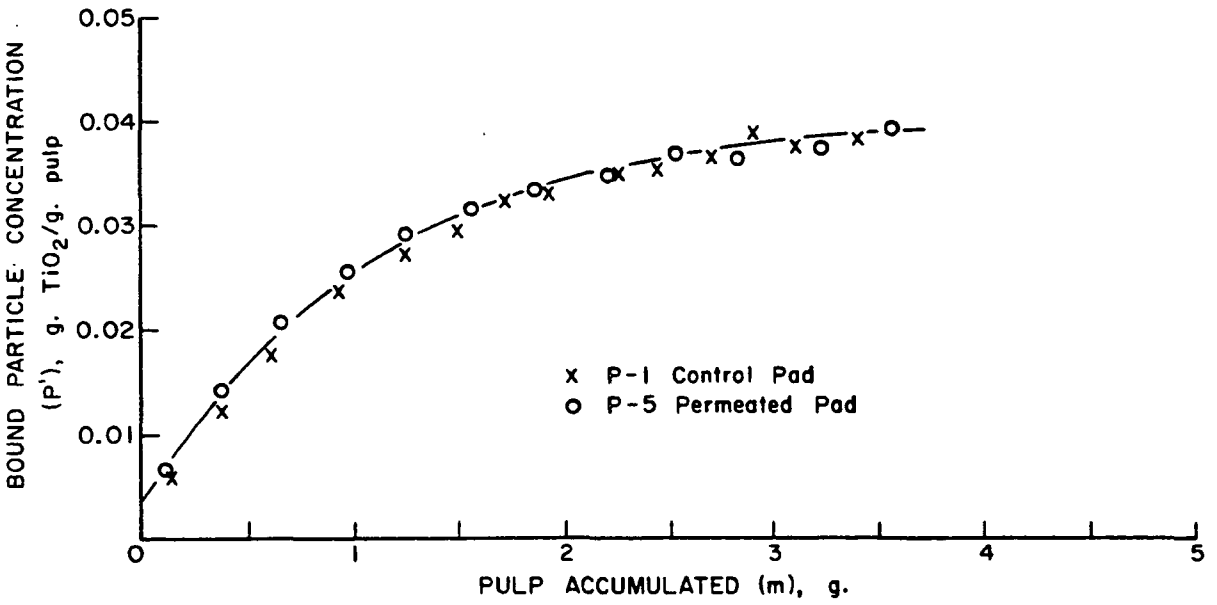


Figure 6. Bound Particle Distributions for Pulp Pads. P-5 was Additionally Permeated at the Same Velocity as Formation

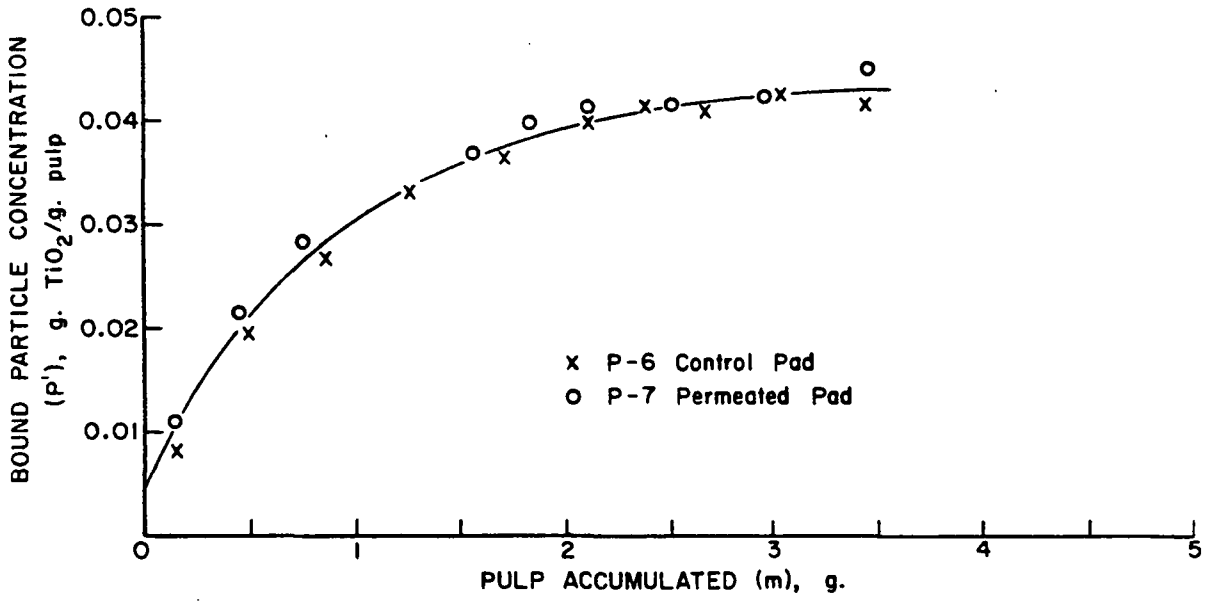


Figure 7. Bound Particle Distributions for Pulp Pads. P-7 was Additionally Permeated with a Particle-Free Fiber Suspension

The difference in the amount of retention between the treated and control pads in Fig. 6 is within the experimental error.

Even though fiber fragments were present in this experiment, the amount of removal was insignificant. As in the first experiment, the permeation was carried out at the same velocity as the pad formation. Thus, the fluid drag forces in the removal test were similar to those which particles and fragments experienced during formation. The particles and fragments were not subjected to any forces which they had not previously experienced during formation. This explains the lack of removal. Another aspect has to do with the migration of fragments through the pad and the possibility of sieving. These experiments do not differentiate between complete lack of removal and an inability to migrate significant distances through the pad.

The third removal experiment was designed to increase the shear level caused by the fluid drag forces on the bound particles at a constant filtration velocity. This would correspond more nearly to the actual increase in shear experienced by the particles during pad formation. This run was carried out at pH 3 using a Type 3 pulp.

The control pad (P-6) was formed at a velocity of 1 cm./sec. until a pressure drop across the pad of approximately 6 p.s.i. was achieved. The second pad (P-7) was formed in exactly the same manner. When the pressure drop across this pad reached 6 p.s.i., the feed was changed to a suspension of particle-free fibers at the same pH as the particle-fiber suspension. This was done without interruption or increase of flow. The filtration was continued until the pressure drop was approximately 14.5 p.s.i.

Pad P-7 had a pressure history exactly like that of Pad P-6 during the particle-fiber phase, and then, due to fibers only, the pressure drop was gradually increased to double that of Pad P-6.

The particle-free fibers were a mixture of the sulfite fibers and nylon fibers which had been dyed black. It was thus possible to distinguish the original upper boundary of Pad P-7. The fiber-only portion of Pad P-7 was removed and discarded. The pads were then split and analyzed as usual. The results are shown in Fig. 7. Again, there is no significant amount of removal.

The increase in shear level in the section of the treated pad containing particles was related to the compressibility of the pulp. As the permeation with the particle-free fibers continued, the lower section of the pad was in continuously increasing states of compression. This increasing state of compression resulted in decreasing porosity and increasing shear levels at the constant filtration velocity. It would be expected that the increases in shear would enhance removal of fiber fragments due to the increase in fluid drag forces. Decreasing porosity, however, should enhance the chances of having the fiber fragments remain in the pad by sieving. It must be concluded that in this constant-rate filtration the shear level increases were not of sufficient magnitude to remove any additional fiber fragments, or if removed, they did not migrate because of their size.

The fourth removal experiment was designed to increase the shear level in the pad by a step change rather than gradual change as described above. The Type 3 pulp was used in the experiment at pH 2.8. Both pads were formed at a velocity of 1 cm./sec. At the end of Pad P-9 formation, the feed was changed from the particle-fiber suspension to water only at the same pH. Simultaneously, the flow rate was upped to 2 cm./sec. and the pad compressed significantly. The

permeation at 2 cm./sec. was continued for six minutes. The pads were then removed and analyzed for titanium dioxide content. The results are shown in Fig. 8. Within experimental error, the distributions are the same.

The increase in shear level in this pad was quite large. The permeation velocity was double that of the formation velocity. In addition to this increase, there was the increase due to the accompanying change in the state of compression of the pad. As discussed in the visual observations, step changes in shear usually resulted in the loss of fiber fragments from the fiber. In this experiment, this should have occurred also. In addition, there were fiber fragments initially present due to the use of the Type 3 pulp. Obviously, the step increase did not result in any significant loss or redistribution of these fragments.

The final phase of the removal studies consisted of an experiment to determine if changes in colloidal environment had any effect on the removal of bound particles. In removal Experiment 5, the highly classified Type 1 pulp was used. The pH of the suspension was set at 3. A control pad was formed at 1 cm./sec. and removed. A second pad was formed at 1 cm./sec. and, without interruption of flow, was permeated an additional 10 minutes with distilled water at pH 6.8. The results are shown in Fig. 9. Significant amounts of titanium dioxide were lost by each layer in the second pad. Visual observations of the effluent during the permeation with distilled water showed the particles being removed to be fairly well dispersed. There appeared to be little or no pulp fines associated with them. Initially, the turbidity of the effluent was very high, but cleared considerably by the end of the permeation.

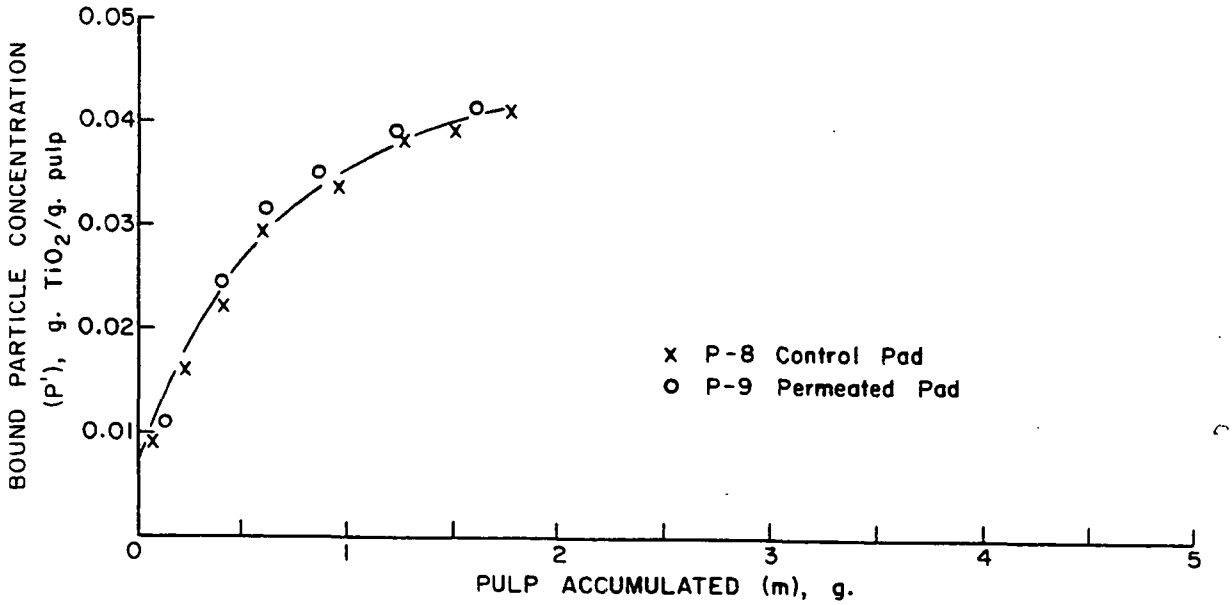


Figure 8. Bound Particle Distributions for Pulp Pads. P-9 was Additionally Permeated at Double the Velocity of Formation

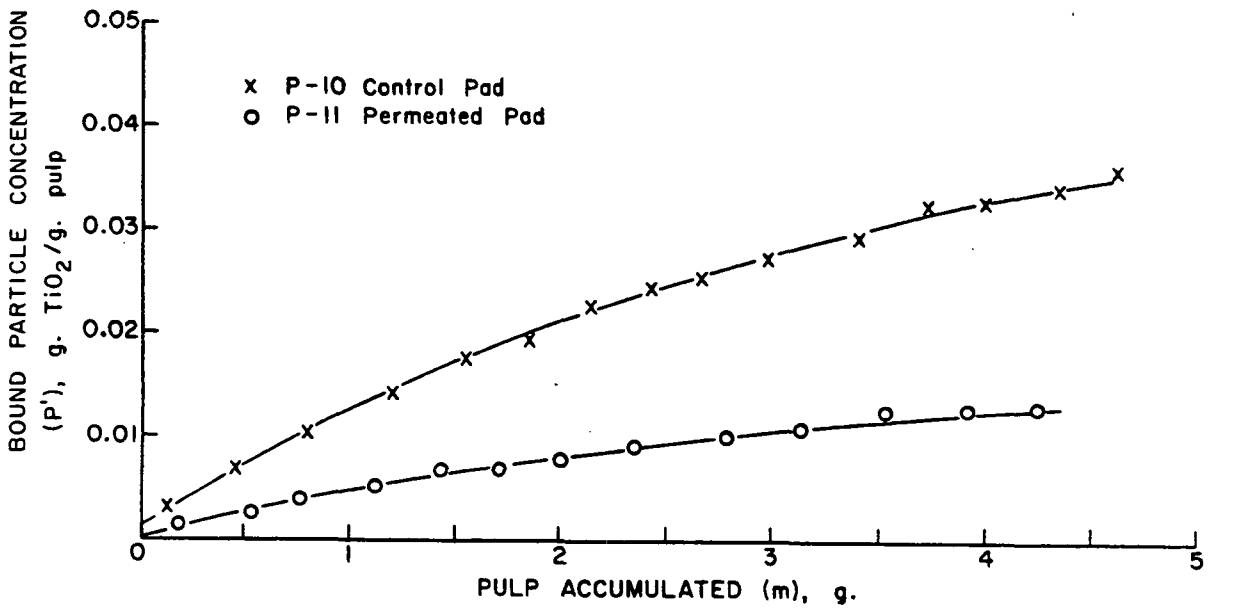


Figure 9. Bound Particle Distributions for Pulp Pads. P-11 was Additionally Permeated with Distilled Water at the Same Velocity as Formation

Each layer in Pad P-11, the permeated pad, lost approximately 60% of its retained particles. This uniform loss indicated that, once the particles are removed, they are not recaptured. If the removed particles were recaptured, the distributions would not be expected to be similar in shape. The distribution in the permeated pad would probably show more net loss in the upper layers then in the lower layers.

This phenomenon is not unknown in colloidal chemistry. It is called repeptization (18). The ease with which a flocculated system can be redispersed by a change to nonflocculating conditions depends on the magnitude of the shear force and the ion used in initially flocculating the system. Systems flocculated by the use of multivalent ions are more difficult to redisperse than if the systems were flocculated by monovalent ions. This behavior is at least partially due to the difficulty of expelling the polyvalent ions from the double layer (greater adsorbability). Changes in the quantity of potential determining ions also lead to repeptization.

The action which leads to repeptization is visualized as the restoring of the repulsive potential to the flocculated particles. When a condition is reached where the repulsive force and the fluid drag force exceed the attractive force, the particles will redisperse.

In this experiment, the change in the hydrogen ion concentration would result in a change in the repulsive potential. The higher repulsive potential in the presence of the fluid drag force was obviously sufficient to overcome the attractive force and lead to a large amount of removal. It was felt that continued permeation with distilled water would have resulted in the loss of even more particles than observed in Fig. 9. However, complete removal of the particles in the treated pad would probably be impossible due to the following

reasons. First, it must be assumed that the fiber surface, due to its non-homogeneous nature, is composed of a distribution of attractive potential sites making some particles hold to the surface more strongly than others. It must also be kept in mind that the magnitude of the fluid drag force on a particle depends on its location on the fiber and the fiber's location within the pad. Some particles are also retained by mechanical entrapment; therefore, retained independently of the colloidal forces. The particles remaining in the pad after permeation could be there for any of the above reasons or combinations of them.

An additional experiment of this type was performed using the rayon fibers. The details of the experiment and results are given in Appendix IX. Little or no removal was observed when a duplicate pad was permeated with distilled water at pH 6.3 for 10 minutes. The retention behavior of the rayon fibers under a variety of colloidal conditions was not investigated. A satisfactory explanation of this observation cannot be given, but possible reasons for this behavior are discussed in Appendix IX.

## REMOVAL SUMMARY

Some particle removal was achieved during the permeation in Experiments 1 through 4 as evidenced by visual observations of the effluent. The majority of the removal seen in the effluent probably occurred immediately at the septum. These amounts were quite small and were undetectable in the distribution curves.

The microscopic observations had shown that individual particle removal was quite small. Retention of single particles could be considered irreversible. This fact was specifically substantiated by Experiment 1. The Type 1 pulp used in this experiment was relatively undamaged and free of fiber fragments. Permeation at the same velocity as formation showed no significant loss of particles.

The microscopic visual observations also showed the major removal mechanism was the loss of fiber fragments with attached particles. In Experiments 2 through 4, the Type 3 pulp was used. This pulp had received treatment designed to increase the amount of loss due to fiber fragments. The permeation techniques were designed to test for removal at three different shear conditions. In Experiment 2, the shear level during permeation was the same as formation and the pad structure did not appreciably change. The pad in Experiment 3 experienced a continuous increase in shear and a continuous increase in the state of compression. The pad in Experiment 4 had a step change in shear and a step change in the state of compression. No significant loss or redistribution of titanium dioxide could be detected in the experiments.

The removal observed in Experiment 5 could be explained in terms of repeptization. This removal mechanism will not be operating in experiments carried out in a fixed colloidal condition. It was, therefore, concluded that distributions obtained at fixed colloidal conditions were primarily function of attachment and that once a particle became bound, it was not removed.

# PARTICLE ATTACHMENT

## CONCEPTS OF ATTACHMENT

### BACKGROUND

As discussed earlier, quantitative treatment of the retention process has been based on the application of conservation of mass to a particular retention system. From the particle distribution curves that result, the retention process can be described in terms of a collection efficiency or an effective rate constant. In the absence of removal, the retention rate is essentially the same as the attachment rate.

The accepted method of treating the attachment process has been to assume that the collection efficiency was composed of two parts. The first part was visualized as the transport of the particles to the fiber surface. The second part was the adhering of the particle to the fiber surface. Particle transport or collision probability has been considered a function of the hydrodynamics of the system, while the probability of the particle adhering to the surface of the fiber has been considered a function of the colloidal state of the system.

The pattern of the investigators has been to fix colloidal variables and study the effects of hydrodynamic variables. The converse approach has also been used. That is, fix hydrodynamic variables and study the effects of changing colloidal variables. Attempts have been made to correlate changes in either hydrodynamic or colloidal variables with observed changes in collection efficiency.

PARTICLE TRANSPORT

The relationship between hydrodynamic variables and particle transport can best be discussed by descriptions of the transport mechanisms important in the titanium dioxide-fiber system. These are interception, impaction, and diffusion.

Interception is simply a means by which the particles contact a fiber surface due to their size. When a fluid flows past an object, the streamlines begin to curve around the object at an appreciable distance upstream. The interception mechanism assumes that the particles follow the streamlines. The particles will collide with the object if the streamline containing the center of the particle passes less than one half the diameter of the particle away from the surface of the fiber.

In the normal treatment of interception, the streamlines are taken as those which would occur if no particles were present. The effect of particles on the fluid motion is ignored. The probability of a collision is then determined by geometrical considerations only.

The impaction mechanism of particle transport depends on particle density. If the particle has a density greater than the fluid, its inertia will resist the accelerations caused by the curving of fluid streamlines.

The inertia of the more massive particle will cause it to follow a less curved trajectory than the fluid streamlines, and thus move more directly toward the fiber. The particle will then be able to move across the streamlines and have a greater probability of striking the fiber than when inertial forces are negligible. In the normal treatment of impaction, the movement of particles relative to fluid is taken to be resisted by viscous forces according to Stokes'

law. A simple force balance of particle inertia and viscous resistance, superimposed on the unperturbed streamlines then gives the contribution by impaction.

Diffusion of particles is due to their Brownian motion. This motion results from collisions with fluid molecules. Einstein (19) has shown that the diffusion coefficient of a particle should be

$$D = kT/3\mu d\pi \qquad (11)$$

where

$D$ = diffusion coefficient, cm.$^2$/sec.,

$k$ = Boltzmann's constant, $1.380 \times 10^{-16}$ ergs/°K,

$T$ = absolute temperature, °K,

$d$ = diameter of particle, cm., and

$\mu$ = viscosity of fluid, g./cm. sec.

Brownian motion becomes more intense with smaller particles, in less viscous fluids, and at higher temperatures. This random motion superimposed on the fluid motion may result in a particle whose center was originally in a streamline which would not pass close enough to a fiber for a collision to occur, moving across the streamlines and colliding with the fiber. Of course, it can also result in a particle whose center was originally on a streamline which would pass closely enough for a collision to occur, moving across the streamlines and not colliding. If no concentration gradients existed, there would be no net effect of diffusion. However, concentration gradients do exist, and diffusion can increase the probability of collisions. Quantitative treatment of this mechanism is inherently more complicated than interception and impaction because of the addition of a random process and the need to consider the particle concentration gradients.

From the above discussion, it can be seen that the controlling transport mechanism in a given retention system depends primarily on particle and fiber size, particle density, and the velocity range. Statements regarding the controlling transport mechanism have usually been based on examination of the response of the collection efficiency to velocity changes. If diffusion is the controlling mechanism, the collection efficiency would be expected to decrease with increasing velocity. This is due to the fact that the particle is in the vicinity of the fiber surface for a shorter period of time. If the particle is in the fiber vicinity a shorter period of time, its motion due to Brownian diffusion becomes small compared to its motion past the fiber. If impaction is the controlling transport mechanism, the collection efficiency will increase with increases in velocity. Increases in velocity result in increases in the inertia of the particles, making it more favorable for the particle to cross streamlines and collide with the fiber. The interception mechanism of particle transport is unaffected by velocity changes provided the streamlines about the fibers do not change significantly. This mechanism is more strongly dependent on particle size than velocity. The collection efficiency should not change appreciably with changes in velocity when interception is the mechanism of particle transport.

## ADHESION PROCESS

The relationship between colloidal variables and adhesion of the particle to the fiber surface is more obscure than the relationship between hydrodynamic variables and the transport of the particle. Since a detailed knowledge of what actually occurs at the fiber surface is not available, the adhesion step is assumed to be described by a distribution function. Once the particle collides with the fiber surface, it is visualized as either adhering or bouncing off, depending on the colloidal forces operating at the site of collision. Adjustment

of the colloidal variables from poor to favorable flocculating conditions is visualized as allowing more and more of the collisions to result in the particles adhering to the surface.

Treatment of the attachment process as described above has led to the concept of the collection efficiency being composed of a collision probability and an adhesion probability. This has allowed for the separation of colloidal and hydrodynamic effects. Utilizing the separate concept of collection efficiency, Johnson (11) and Han (10) have fixed the colloidal environment to favorable flocculating conditions and have investigated the effects of hydrodynamic variables such as velocity, porosity, and fiber diameter on retention. Based on the response observed in the collection efficiency to changes in these variables, they have concluded that the attachment process is diffusion controlled.

Williams and Swanson (9) have studied the effects of changing colloidal environment at fixed hydrodynamic conditions. They found increases in the amount of retention prior to and during pad formation as the repulsive barrier was lowered. The observed collection efficiency was correlated with the amount retained prior to pad formation and the amount retained during a filtration.

All of these investigators have pointed out the need to further understand the interrelationship between colloidal and hydrodynamic forces acting in the vicinity of the fiber surface. Han (10) describes the retention process in the following manner, pointing out the need of further understanding of the adhesion step:

> "When small particles are suspended in a fluid, they are subject to various forces which govern their motions relative to the fluid, resulting in collisions with each other. If their sizes are much smaller than 1 μm. in diameter, the suspended

particles exhibit strong Brownian motion superimposed on their movement with the fluid. By the kinetic theory Brownian motion represents a diffusional characteristic of small particles.

"If solid boundaries or objects are placed in a field of flow, the particles will also collide with the solids primarily due to diffusion if the particle inertia is negligible. The frequency of collision may be determined from the particle concentration and diffusivity, the geometry of the solids, and the flow pattern. On collision they may adhere to or bounce off the solid surface. Whether attachment or detachment will result depends on the forces operating at the site of collision. In the absence of repulsive forces, the particles tend to agglomerate with each other or to adhere to a solid surface when they come into close proximity where the Van der Waals-London attractive forces are operating.

"In aqueous suspensions, the dispersion of hydrophobic particles may be achieved by introducing certain electrolytes, the ions of which tend to adsorb preferentially on the particle surfaces. Owing to the necessity of electrostatic neutralization, the charged particles will be surrounded by a diffused layer of oppositely charged ions. The repulsive forces so created will lessen the tendency toward particle flocculation even in a concentrated suspension. In such a colloidal condition the state of dispersion is a delicate balance between the attractive and repulsive forces in the critical range of ionic concentrations.

"The adhesion of particles to fibers is not well understood, but probably follows similar physicochemical laws. In addition to the natural attractive forces and the imposed repulsive forces, whether a small particle will or will not adhere to a fiber on their close encounter is also dependent on the hydrodynamic forces. At present, we are unable to analyze the various forces acting at the sites of collision. We merely assume that the probability of particle retention exists in the a posteriori sense."

It was felt that an experimental program designed to investigate the effects on retention of velocity changes over a range of colloidal conditions would help in the understanding of the attachment process. The effects of velocity under favorable flocculating conditions had been investigated and the effects of colloidal environment at a fixed velocity had also been investigated, but

velocity effects at colloidal conditions where significant repulsive forces existed were unknown. Hence, there had been little speculation on the possible effects of the kinetic energy of the particles or on the possible interaction between the colloidal forces and hydrodynamic forces on collision probability.

## COMPRESSIBILITY CONSIDERATIONS

In the derivation of the retention equations the porosity variable is explicitly eliminated by changing the position coordinate, $z$, to the mass coordinate, $m$. Thus, compressibility enters into consideration only in its effect on the collection efficiency. In the absence of compressibility, the hydrodynamic and colloidal states would be expected to be the same throughout the pad. It has been shown by Williams and Swanson (9) and by Grace (12) that $E$ is not constant within a pad in the titanium dioxide-pulp system. Although there was previous speculation that this behavior might be due to removal of particles, the results of this work would indicate that removal is not the explanation. It is most probable that variation in $E$ within the pad is directly associated with the compressibility of the pads.

Compressibility can affect the retention rate in a number of ways. In a compressed pad, the porosity (or void space) is decreased, and contact between fiber surfaces is increased. The possible consequences of these changes are discussed below.

A porosity dependence on collection efficiency might be expected as the porosity determines the closeness of approach of the particles to the fiber surface. In a constant-rate filtration of compressible wood fibers, there is no control over porosity. It is highest toward the top of the pad and decreases toward the septum. If porosity has a pronounced effect on retention, the collection efficiency should be expected to vary from top to bottom in the pad.

Changes in porosity are accompanied by changes in the local velocity around the fibers. This relationship is given by Equation (12), if the superficial fiber velocity is assumed negligible:

$$u = \frac{U_o}{\varepsilon} \tag{12}$$

where

$u$ = local velocity, cm./sec.,

$U_o$ = superficial velocity, cm./sec., and

$\varepsilon$ = porosity.

Thus, not only will a compressible pad have a porosity distribution but also a local velocity distribution. Changes in local velocity may also be expected to affect the collection efficiency as the local velocity about the fibers should affect the particle trajectories.

In writing the retention equations in terms of a collection efficiency, it is necessary to introduce a term representing the fiber surface area available for retention. In solving these equations, this area is normally considered constant, and any effects due to changing surface area are lumped into the collection efficiency. Since compression is brought about by fiber-to-fiber contact, it would be expected that compression will decrease the available surface exposed to particles and hence (from this standpoint) tend to decrease the collection efficiency. There is very little known about the actual area available for retention in a compressed pad. Han (10) used the projected surface of the fibers in his determinations of E. Grace (12) used the hydrodynamic specific surface area. Nelson (13) defined an attenuation coefficient involving $(1 - \varepsilon)$ as well as the projected area to account for surface not exposed to fluid flow and thus not contributing to collection of particles.

Neither Han nor Grace seriously considered variable area, and Nelson's general equations have been too complex to solve. An attempt to quantitatively determine the effect of compression on surface exposed to flow was made by Labrecque (20). He used an optical technique on dry pads and found a linear relation between the contact area and the degree of compression. It is not known if these results are applicable to a wet system or if the area he measured is proportional to the retention area. In summary, the effect of compressibility on retention area is unknown, except that compression will decrease area to some extent.

The state of compression is usually expressed as the pad density or mass of fibers per unit pad volume. It is a function of the compacting load or pressure drop across the pad. As the pressure drop across the pad increases, the rate of compression of the pad increases. This relationship is given by:

$$c = Mp^N \tag{13}$$

where

$c$ = mat density, g./cm.$^3$,

$p$ = compacting load, dynes/cm.$^2$, and

$M$ and $N$ = empirical constants.

The mat density is related to the porosity by the following equation:

$$c = (1 - \varepsilon)/V \tag{14}$$

where $V$ = fiber specific swollen volume, cm.$^3$/g. From this equation and Equation (12) the relationship between local velocity and mat density may be found.

From the above discussion, it can be seen that compressibility changes can be determined from the load or pressure drop history of the pad. This permits a first attempt at examining the effects of compression on the retention

rate. The second part of this study of attachment was aimed at an investigation of compressibility effects.

## ATTACHMENT STUDIES

### VISUAL OBSERVATIONS

Motion pictures have been made of a single fiber being permeated by a suspension of titanium dioxide particles.[1] Under good flocculating conditions, the particles easily adhere to the fiber. As is well known, the wood pulp fiber is quite fibrillated. In the wet state, these fibrils extend from the fiber surface. As can be seen from the trajectories of the free particles, the fibrils distort the streamlines about the basically cylindrical fiber. This results in a very complex flow pattern about an individual fiber. As the particles try to follow the streamlines about the fiber, some of them collide with the fibrils and adhere to them. Many of the fibrils are not visible until a titanium dioxide particle is attached to them. A large percentage of the retained particles are mobile within certain limits due to their attachment to fibrils. Fluctuation of the flow past the fiber causes the particles to "flop back and forth" as if suspended from a string. During constant flow, fibrils on the trailing edge of the fiber collect particles. They appear to be suspended in the flow by an invisible thread. The fibrils vary in length from quite short to some as long as a fiber diameter. The fibrils act as excellent collectors and become heavily laden with particles. However, under good flocculating conditions, the particles appear to adhere equally well to the actual fiber surface, the extended fibrils, or onto other retained particles. There is always a heavier build-up of particles on the leading edge of the fiber, but retention is in general uniform.

---

[1] Available at The Institute of Paper Chemistry.

Shown in Fig. 10 are scanning electron micrographs of fibers removed from a pad formed under good flocculating conditions. In Fig. 10A, particles are seen on the fibrils, the fiber body, and around the fiber pit at the right of the micrograph. A surprising visual observation from the motion picture films was the flow of particles down the lumen of the fiber. This internal flow is slow compared to the external flow, but nevertheless real. It is seen as particles flowing down the axis of the fiber while the major part of the flow is perpendicular to this axis. The suspension probably entered through pit openings on the leading edge of the fiber and exited through the pits on the trailing edge. This probably explains the retention observed around the pits. Figure 10B also shows retention on a section of a fiber. In the lower left of the micrograph a large fibril may be seen. Figure 10C shows an enlargement of fibrils extended from the fiber surface. In all the micrographs, the effects of particle-particle flocculation is evidenced by the large clumps of particles.

Permeation of fibers with a suspension of titanium dioxide particles under poor flocculating conditions resulted in very small amounts of retention. The major part of this retention occurred on the larger fibrils. Particles were also observed to strike the fiber surface, tumble around with no apparent affinity, and enter the fluid stream again. However, the number of these events was small.

The Brownian motion of the particles appeared small in comparison to their motion due to the fluid velocity. The complexity of the flow pattern about the fiber results in a tortuous path for the particles near the fiber to follow. Particles in the streamlines close to the fiber seem to have a high probability of colliding with either the fiber or a fibril. The effective retention diameter of the fiber is probably much larger than its geometrical

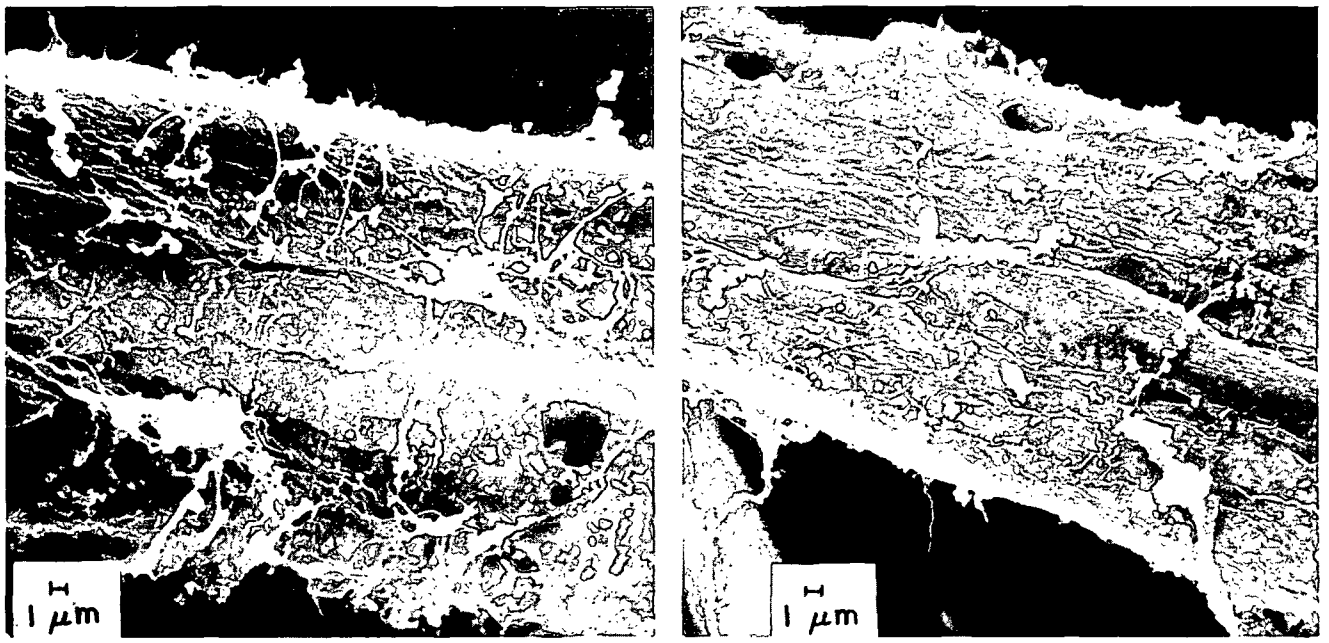


A B

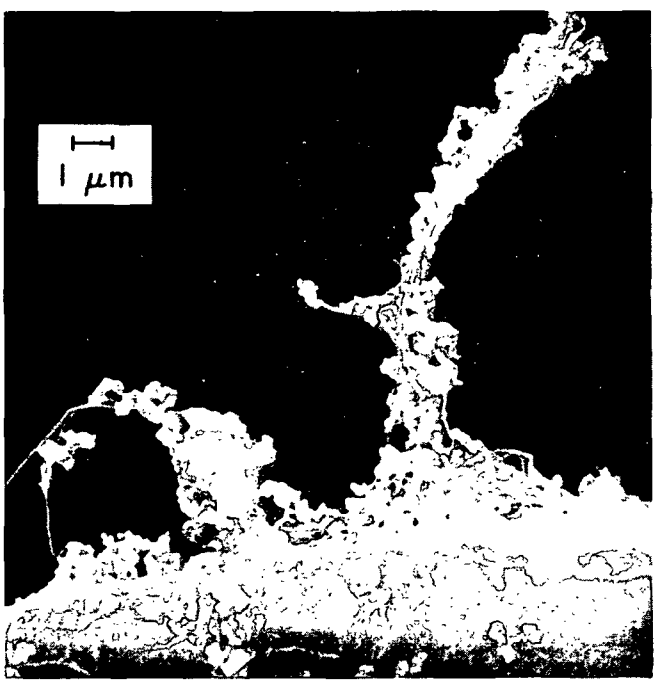


C

Figure 10. Scanning Electron Micrographs of Fibers Removed from a Pad Formed Under Good Flocculating Conditions. A and B Sections of Fiber Surface. C Enlargement of Fibrils

diameter. From visual observations alone, it would be difficult to determine whether the collision process was the result of Brownian diffusion, interception, or impaction or whether the colloidal forces actually change particle trajectories.

FILTRATION EXPERIMENTS

In order to help clarify the attachment process, the effects of two different forming velocities over a range of pH's were investigated. Suspensions were made which contained enough fiber and particles to form two pads. The pH of the suspension was then adjusted with either HCl or NaOH. Constant-rate filtrations were carried out at forming velocities of both 1 and 2 cm./sec. The results are shown in Fig. 11 through 17. The data are given in Appendix V. It should be noted that the scale for the bound particle distributions in Fig. 11 through 13 are one half the scale of Fig. 14 through 17.

Figure 11 shows the results of the filtration at pH 11.4 Overall retention is very low and the bound particle distribution at a forming velocity of 2 cm./sec. is only slightly higher than the bound particle distribution at 1 cm./sec. Both distributions are slightly concave up.

As the pH is lowered to 10.1, the distributions change to those found in Fig. 12. The bound particle distribution at 2 cm./sec. is now significantly higher than at 1 cm./sec. Both distributions show upward curvature.

Further lowering of the pH to 5.9 does not result in any significant change in the distribution curves of either the 1 or 2-cm./sec. pads. These results, shown in Fig. 13 are essentially the same as those obtained at 10.1.

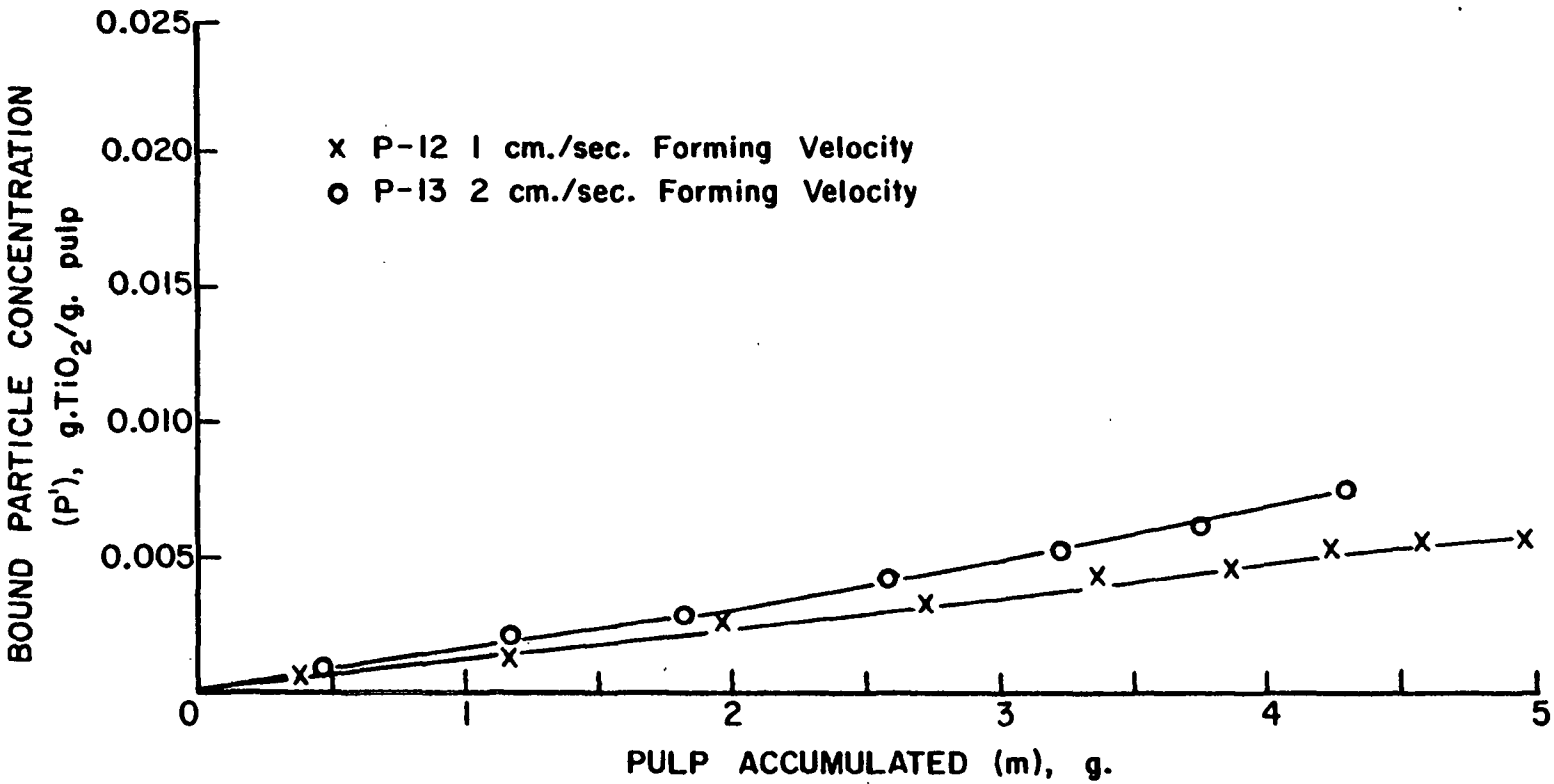


Figure 11. Bound Particle Distributions for Pulp Pads. Pads Formed from Suspension at pH 11.4

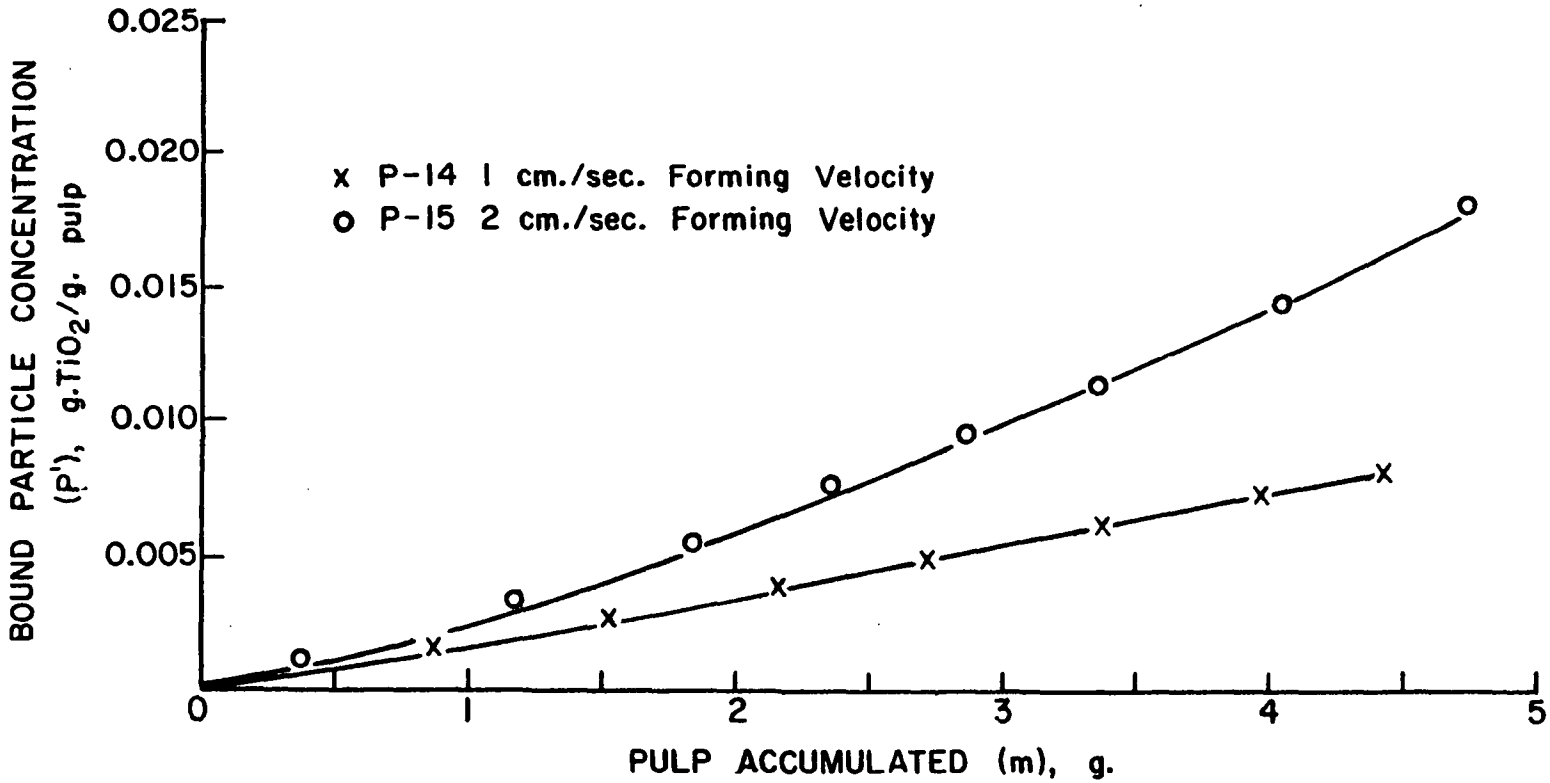


Figure 12. Bound Particle Distributions for Pulp Pads. Pads Formed from Suspension at pH 10.1

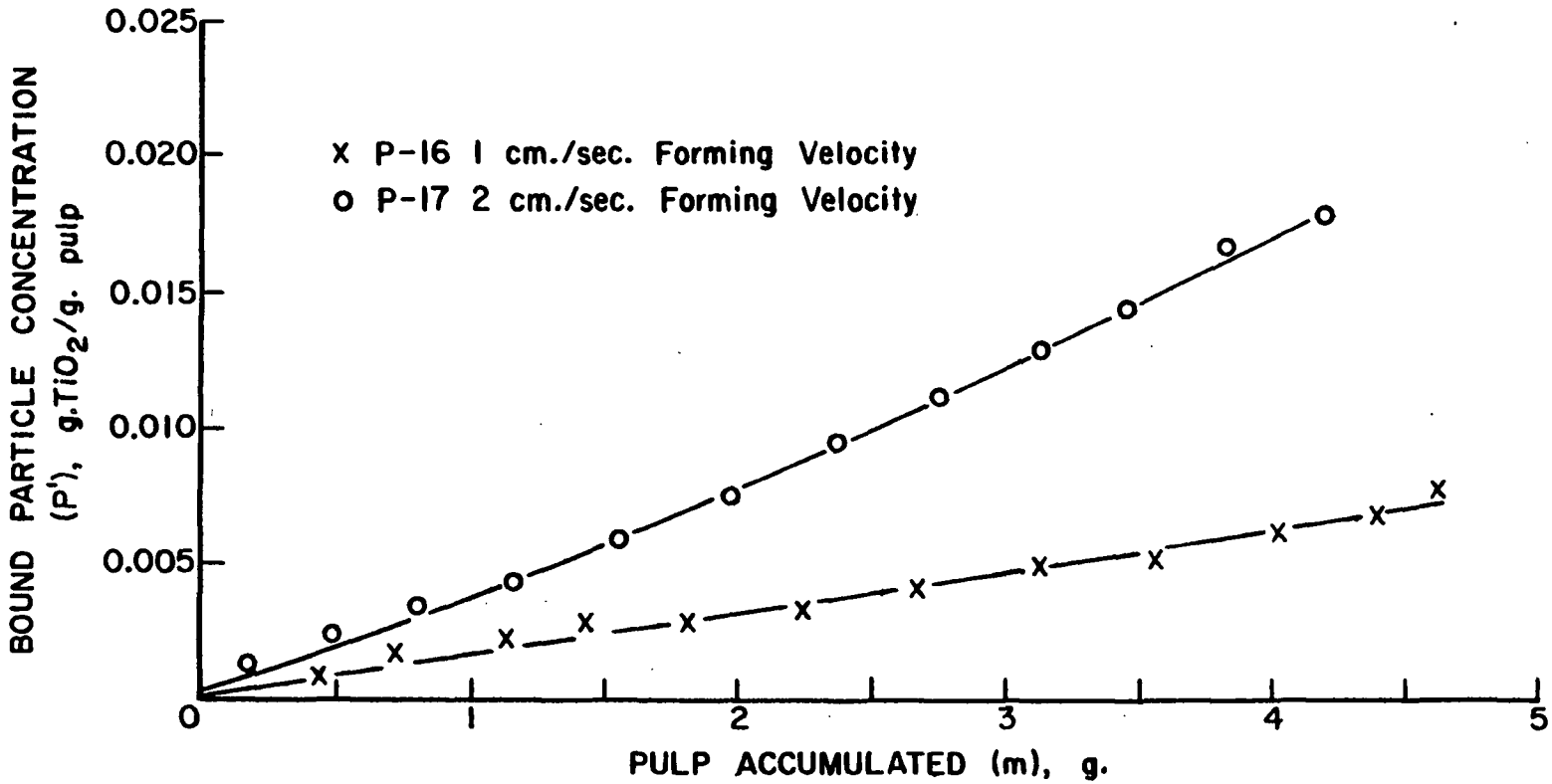


Figure 13. Bound Particle Distributions for Pulp Pads. Pads Formed from Suspension at pH 5.9

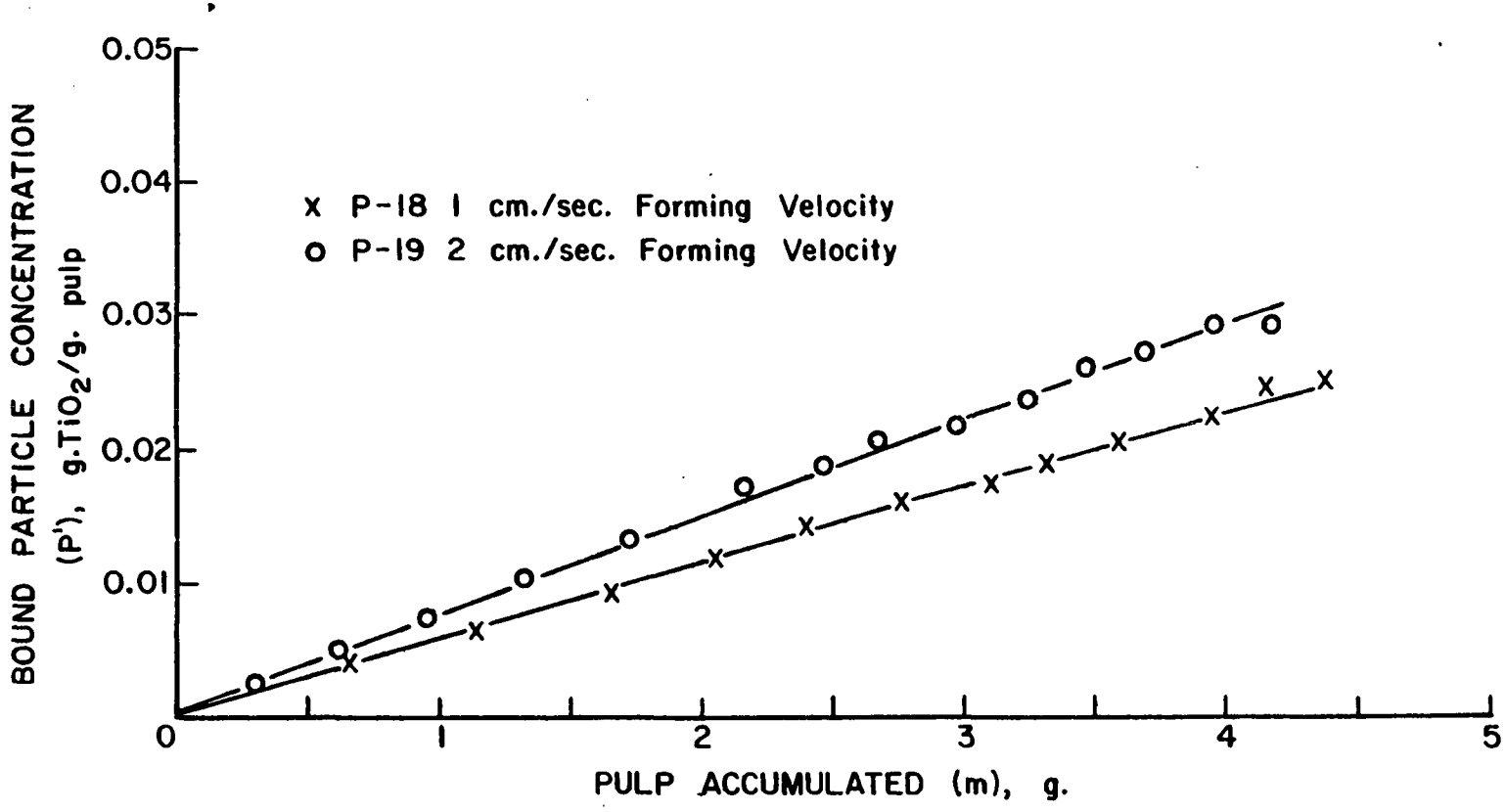


Figure 14. Bound Particle Distributions for Pulp Pads. Pads Formed from Suspension at pH 5.0

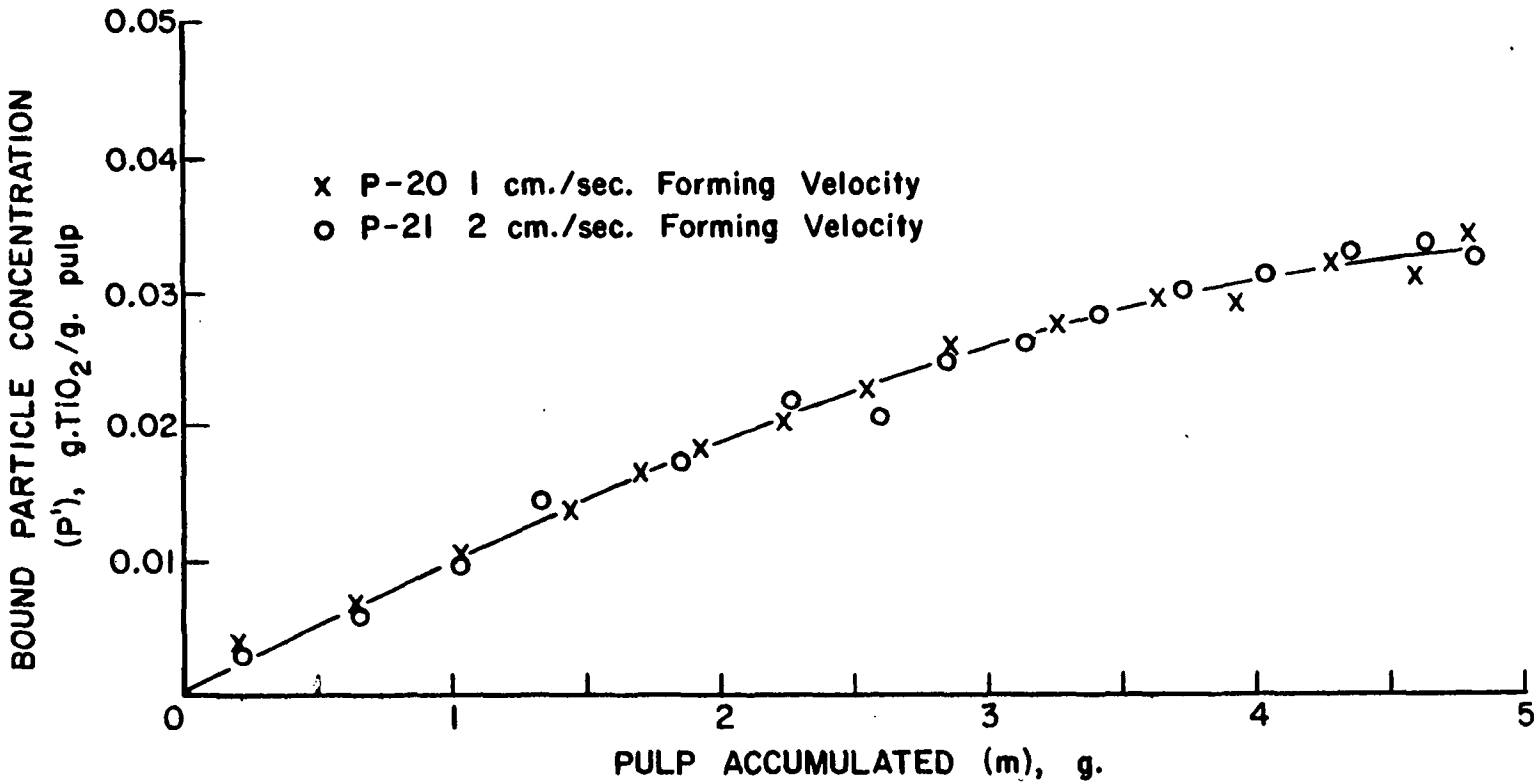


Figure 15. Bound Particle Distributions for Pulp Pads. Pads Formed from Suspension at pH 4.5

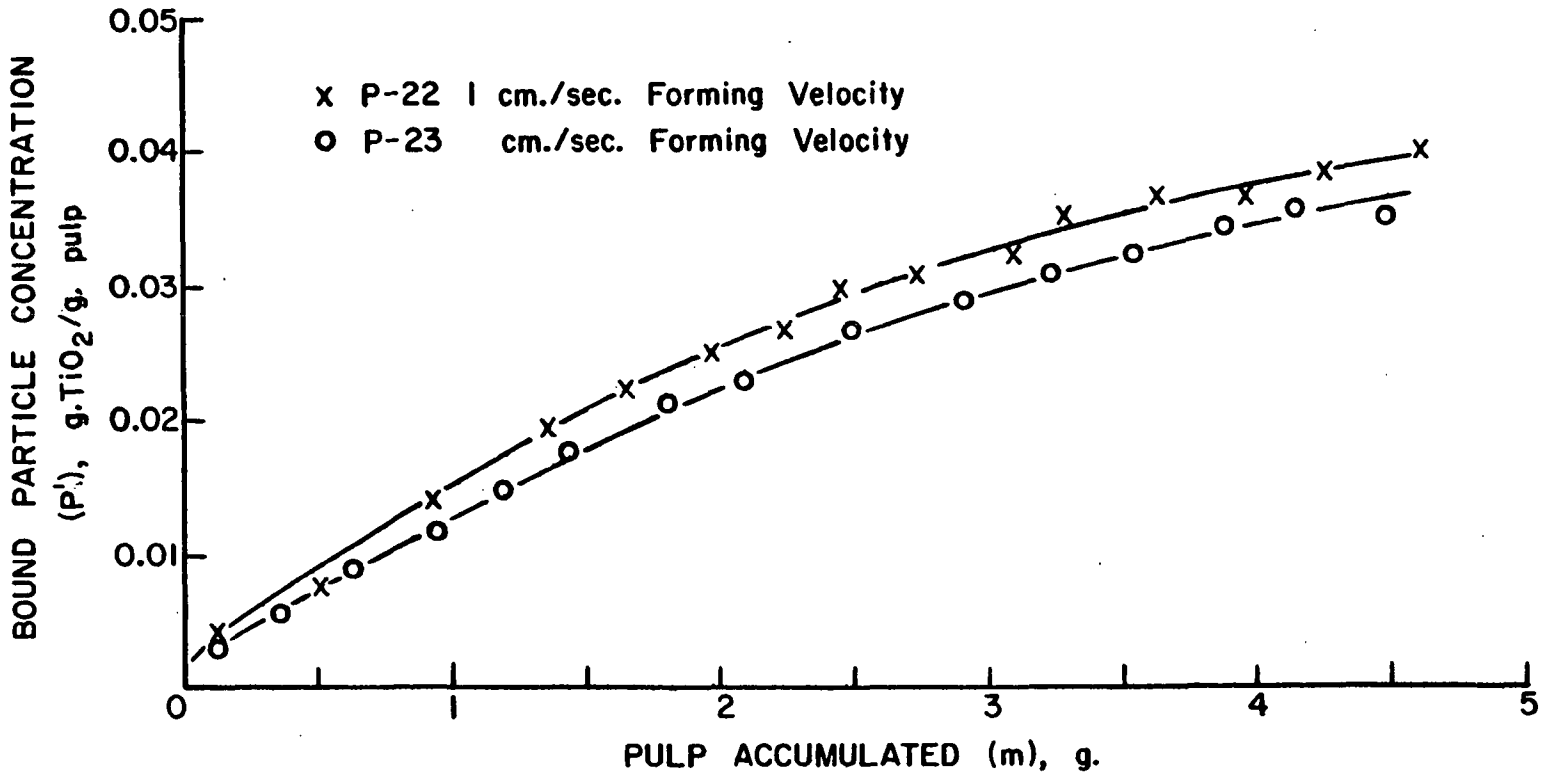


Figure 16. Bound Particle Distributions for Pulp Pads. Pads Formed from Suspension at pH 4.0

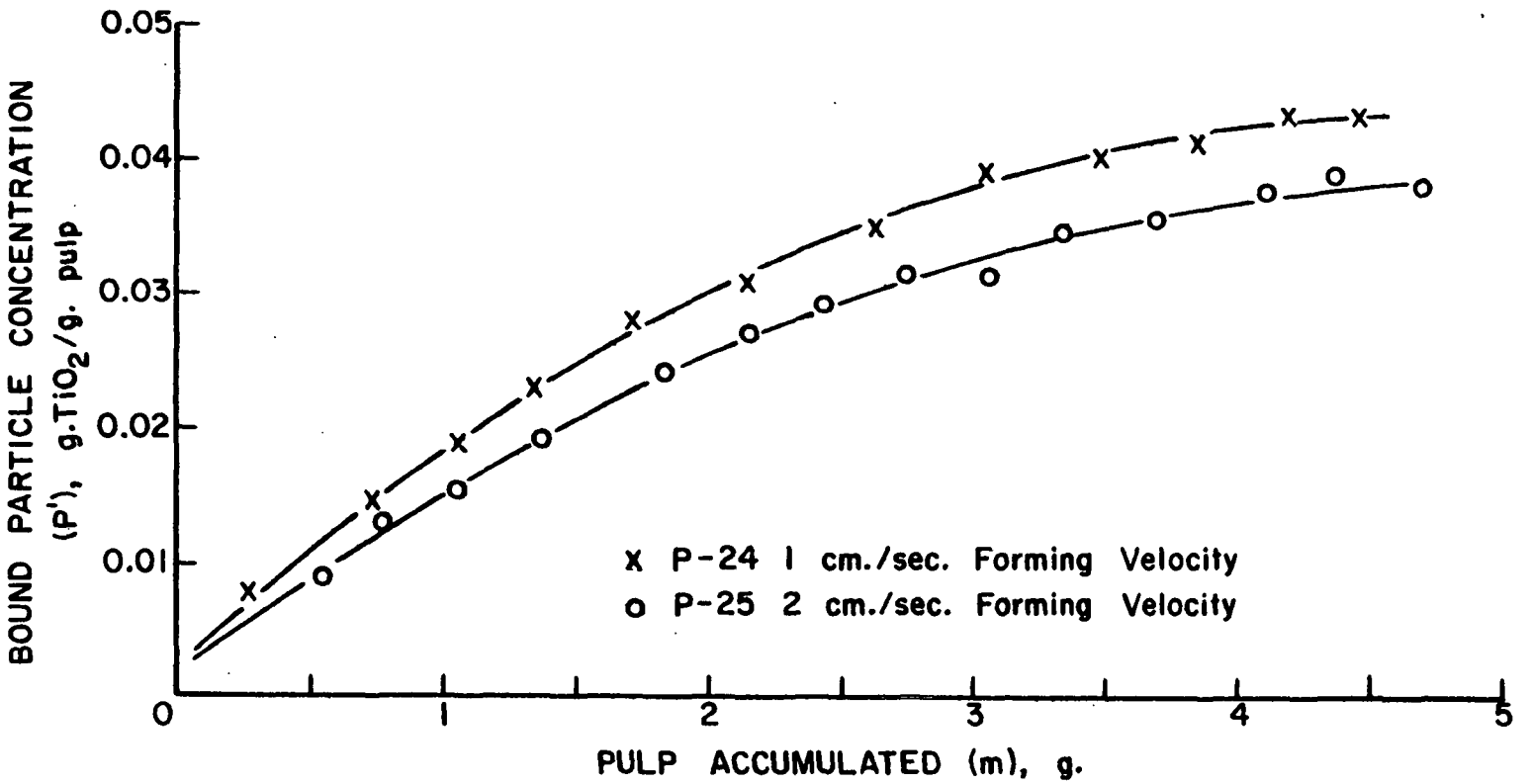


Figure 17. Bound Particle Distributions for Pulp Pads. Pads Formed from Suspensions at pH 3.5

Figure 14 shows that at pH 5.0 the overall level of retention is again increased. The distribution at 2 cm./sec. is still higher than at 1 cm./sec. The difference between the amount retained at the two different velocities is now not as large as before. The concavity of the distributions is also not as pronounced. The curves are essentially linear.

At pH 4.5, the distributions as shown in Fig. 15 are the same. The level of retention has again improved. The curvature of the distribution is now the opposite of the distribution obtained at the higher pH's.

Figure 16 shows the distributions obtained at pH 4.0. The amount of retention has improved. The distribution at 1 cm./sec. is now higher than at 2 cm./sec. The shape of the distribution curves is similar to the curves of Fig. 15.

As the pH is lowered to 3.5, the level of retention again increases as shown in Fig. 17. The distribution obtained at 1 cm./sec. is significantly higher at 2 cm./sec.

Additional experiments were performed at pH's 12.0, 2.6, and 2.1. Various problems were encountered at these extremes in pH. Briefly, at pH 12 the fibers became quite swollen and gelatinous. The overall retention at this pH was higher than the retention at pH 3.5. This is believed to be due to significant amounts of mechanical entrapment on the fibers. At pH's 2.6 and 2.1, extensive fiber-fiber flocculation was encountered. This resulted in poorly formed pads with levels of retention below those observed at pH 3.5. The results of these filtrations are discussed in detail in Appendix X.

The amount retained at an arbitrary level of 3.5 g. of pulp accumulated was calculated for each pad (pH 11.5 through pH 3.5). This quantity is simply

the area under the distribution curve up to an accumulated mass of 3.5 g. This amount of titanium dioxide was divided by the total amount of titanium dioxide which had passed through the pad at this time. This quantity was defined as the percent retention and is an indication of the extent of retention of the system. The results are shown in Fig. 18.

The general shape of either the 1 or 2-cm./sec. curve is as predicted for a hydrophobic colloid. That is, there appears to be a critical electrolyte concentration range (pH 6.0 to pH 3.5) where the retention level rises rapidly. This range is visualized as the region where the repulsive potential is beginning to be "collapsed" by the addition of electrolytes. As the repulsive potential is lowered, the level of retention increases significantly.

Hydrophobic colloid theory also predicts little flocculation in the regions where the repulsive potential is high. Addition of electrolyte in this region lowers the repulsive potential, but significant improvements in the amount of flocculation do not occur until the critical level of electrolyte is reached. The region (from pH 11.4 to pH 6.0) in Fig. 18 may be interpreted as the region of high repulsive potentials.

After "collapse" of the repulsive potential, there should also be another region where the amount of retention is independent of the electrolyte concentration. This would correspond to the leveling off of the curves in Fig. 18 as indicated by the dashed lines. However, extensive fiber-fiber flocculation was encountered during retention experiments at these low pH's. The results were poorly formed pads with levels of retention below those observed at pH 3.5. These data are discussed in Appendix X.

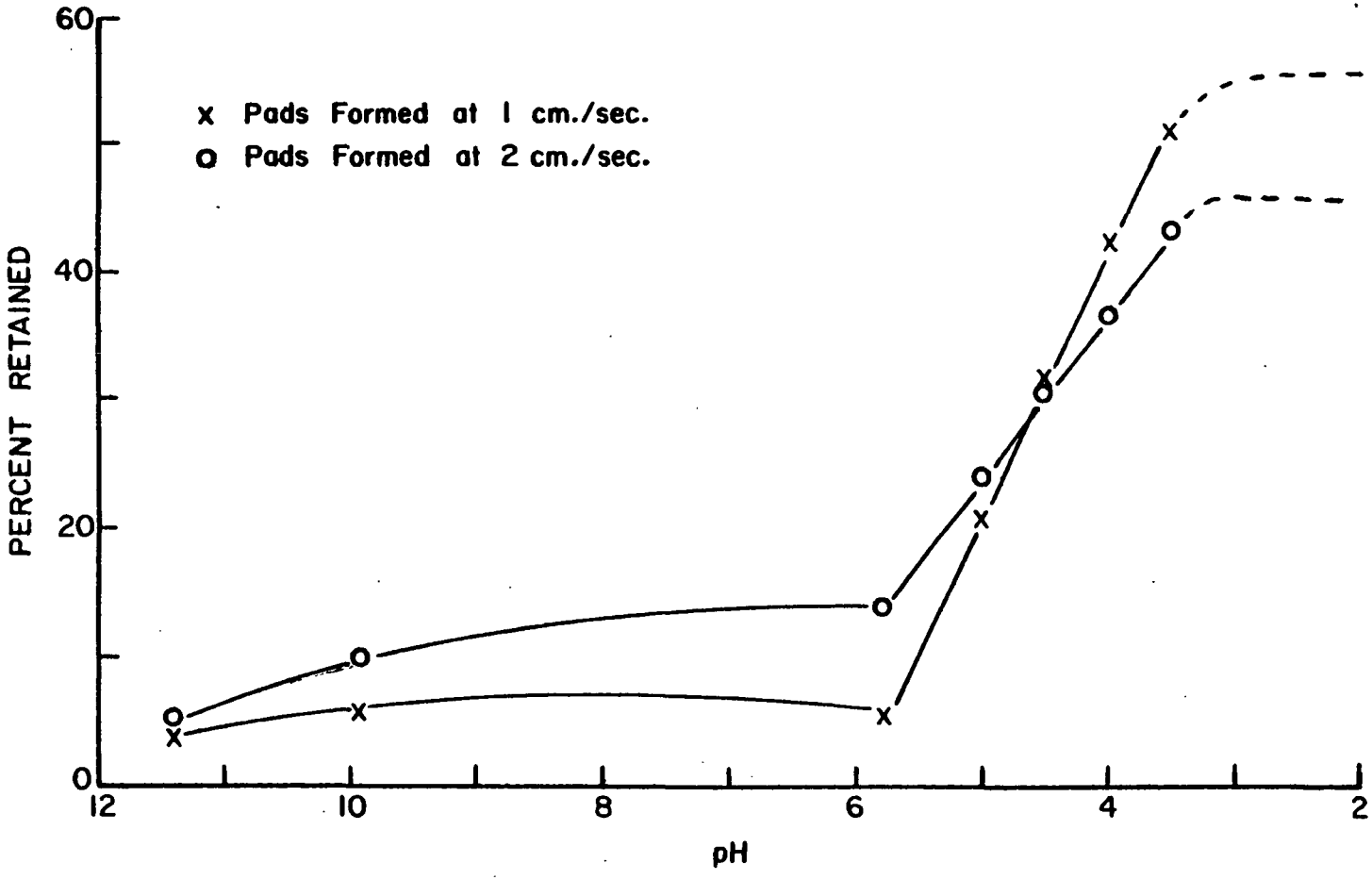


Figure 18. Relationship Between Percent Retained in 3.5 Gram Pad and pH

The effect of pH on this system is more complex than the effect of a neutral electrolyte such as NaCl. Webb (15) has extensively studied the colloidal behavior of titanium dioxide, and Walkush (17) has investigated the colloidal behavior of a pulp system. The hydrogen ion probably affects the charge on both the titanium dioxide and pulp fibers by a combination of methods. There are generally two accepted methods by which the repulsive potential may be changed. These methods will be discussed briefly.

The repulsive potential may be changed by the addition of ions responsible for the surface charge. These ions are called the potential determining ions. If some of the surface charge of the titanium dioxide and pulp fibers is caused by hydroxyl groups, or by carboxyl groups on the pulp fiber, the addition of hydrogen ions would tend to lower the surface charge and lead to flocculation. Conversely, the addition of hydroxyl ions would tend to increase the surface charge and promote stability.

The repulsive potential may also be changed by the addition of counter-ions. For example, on a negatively charged particle, the addition of sodium ion tends to lower the repulsive potential to a point of "collapse" of the double layer. This process also leads to flocculation of the particles.

The above discussion points out the difficulty in predicting the relative magnitude of the repulsive potential over the wide pH range used. For example, in order to raise the pH above that of the distilled water requires the addition of NaOH. The effect of the hydroxyls should be to raise the negative surface charge on the titanium dioxide and fibers, while the effect of the sodium ion should aid in the "collapse" of the repulsive potential. Thus, in the range of pH's from 7 upward, it is not possible to predict the net result of adding the NaOH.

The situation is less complex in the acidic regions of pH. Addition of HCl should result in a continuous lowering of the potential. The hydrogen ion can act as both a potential-determining ion and a counter-ion in lowering the repulsive potential. The results of Fig. 18 confirm this prediction.

Another problem involved with the pulp fibers is the possible chemical attack in both highly acidic and highly basic media. This problem is not too severe at the temperatures (17-20°C.) and contact times (1 hr. maximum) involved in this series of experiments.

The region of particular interest for the purpose of this work is from pH 6 to pH 3.5. The pulp is relatively stable at these pH's under the experimental conditions.

Despite the above complications, it can be seen that either curve in Fig. 18, taken separately, corresponds to a typical hydrophobic colloid response to an electrolyte. However, the curves taken together show different effects of velocity at different colloidal conditions. At pH's above 4.5, the bound particle distributions are higher at forming velocities of 2 cm./sec. At pH's below 4.5, the bound particle distributions are higher at forming velocities of 1 cm./sec. The bound particle distributions are the same at pH 4.5. Thus, if an attempt was made to determine the controlling mechanism of particle transport by changes in velocity alone, different results would be obtained at different pH's. The results of this series of experiments cannot be explained by a collection efficiency composed of a collision probability and an adhesion probability. If this simplified concept of the attachment process were correct, the ratio of the amount of retention at 1 and 2 cm./sec. forming velocity should be a constant. For example, if the collection efficiency is expressed as $\underline{E} = \alpha\beta$ where $\alpha$ is the adhesion probability and $\beta$ is the collision probability, then $\beta$

should be unaffected by changes in pH. The collection efficiency at 1 cm./sec. forming velocity can be written as $\underline{E}_1 = \alpha_1\beta_1$, and at 2 cm./sec. as $\underline{E}_2 = \alpha_2\beta_2$. The ratio of the collection efficiencies at any pH is then $\underline{E}_1/\underline{E}_2 = \beta_1/\beta_2$. At pH's above 4.5, this ratio is greater than 1. At pH 4.5, it is approximately 1, and at pH's below 4.5, it is less than 1. The fact that the ratio of the collection efficiencies is not a constant shows a need for a better model of the attachment process. The discussion which follows provides a more detailed consideration of possible events leading to attachment.

## DETAILED CONSIDERATION OF ATTACHMENT PROCESS

### Energy Interactions

Figure 19 taken from Kruyt (18) shows a typical series of curves which represents schematically the energy of interaction between colloidal particles. Curves 1 through 3 represent the net energy of interactions as the repulsive potential is lowered.

These curves are the net result of adding the repulsive potential due to the charge on the particles and the attractive potential due to Van der Waals-London forces. Examination of the curves shows a minimum in the interaction depicted by the letter R. The curves are seen to rise rapidly at distances smaller than the distance at R. This abrupt rise in repulsive potential is visualized as arising from the overlap of electronic clouds and is termed the Born repulsion. The Born repulsion is important in preventing the net attractive energy from becoming infinitely large near the surface. Due to this repulsion, there is a minimum in the potential curves denoted by R.

A retained particle may be defined in terms of these curves. A retained particle is a particle which is located in an energy "well" which is deep

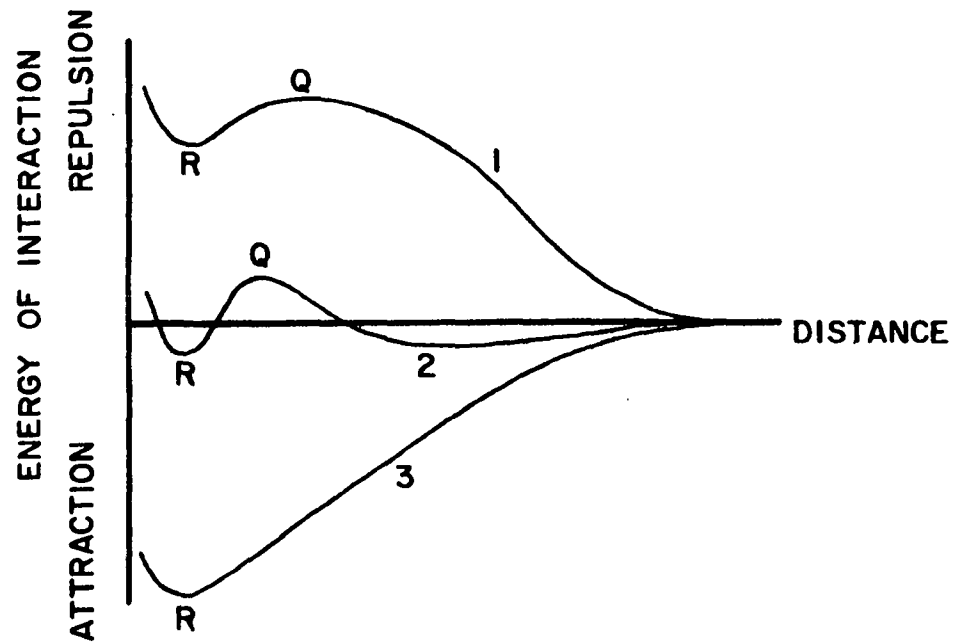


Figure 19. A Series of Potential Curves Illustrating Schematically the Energy of Interaction Between Colloidal Particles as the Repulsive Potential is Lowered

enough to prevent escape of the particle by thermal motion or fluid drag forces. In the absence of fluid drag forces, the depth of the well needed to prevent escape by the thermal motion of the particle is approximately equal to $kT$, where $k$ is the Boltzmann constant and $T$ is the absolute temperature. When fluid drag forces are present, the "well" must be somewhat deeper.

To begin the discussion of the possible events leading to attachment, it is simplest to neglect any terms responsible for the dissipation of energy in the system. The consequence of this will be considered later. For the present, consider a particle approaching a fiber which will interact according to Curve 1 of Fig. 19. Curve 1 represents a system where the well is less than $kT$ in depth. Particles approaching the fiber would have to overcome a very large repulsive potential to reach the well at $R$. If the particle should have this much kinetic energy, it would not remain in the well as its thermal energy is greater than the well depth. Very few particles should be retained in a system under these colloidal conditions.

Curve 2 represents a system which should be capable of retaining some particles. A net repulsive potential exists at the larger distances, but the attractive potential predominates near the surface. The well is greater than $kT$ in depth, so particles should be difficult to remove once they are in. For a particle to get into the "well," it must get over the energy "hill" designated by the letter $Q$ in Fig. 19. Under colloidal conditions such as this, the kinetic energy of the particle becomes very important. If the kinetic energy of the particle is large enough, it should be able to cross over the energy "hill" and proceed toward the "well." Conversely, if the particle does not possess enough kinetic energy to cross the "hill," no retention is possible.

If the approach velocity is denoted by $\underline{V}_o$, then the criteria for the particle to "cross" the repulsive barrier may be expressed as

$$1/2\ m_\rho V_o^2 > Q \qquad (15)$$

where $\underline{m}_\rho$ = mass of particle. This may be considered the lower limit of kinetic energy for retention to occur under any colloidal conditions.

There is another aspect of particle kinetic energy which must also be considered. If there is no energy dissipation in the system, particles which cross the repulsive barrier will continue a course into the "well" and then back out again due to the Born repulsion. In this situation, there would be no retention regardless of the height of the hill or the depth of the well. Due to conservation of energy, there would be only conversion of potential energy and kinetic energy and a particle with sufficient energy to cross the barrier from one side would have the same ability to return. In order for retention to take place, some of the kinetic energy of the particle must be dissipated along its path. This dissipation can occur by a number of methods which are discussed below.

The change in the kinetic energy of the particle due to the presence of the potential field is resisted by the fluid motion. Thus, some of the particle energy is dissipated in overcoming the effects of the drag of the fluid. This can be considered somewhat analogous to a frictional loss and is a velocity-dependent term. Another method of energy dissipation is by an energy transfer on collision. This phenomenon is analogous to a partially elastic collision. In a partially elastic collision, there is a transfer of energy between the elements of the colliding system.

If a particle collides with the fiber surface, there should be some transfer of energy from the particle to the fiber. This leaves the particle at a lower energy level after collision.

By these methods of energy dissipation, the kinetic energy of the particle can be lowered a sufficient amount to result in the particle remaining in the well. If the total energy dissipated is denoted by $J$, then the particle will remain in the well if:

$$1/2\ m_p V_o^2 - J < Q. \tag{16}$$

A "bounce off" will occur if the kinetic energy of the particle, $1/2\ m_p V_o^2 - J$, is greater than the energy barrier, $Q$.

From the above discussion, the range of kinetic energies of the particles for attachment to occur may be set. The limits are between $Q$ and $J + Q$ and may be expressed by the following inequality:

$$J + Q > 1/2\ m_p V_o^2 > Q. \tag{17}$$

Thus, if the kinetic energy of the particle is less than the height of the "hill," denoted by $Q$, the particles cannot cross the barrier. If the kinetic energy of the particles is greater than $Q$, the particles can cross the barrier and may be retained if the energy dissipation term, $J$, is large enough to prevent the particle from returning across the barrier, $Q$. The particles will "bounce off" if the kinetic energy is greater than $J + Q$.

Force Interactions

The above discussion has considered attachment from an energy point of view. The influence of fluid motion is more readily handled in terms of forces. Meyer (21) has considered the problem of the retention of small particles in the

presence of a potential field. From a consideration of the forces acting on the particles, he has suggested an equation relating the net force on the particle to the colloidal forces and the fluid drag forces. This equation is useful in that it vividly points out the interrelationships between colloidal forces and hydrodynamic forces in determining particle trajectories. A discussion of his interpretation of the problem and the presentation of his equation will help in further clarifying the complexity of the attachment process.

Figure 20 depicts a single idealized fiber being permeated by a suspension of particles. It is assumed that the colloidal forces acting on the particle are of a central force type and that the direction of the force is that of a radius vector connecting the centers of the particle and the center of a circular-cross-section fiber. The effect of the fluid drag forces are assumed to be described by Stokes Law.

The particles in the fluid in the region near the fiber experience accelerations as a result of forces acting upon them which distract them from the streamlines they would follow if they were free of mass and in a nonperturbing environment. As a consequence of the colloidal forces, the particle trajectories may be affected. An attempt to describe the interplay of the various forces on the particle requires a knowledge of the streamlines about the fiber. This would describe the path of a massless particle in the absence of colloidal forces. Streamlines about fibers of cylindrical shape can be described. In this discussion, the symbol $\underline{\vec{V}}_f$ will be used to describe the unperturbed field of velocities about the fibers and will be assumed the path of the particle if no other forces act.

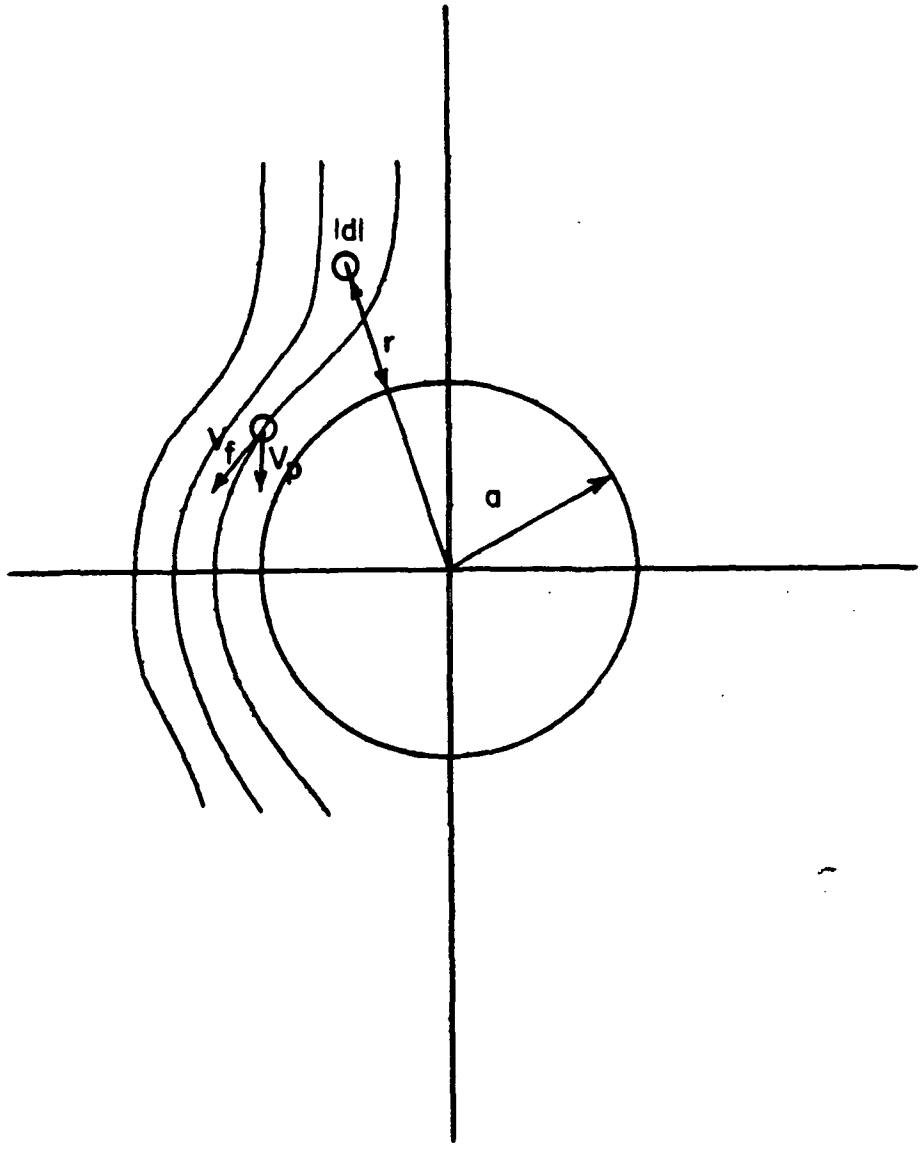


Figure 20. Pictorial Representation of Particle in Vicinity of Cylindrical Fiber Being Acted upon by Colloidal and Hydrodynamic Forces

The motion of an individual particle of mass $m$, located at position vector $\vec{r}$, can be described by a particle velocity $\vec{V}_p$, which is the time derivative of the position vector, or

$$\vec{V}_p = d\vec{r}/dt. \tag{18}$$

From an equation of motion governing $\vec{V}_p$, particle trajectories can be computed. Newton's second law, applied to the particle, gives this equation of motion:

$$\frac{d}{dt}(m_p \vec{V}_p) = \vec{F}. \tag{19}$$

This equation is perfectly general; however, problems arise when a complete description of $\vec{F}$ is attempted. $\vec{F}$ is composed of the attractive forces, the electrostatic repulsive force, the Born repulsion, and all the dissipative forces in the system such as the fluid drag forces and the forces responsible for energy transferred during a collision. Mathematical descriptions of all these forces are not available as the actual interactions of colloidal particles on contact are not themselves completely understood. Meyer has chosen to include in his model of $\vec{F}$ a generalized expression for the colloidal forces of the following form:

$$\vec{F}_1 = \vec{r} \sum_{i=1}^{q} \frac{f_i}{(r - a - \frac{d}{2})^{n_i}} \tag{20}$$

where $\vec{F}_1$ is the sum of the colloidal forces acting on the system; $f_i$ and $n_i$ are parameters to be determined from experimental data. The parameter $f_i$ is associated with such things as the surface charges, the conductivity of the fluid, and the Hamaker constant (22), utilized in describing attractive forces.

Meyer visualized the above colloidal forces being resisted by the fluid drag forces having the following form:

$$\vec{F}_2 = 3\pi\mu d(\vec{V}_f + \vec{V}_p). \tag{21}$$

The fluid drag force is the only dissipative term included in this model. The total force on the particle, $\vec{F}$, may then be written as the sum of the above forces, $\vec{F}_1$ and $\vec{F}_2$.

$$\vec{F} = \vec{r} \sum_{i=1}^{q} \frac{f_i}{(r - a - \frac{d}{2})^{n_i}} + 3\pi\mu d(\vec{V}_f + \vec{V}_p). \tag{22}$$

This treatment is important in that it points out the interrelationship between the colloidal forces and the hydrodynamic forces in determining particle trajectories. The treatment from energy considerations has pointed out the importance of both colloidal and hydrodynamic factors in determining if the particle will adhere to a surface or "bounce off." The observed retention in any system whose primary retention mechanism is coflocculation will be the result of the complex interplay of these colloidal and hydrodynamic factors.

System Nonideality

All of the discussion of the attachment process thus far has been based on an ideal system. Recognition must now be made of the "nonideality" of the wood pulp fiber system.

To begin with, the wood pulp is far from being an ideal, smooth, cylindrical fiber. The visual observations have shown the fibrillar nature of the surface. These fibrils stick out from the fiber surface in all directions and are of various lengths. They appear to be very effective collectors of particles. Due to these fibrils, flow patterns about the wood pulp fiber are

extremely complex and would vary considerably along the fiber axis. There is certainly a local velocity distribution about an individual fiber being permeated at a constant superficial velocity. Thus, even when forming pads at a constant superficial velocity, a rather large distribution of local velocities would be expected.

In addition to the geometrical nonideality of the wood pulp fiber, there is also a surface nonideality. Surface irregularities on the wood pulp may arise from variations in the order of the surface. Theories on the structure of the cellulose fiber consider it to be composed of regions of high order (crystalline regions) and low order (amorphous regions). Surface irregularities may also arise from variations in the chemical composition of the surface. The presence of polymers other than cellulose are to be expected as wood pulp fibers contain varying amounts of hemicellulose polymers. The chemical treatments of pulping and bleaching also alter the surface of the fiber causing the formation of carboxyl groups. The result of these surface irregularities should be a distribution of both attractive and repulsive energy sites on the fiber.

From these considerations, it may be concluded that the kinetic energies of the particles passing through a fiber pad are distributed about some mean kinetic energy. The distribution arises from the velocity distribution and also from the particle size distribution. The shape of the kinetic energy distribution and the width of the distribution are unknown. However, there should exist some mean kinetic energy which is somehow related to the filtration velocity. Thus, the mean kinetic energy of the particles at a filtration velocity of 2 cm./sec. should be higher than the mean kinetic energy of particles at a filtration velocity of 1 cm./sec. In addition to the kinetic energy distribution, there is probably the energy site distribution due to variations in the fiber surface. These two distributions should be important in determining the amount of retention.

The attachment process has now been considered in some detail. It is not certain just how important some of the concepts discussed are. However, the results shown in Fig. 18 do indicate an interrelationship between the colloidal and the hydrodynamic variables. The above discussion has considered several possible methods in which these variables could interact. Some of these concepts can be used to qualitatively explain the results of Fig. 18.

APPLICATION OF CONCEPTS TO EXPERIMENTAL RESULTS

From pH 6 to pH 3.5, it can be safely assumed that the repulsive potential of the system is being lowered. As the repulsive potential is lowered, the amount of retention should increase as predicted from hydrophobic colloid theory. This increase is observed for both formation velocities as shown in Fig. 18.

According to the concepts previously discussed, when a relatively large repulsive potential is present, only the particles with sufficient kinetic energy to cross this barrier may be retained. Once the particle crosses this barrier, a sufficient amount of its kinetic energy must be dissipated to prevent a "bounce off" and the "well" must be of sufficient depth to prevent its escape by thermal motion and fluid drag forces. At pH's above 4.5, more of the particles at a formation velocity of 2 cm./sec. appear to fit this criterion.

Meyer's force balance can also be used to predict this same result. If the generalized expression for the colloidal forces includes a large repulsive term, then the majority of the particles should veer around the fiber. Only those particles whose velocity, $\vec{V}_p$, is of sufficient magnitude and in the proper direction to overcome the repulsive force should be retained. Again, more of the particles at a formation velocity of 2 cm./sec. should fit this criterion when the repulsive force is large.

As the repulsive force becomes smaller, it would be expected that more particles at both 1 and 2 cm./sec. would meet the requirements for becoming retained. This is observed. However, more particles are retained at 1 cm./sec. than at 2 cm./sec. at low repulsive potentials. There could be several different explanations for this. From energy considerations, there should be more "bounce off" of the particles at the higher velocities.

For the particle to be retained, the "well" must be deep enough to prevent its escape by thermal motion and fluid drag. The higher the velocity, the more the fluid drag contributes to this escape mechanism requiring deeper wells for attachment. However, this process has essentially been tested for in the removal studies. It should be recalled that no removal was observed when pads formed at 1 cm./sec. were permeated at 2 cm./sec. with fluid at the same colloidal conditions as formation. Hence, this process does not appear to contribute to the difference in the amount of retention at the low repulsive potentials.

A final reason for the observed lower retention at the higher forming velocity under low repulsive potential could be related to geometrical differences in the wood pulp fiber at different velocities. The fibrillar network on the wood pulp fiber accounts for a large fraction of the retained particles. Changes in this network could produce changes in the amount of retention. There could be a distinct difference in the geometry of the fiber at 2 cm./sec. when compared with 1 cm./sec. The fibrils, reacting to the fluid drag forces, are bent in the direction of flow. This bending of the fibrils could result in a lower retention area at the higher velocity and therefore lower amounts of retention.

CONSIDERATION OF SIEVING EFFECTS

To complete the discussion on this series of experiments, attention must be drawn to the fact that there is always some retention regardless of the colloidal conditions. This could be because there are always some particles which fit the criteria for becoming retained. With the aforementioned distributions of both velocity and retention sites, there may be some particles which can become retained under a wide variety of conditions. Another possibility which must be considered is that of sieving. As discussed previously, sieving is one of the mechanisms which could be operating in the retention of fillers. The extent to which this mechanism operates depends primarily on particle size and the three-dimensional network formed by the retention medium. The extremely small size of the titanium dioxide particles used in this study would make retention by sieving highly unfavorable. The large change in the amount of retention due to changes in colloidal environment supports the contention that coflocculation is the dominant retention mechanism. However, some of the observed retention under poor flocculating conditions could be due to sieving. In this series of experiments, the maximum amount of particles which could be retained by sieving would be the minimum amount of retention observed. For example, the results shown in Fig. 11 could be due to the sieving mechanism. Since sieving is a function of the network formed by the retention mechanism, it would be expected that more retention would occur at the higher formation velocity because the pad is more highly compressed. As can be seen in Fig. 11, the retention is slightly higher at 2 cm./sec. forming velocity.

There is no way to be certain about the retention observed in Fig. 11 being due solely to sieving, but if it is, then a significant portion of the

total retention observed in Fig. 12 and 13 could also be due to sieving. If it is assumed that the retention observed in Fig. 11 is by a sieving mechanism, and that this retention can be used as an approximation of the amount retained by sieving in Fig. 12 and 13, then the amount retained by coflocculation can be approximated by subtracting the result of Fig. 11 from Fig. 12 and 13.

This resulted in an approximately linear curve for these figures. The upward concavity was essentially removed. It could therefore be speculated that the upward concavity in Fig. 12 and 13 is the result of retention by both sieving and coflocculation with the amount retained by sieving being a significant portion of the total retention.

In the remainder of this series of experiments, retention by coflocculation becomes the dominant mechanism. Under good flocculating conditions, the amount retained by sieving becomes even more difficult to predict. This is because the free particle concentration decreases rapidly, making the number of particles reaching the lower sections of the pad much smaller than at poor flocculating conditions. The amount retained by sieving under good flocculating conditions is usually considered negligible. However, under favorable flocculating conditions, there is a potential particle size increase due to flocculation between the particles themselves. The extent to which "self" flocculation occurs and its effect on the amount retained by sieving is not known.

Another possible reason for the upward concavity in Fig. 11, 12, and 13 could be due to the compressibility of the pulp pads. If increases in the state of compression of the pad caused the retention rate by coflocculation to increase more rapidly than the change in free particle concentration caused the rate to decrease, then the retention rate would have an upward curvature. In these three experiments, the retention is so low that the free particle

concentration does not change appreciably from the beginning of the filtration to the end. Hence, the compressibility effects on retention should be more pronounced. Compressibility effects are considered in more detail in the next section.

## COMPRESSIBILITY EFFECTS ON ATTACHMENT

In a constant-rate filtration, the pad-forming process and the retention process occur simultaneously. Constant-rate filtrations of compressible fibers result in pads which vary in density from the upper surface to the septum. The pad density is least at the surface and continuously increases toward the septum. The extent to which the pad is compressed at any given amount of pulp accumulated depends upon the pressure drop.

The change in the state of compression of a pad during a filtration results in the local conditions at a given layer in the pad continuously changing. It is to be expected that these changes should be reflected by changes in the collection efficiency. The three local variables which should be of importance to the collection efficiency are: pore size, local velocity, and retention area. These variables, the changes they undergo during a constant-rate filtration, and the consequences of the changes will be considered.

### Pore Size

Pore size will be used to describe the size of the void space between the fibers in the mat where the fluid and free particles can flow. The fibers in the pad form a three-dimensional network, leaving pores with a potentially definable size and geometry. Compression of the pad results in a decreasing pore size. The effect of decreasing pore size should result in an increase in the number of particles passing closer to the fiber surface. This action should

lead to more collisions between the particles and fibers, thus increasing the collection efficiency. When this is the dominant effect of compression, the collection efficiency should increase with increasing amounts of pulp accumulated, m.

Local Velocity

Local velocity was defined by Equation (12) which was discussed earlier. Increasing states of compression result in increases in local velocity. Therefore, the local velocity will increase from the top of the pad to the septum.

As seen in the preceding section, velocity effects are related to colloidal variables. At high repulsive potentials, more retention was observed at the higher velocity. It would therefore be expected that increases in local velocity at conditions where the repulsive potential is high would result in increases in collection efficiency. At low repulsive potentials, it would be expected that increases in local velocity would cause the collection efficiency to decrease. If local velocity changes are the dominant effect of compression, the collection efficiency may increase or decrease, depending on the colloidal state of the system.

Retention Area

The retention area can be defined as the fiber surface area available for retention. The visual observations have shown that the retention area is quite complex and very important in the wood pulp fiber system. This is due to the fibrillar nature of wood pulp fibers. There are two major problems involved with this variable. The first problem is how to describe it in terms of measurable areas such as the fiber projected area or the hydrodynamic surface area. It is probably more closely related to the hydrodynamic surface area. The second problem is that to date there is no way to predict how the retention

area varies with the state of compression in the pad. The functional relationship between retention area and compressibility could be quite complex. As the pad is compressed, more fibers are brought into contact with each other. This results in additional areas into which flow is denied; hence, less area available for retention. The mechanisms of fiber deformation and contact in compressible pads are not fully understood, making it impossible to be very specific about changes in retention area. In general, it may be postulated that retention area should decrease as the state of compression increases. If loss of retention area is the dominant effect of compression, then the collection efficiency should decrease with increasing pulp mass, m.

Determination of Collection Efficiency

The retention rate may be expressed in terms of the collection efficiency in the following manner:

$$\phi = ES\rho_w U_o s(P_{oo} - P'). \tag{23}$$

The retention rate is also given by

$$\phi = s\rho_w A U_o \frac{dP'}{dm} . \tag{24}$$

Therefore,

$$s\rho_w A U_o \frac{dP'}{dm} = ES\rho_w U_o (P_{oo} - P') \tag{25}$$

or

$$A \frac{dP'}{dm} = ES(P_{oo} - P'). \tag{26}$$

Rearranging,

$$\frac{ES}{A} = \frac{dP'/dm}{P_{oo} - P'} . \tag{27}$$

In the above equations, $\underline{A}$ is the cross-sectional area of the mat, which is a constant; $\underline{S}$ is the fiber specific surface. This quantity should be related to the retention area and has always been assumed a constant. These terms will be lumped with the collection efficiency to give a pseudocollection efficiency, $\underline{E}'$, which should be proportional to $\underline{E}$.

$$E' = \frac{ES}{A} = \frac{dP'/dm}{P_{oo} - P'} \tag{28}$$

Thus, $d\underline{P}'/d\underline{m}$ is the slope of the bound particle distribution curve. $(\underline{P}_{oo} - \underline{P}')$ is the free particle concentration. These quantities may be determined from the bound particle distribution for any value of the mass of pulp accumulated, $\underline{m}$. This procedure allows the changes in the pseudocollection efficiency to be determined throughout the pad. These changes should be interpretable in terms of the compressibility effects discussed previously.

The major problem involved in this procedure is the accuracy with which $\underline{E}'$ may be determined. This method of determining changes in the pseudocollection efficiency has a great deal of uncertainty involved in its calculation due to several reasons.

The first reason for the error is the uncertainty involved in the determination of the slope of the bound particle distribution curve, $d\underline{P}'/d\underline{m}$. In determining this slope, problems are encountered near the top of the pad, $\underline{m} = 0$. The initial value of the bound particle distribution, $\underline{P}_o$, is obtained by extrapolation of the curve to $\underline{m} = 0$. Many times, as in Fig. 6 and 7, the slope is changing rapidly and the extrapolation is very difficult to make with certainty. Thus, the slopes at the top of the pad are subject to considerable error. The problem is reversed at the opposite end of the pad, the septum end. Here the slope may be changing very slowly, as also seen in Fig. 6 and 7. This small change in slope is also difficult to quantify.

The second reason for the error involved in $\underline{E}'$ has to do with the uncertainty of the ratio of titanium dioxide to pulp added initially, $\underline{P}_{\underline{oo}}$. This quantity was determined by adding a slurry of titanium dioxide to 100 liters of an aqueous suspension of fibers. Inherent in this quantity is the uncertainty in the concentration of the titanium dioxide slurry and the uncertainty in the mass of pulp used in the filtration. This is essentially a gravimetric procedure. The actual bound particle concentration, $\underline{P}'$, is determined by a combination of a gravimetric and colorimetric procedure. There is, therefore, an error involved in determining the two quantities by two different methods. All of these errors have been lumped into the $\underline{P}_{\underline{oo}}$ error and it is estimated to be ± 5% based on calculated errors in pulp weight and slurry concentration determinations by gravimetric and colorimetric methods.

The error involved in $\underline{P}_{\underline{oo}}$ can result in a significant error in $\underline{E}'$ as $\underline{P}'$ approaches $\underline{P}_{\underline{oo}}$. This occurs at the septum end of the pads. The values of $\underline{E}'$ near the septum have the largest percent error involved in them.

In spite of the problems encountered in the calculation of $\underline{E}'$, it was felt that some trends in the data could be established and the results qualitatively explained. A complete discussion of the method of calculating $\underline{E}'$ and the determining of the error involved in the calculation can be found in Appendix VI.

Determination of the State of Compression

In order to investigate the effects of compressibility on collection efficiency, a method was needed for determining the specific state of compression of the pad at various amounts of pulp accumulated. This was accomplished by applying the static compressibility function [Equation (13)]

using the recorded pressure drop across the pad. The pressure was continuously recorded during each filtration run. From this equation and the relationship between mass of pulp accumulated, $\underline{m}$, and filtration time, $\underline{t}$, it was possible to determine the relationship between the state of compression of the pad, $\underline{c}$, and the mass of pulp accumulated, $\underline{m}$. Details of this procedure are given in Appendix VII.

RESULTS AND DISCUSSION OF COMPRESSIBILITY EFFECTS

Figures 21 and 22 show the calculated values of the pseudocollection efficiency for the pads formed from the Type 2 pulp at both 1 and 2 cm./sec. The details of the calculation can be found in Appendix VI. The estimated error in the pseudocollection efficiency is also shown in the figures. As previously discussed, the range of uncertainty can be large. Most of it occurs due to the uncertainty in the initial ratio of titanium dioxide to pulp, $\underline{\underline{P_{oo}}}$.

The approximate states of compressions are also given in the figures. A discussion of the compressibility determinations can be found in Appendix VII.

Due to the large uncertainty in the pseudocollection efficiency, $\underline{E'}$, the results shown in these figures are not amenable to definitive quantitative treatment, and in some instances are only indicative of trends. The interpretation of these results is based on the assumption that the pseudocollection efficiency can be dominated by different local variables at different states of compression.

As seen in Fig. 21, the pseudocollection efficiency increases throughout these four pads. The changes in local variables in these pads are not as pronounced as the changes of the local variables in the pads formed at 2 cm./sec.

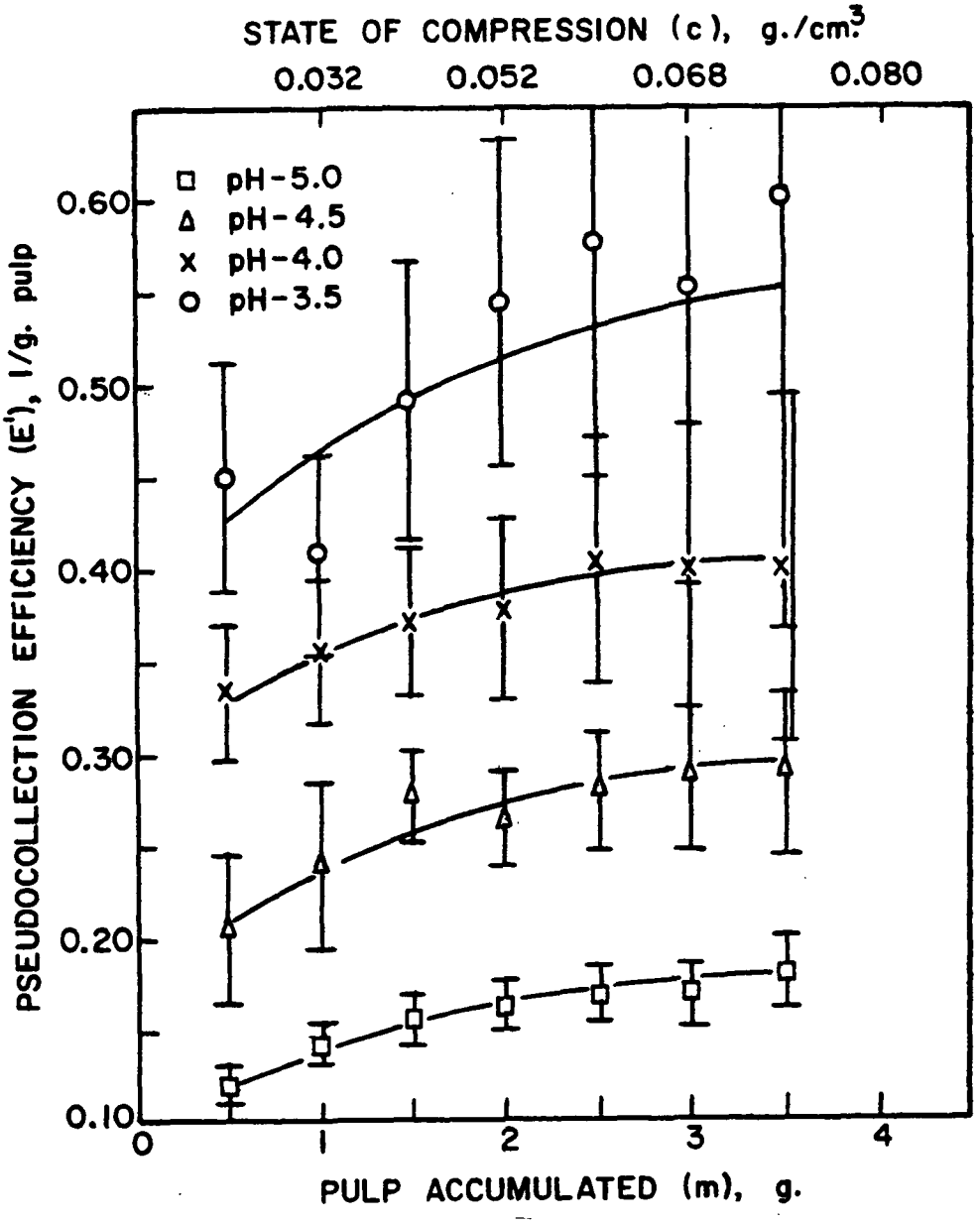


Figure 21. Pseudocollection Efficiencies for Pads Formed at 1 cm./sec.

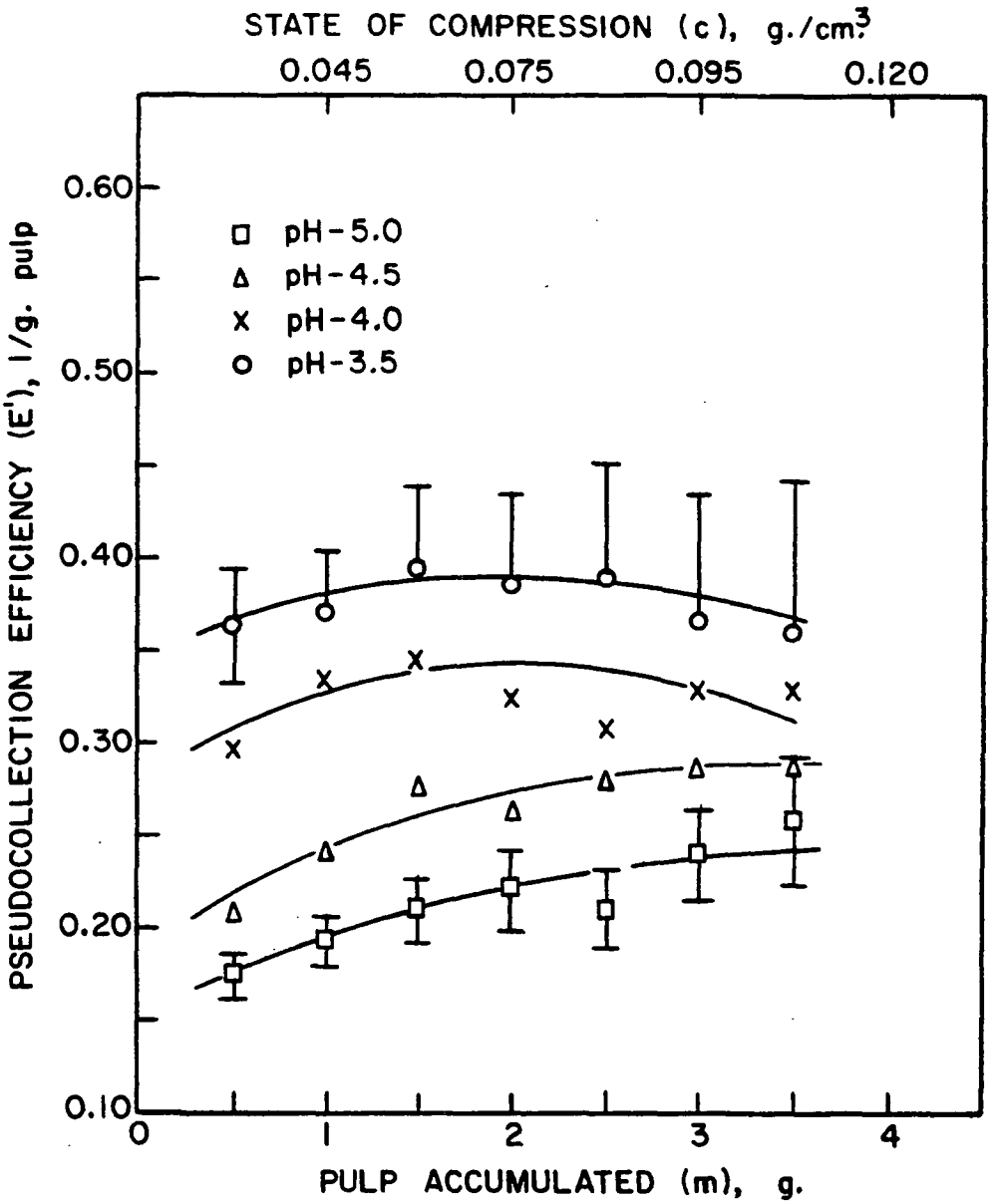


Figure 22. Pseudocollection Efficiencies for Pads Formed at 2 cm./sec.

Over the range of compression experienced by the 1-cm./sec. pads, the local velocity and retention area probably do not change appreciably. It is believed that over the range of compression for these pads, an apparent decrease in pore sizes is the dominant variable causing the pseudocollection efficiency to increase.

In Fig. 22, the pseudocollection efficiency continuously increases at pH's 5.0 and 4.5. At pH's 4.0 and 3.5, there is an increase of the pseudocollection efficiency in the lower layers. The interpretation of this result is based on the fact that the 2-cm./sec. pads have a larger range of compression than the 1-cm./sec. pads.

The initial increase in the pseudocollection efficiency for all of the pads is interpreted similarly to the 1-cm./sec. pads. That is, the dominance of the pore size decreases on the pseudocollection efficiency. This increase occurs over approximately the same range of compression as the 1-cm./sec. pads experienced.

The lower sections of the pad show continued increases in pseudocollection efficiency at pH's 5.0 and 4.5 but decreases at pH's 4.0 and 3.5. It is believed that over these ranges of compression the retention area decreases are beginning to become significant. The difference in the results can be explained in the following manner.

At pH's 5.0 and 4.5, a significant repulsive barrier exists. The amount of retention is low and the rate should be controlled primarily by the ability of the particle to cross the repulsive barrier. For this situation, both the increase in local velocity and the decrease in pore size caused by the increasing state of compression should tend to increase the pseudocollection efficiency.

The decrease in retention area due to compression should tend to decrease the pseudocollection efficiency. The observed result can be interpreted as, over this range of compression, the decreasing pore size and increasing local velocity have more effect in increasing the pseudocollection efficiency than the decreasing retention area.

In contrast to the above situation is the system at pH's 4.0 and 3.5. The repulsive potential is now low and the rate should be controlled less by the colloidal state of the system. Increases in local velocity should now have little or adverse effects on the retention rate. Therefore, at these higher states of compression and under favorable flocculating conditions, both the local velocity changes and the retention area changes are acting to decrease the pseudocollection efficiency while only the pore size decrease is acting to increase it. The observed result is interpreted as the dominance of the local velocity and retention area causing the pseudocollection efficiency to decrease.

In summary, it appears that at low states of compression the pore size changes dominate the changes in pseudocollection efficiency causing it to increase. At higher states of compression, the surface area decrease may become the dominating variable causing the pseudocollection efficiency to decrease. The local velocity changes may obscure the surface area effects under poor flocculating conditions, or may aid the surface area effects under good flocculating conditions.

A final look at compressibility effects may be obtained by examining the pseudocollection efficiency of a Type 3 pulp used in the removal experiments. At a given filtration velocity and mass of pulp, these pads will be at a much

higher state of compression than the Type 2 pulp used above. This is due to the treatment of the pulp in the British disintegrator.

Figure 23 shows the values of the pseudocollection efficiencies from the distribution curves given in Fig. 6 and 7. The details of these filtrations are given in the removal section. The pads were formed under good flocculating conditions at 1-cm./sec. forming velocity. The approximate states of compression are also given in the figure. It should be noted that the state of compression of these pads at 1-g. accumulated pulp is higher than the state of compression of the entire pads formed at 1 cm./sec. of the Type 2 pulp. This means that all the compressibility changes observed in Fig. 21 are occurring in the extreme top of these pads. Any initial increase in the pseudocollection efficiency has been obscured because of the rapid increase in the state of compression for these pads.

The observed decreases in the pseudocollection efficiences in these pads are outside the range of the error limits and may be considered significant changes. These decreases are in keeping with the interpretations for the compressibility effects for the Type 2 pulp. The decreases in the pseudocollection efficiency may be attributed to the dominance of increases in local velocity and decreases in retention area. Both of these variables should undergo significant changes at these very high states of compression.

This section has presented evidence that the compressibility effects on the pseudocollection efficiency are complex. The compressibility effect depends on the colloidal state of the system and the range of compressibility changes encountered in the pad. The pseudocollection efficiency was observed to both increase and decrease with increasing states of compression. These changes are interpretable in terms of the local variables — pore size, velocity, and retention area.

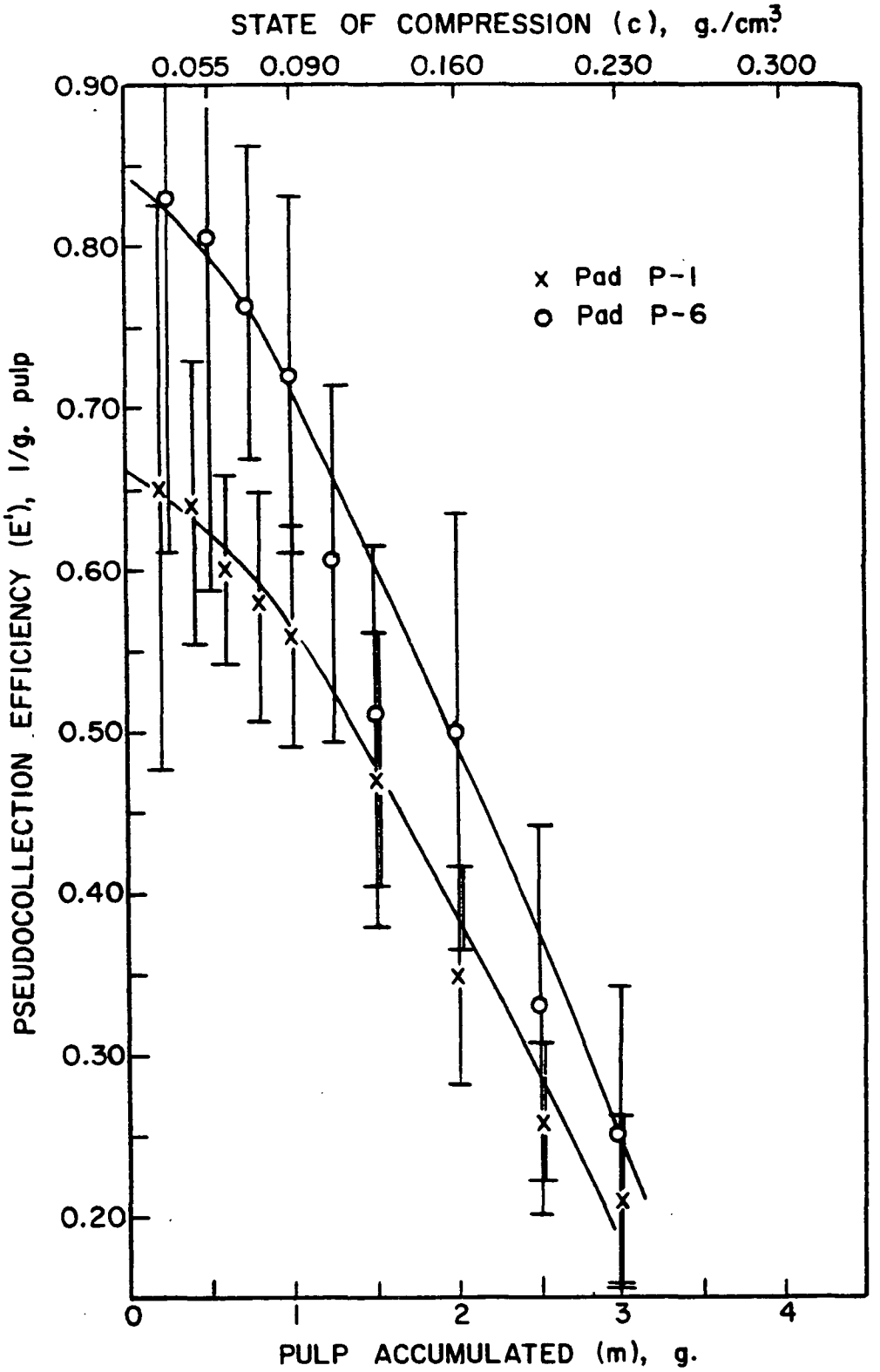


Figure 23. Pseudocollection Efficiencies for Pads Formed at 1 cm./sec., Type 3 Pulp

# CONCLUSIONS

For this system at constant colloidal conditions and over the shear ranges employed, no significant amounts of removal of bound particles were observed. Microscopic observations showed that individual particle removal was insignificant. These observations also showed that the major removal mechanism was the loss of fiber fragments with particles attached. It was concluded that the titanium dioxide-fiber bond was strong enough to withstand the shear forces encountered in this study. These bonds appear to be stronger than the bonds in certain sections of the fiber wall. Filtration experiments were used to quantitatively test for particle removal. No significant loss or redistribution of titanium dioxide could be determined in the experiments. Over this limited range of experimental variables, the retention process can be considered irreversible at constant colloidal conditions. The removal of bound particles, however, was found to be sensitive to colloidal environment. By restoring the repulsive potentials of the system, the particles were readily removed from the fiber surface. This effect was attributed to the repeptization phenomenon.

Visual observations of wood pulp fibers being permeated by suspensions of titanium dioxide have also shown the complexity of the attachment process. The fibrillar nature of the wood pulp fiber makes the flow patterns about it very complex. These fibrils, which extend from the fiber surface, act as excellent collectors of particles.

The previous concept of a collection efficiency composed of a separable collision probability and adhesion probability has been found to be inadequate in describing the attachment process for this system. An interrelationship between the colloidal variables and hydrodynamic variables was proposed to

explain this observation. The interrelationship was visualized as occurring through the kinetic energy of the particles.

Variations in a defined pseudocollection efficiency within individual pads were also observed. These variations were attributed to compressibility effects. Depending on the colloidal conditions, the pseudocollection efficiency increased with increasing compression at low states of compression and decreased when the pad was highly compressed. The results could be qualitatively explained by changes in local values of pore size, velocity, and retention area.

## NOMENCLATURE

$A$ = area of pad, cm.$^2$

$a$ = radius of fibers, cm.

$c$ = state of compression or pad density, g./cm.$^3$

$D$ = diffusion coefficient of a particle, cm.$^2$/sec.

$d$ = diameter of particles, cm.

$E$ = collection efficiency

$E'$ = pseudocollection efficiency, 1/g.

$F$ = resultant force on particle, g./cm. sec.$^2$

$f_i$ = parameter in general expression of colloidal forces

$J$ = energy dissipation term, g. cm.$^2$/sec.$^2$

$K$ = rate constant, 1/sec.

$k$ = Boltzmann's constant, $1.380 \times 10^{-16}$ ergs/deg.

$L$ = distance from septum to mat surface, cm.

$M$ = empirical constant in compressibility equation

$M_T$ = total mass of fibers in pad, g.

$m$ = fiber mass coordinate, cumulative from surface, g.

$m_i$ = mass of fibers in $i$th layer, g.

$m_p$ = mass of particle, g.

$N$ = empirical constant in compressibility equation

$n_i$ = parameter in general expression of colloidal forces

$P$ = free particle concentration, g. particles/g. fluid

$P'$ = bound particle concentration, g. particles/g. fiber

$P_o$ = free particle concentration in suspension

$P_o'$ = prepad retention; bound particle concentration in suspension

$P_{oo}$ = initial particle concentration, g. particles/g. fiber

$p$ = pressure, dynes/cm.$^2$

$Q$ = maximum energy of interaction between colloidal particles, g. cm.$^2$/sec.$^2$

$R$ = minimum energy of interaction between colloidal particles, g. cm.$^2$/sec.$^2$

$r$ = distance between colloidal particles, cm.

$S$ = fiber specific surface, cm.$^2$/g.

$s$ = consistency, g. fibers/g. fluid

$T$ = absolute temperature, °K

$T_i$ = total mass of particles in $i$th layer, g.

$T_T$ = total time of filtration, sec.

$t$ = elapse time in filtration, sec.

$U_o$ - forming velocity, cm./sec.

$U_f$ = fiber superficial velocity, cm./sec.; fiber flux in suspension, cm./sec.

$U_w$ = fluid superficial velocity, cm./sec./ fluid flux in suspension, cm./sec.

$u$ = local fluid velocity, cm./sec.

$V_f$ = fluid streamline velocity about fiber, cm./sec.

$V_p$ = particle velocity in vicinity of fiber, cm./sec.

$V_o$ = approach velocity of particle to fiber, cm./sec.

$W_i$ = total mass of particles and fiber in $i$th layer, g.

$Z$ = position coordinate from septum, cm.

$\alpha$ = colloidal probability of particle adhering to fiber surface

$\beta$ = hydrodynamic probability of particle colliding with fiber surface

$\varepsilon$ = porosity in pad

$\varepsilon'$ = porosity in suspension

$\mu$ = fluid viscosity, g./cm. sec.

$\rho_f$ = fiber density, g./cm.$^3$

$\rho_w$ = fluid density, g./cm.$^3$

$\Psi$ = slope of bound particle distribution curve

## ACKNOWLEDGMENTS

The author wishes to acknowledge the guidance extended to him by his Thesis Advisory Committee: Dr. Thomas M. Grace (Chairman), Dr. Dale G. Williams, and Mr. Nai L. Chang.

Appreciation is also expressed for the helpful discussions of other faculty members and the valuable assistance given by many of the Institute staff members. Special recognition is due to the U. S. Forest Products Laboratory, Madison, Wisconsin, for providing the Scanning Electron Micrographs.

Finally, my sincere gratitude to my wife, Harriette, who has patiently waited for her tree.

## LITERATURE CITED


1. Libby, C. E. Pulp and paper science and technology. Vol. II. p. 85. New York, McGraw-Hill, 1962.

2. Brill, H. C., Tappi 38:522 (1955).

3. Weiner, J., and Byrnes, J. Retention of fillers by papermaking fibers. Supplement I. Bibliographic Series 186. Appleton, Wis., The Institute of Paper Chemistry, 1965.

4. Groen, L. J. Formation and structure of paper. Vol. II. p. 697. London, Tech. Sect. Brit. Paper and Board Makers' Assocn., 1962.

5. Steenberg, B. Formation and structure of paper. Vol. II. p. 740. London, Tech. Sect. Brit. Paper and Board Makers' Assocn., 1962.

6. Haslam, J. H., and Steele, F. A., Tech. Assoc. Papers 19:249 (1936).

7. Jirgensons, B., and Straumanis, M. E. A short textbook of colloid chemistry. 2d ed. p. 14. New York, Macmillan, 1962.

8. Mason, S. G., Tappi 33:413 (1950).

9. Williams, D. G., and Swanson, J. W., Tappi 49:147 (1966).

10. Han, S. T., Tappi 47:782 (1964).

11. Johnson, R. C., Tappi 46:304 (1963).

12. Grace, T. M. Unpublished work, 1968.

13. Nelson, R. W., Tappi 47:752 (1964).

14. Williams, D. G. Unpublished work, 1965.

15. Webb, J. T. An investigation of electric-double-layer concepts and colloidal stability of titanium dioxide dispersions. Doctor's Dissertation. Appleton, Wis., The Institute of Paper Chemistry, 1971. 231 p.

16. Han, S. T., and Chang, N. L., Tappi 42:688 (1969).

17. Walkush, J. C. The coagulation of cellulose pulp fibers and fines as a mechanism of retention. Doctor's Dissertation. Appleton, Wis., The Institute of Paper Chemistry, 1970. 202 p.

18. Kruyt, H. R., ed. Colloid science. Vol. 1. New York, Elsevier, 1952.

19. Glasstone, S. Textbook of physical chemistry. 2d ed. p. 261. New York, D. Van Nostrand, 1946.

20. Labrecque, R. P. An investigation of the effects of fiber cross-sectional shape on the resistance to the flow of fluids through fiber mats. Doctor's Dissertation. Appleton, Wis., The Institute of Paper Chemistry, 1967. 94 p.

21. Meyer, H. Unpublished work, 1969.

22. Verwey, E. J. W., and Overbeek, J. Th. G. Theory of the stability of lyophobic colloids. New York, Elsevier, 1948.

23. Ingmanson, W. L. An investigation of the mechanism of water removal from pulp slurries. Doctor's Dissertation. Appleton, Wis., The Institute of Paper Chemistry, 1951. 119 p.

24. Lapinoja, V. M. Study of changes in cellulose fine structure in the wet state during tracheid wall component removal by sodium chlorite pulping. Doctor's Dissertation. Appleton, Wis., The Institute of Paper Chemistry, 1972. 195 p.

25. Beckman Instruments, Inc. Model DB Spectrophotometer Instruction Manual S66-D. Fullerton, Calif., 1963.

# APPENDIX I

## DERIVATION OF RETENTION EQUATIONS

The following is a derivation of the general retention equations adapted from the method used by Grace (12).

Assume that a fiber mat is being formed on a supporting septum from a system consisting of fibers, particles, and water. A spatial coordinate, $z$, can be defined with its origin at the septum. The mat grows in the plus $z$ direction. The process is assumed homogeneous in the other two space directions.

The retention rate, $\phi$, can be defined as the net mass rate of particles becoming bound per unit mass of fibers. The dimensions of $\phi$ are mass of particles/(time x mass of fiber), or time$^{-1}$. With the retention rate describing the interchange between free and bound particles, differential material balances for fiber, water, free particles, and bound particles can be formulated.

Application of the principle of conservation of mass to an incremental thickness of the mat results in the following equations.

$$\frac{\partial}{\partial z} \rho_f U_f = \frac{\partial}{\partial t} \rho_f (1 - \varepsilon) \tag{29}$$

$$\frac{\partial}{\partial z} \rho_w U_w = \frac{\partial}{\partial t} \rho_w \varepsilon \tag{30}$$

$$\frac{\partial}{\partial z} \rho_w U_w P = \frac{\partial}{\partial t} \rho_w \varepsilon P + \rho_f (1 - \varepsilon)\phi \tag{31}$$

$$\frac{\partial}{\partial z} \rho_f U_f P' = \frac{\partial}{\partial t} \rho_f (1 - \varepsilon)P' - \rho_f (1 - \varepsilon)\phi \tag{32}$$

where

$\rho_f$ = fiber density,

$\rho_w$ = fluid density (water),

$U_f$ = superficial fiber velocity,

$U_w$ = superficial fluid velocity,

$\varepsilon$ = interfiber porosity,

$P$ = free particle concentration, mass/mass,

$P'$ = bound particle concentration, mass/mass,

$\phi$ = retention rate,

$t$ = time, and

$z$ = position up from septum.

Equation (29) can be substituted into Equation (32) to yield

$$\rho_f U_f \frac{\partial P'}{\partial z} = \rho_f(1 - \varepsilon) \frac{\partial P'}{\partial t} \rho_f(1 - \varepsilon)\phi \tag{33}$$

and Equation (30) can be substituted into Equation (31) to give

$$\rho_w U_w \frac{\partial P}{\partial z} = \rho_w \varepsilon \frac{\partial P}{\partial t} + \rho_f(1 - \varepsilon)\phi. \tag{34}$$

If the two densities are constant (a reasonable assumption), Equations (29) and (30) can be combined to yield

$$\frac{\partial}{\partial z} (U_w + U_f) = 0 \tag{35}$$

with the solution,

$$U_w + U_f = U_o (t). \tag{36}$$

$U_o$ can be interpreted to be the forming velocity and is at most a function of time.

Since fiber mats are in general compressible ($\varepsilon$ not constant), a fixed coordinate system is not very useful since it does not correspond to a specific layer in the mat. It is desirable to transform the retention equation to a

coordinate system based on the mat itself. Nelson (13) has developed a convenient coordinate system based on the cumulative mass of fiber from the upper surface of the mat. This coordinate, m, is defined in the following manner:

$$m = \rho_f A\int_z^L (1 - \varepsilon)dz' = \rho_f A\{\int_o^L (1 - \varepsilon)dz' - \int_o^z (1 - \varepsilon)dz'\} \tag{37}$$

where L(t) is the thickness of the mat at time t, and A is the area of the mat.

In order to transform the continuity equations from z-t coordinate system to the m-t coordinate system, the following transformation relations are required:

$$\frac{\partial}{\partial z} \rightarrow \left(\frac{\partial m}{\partial z}\right)_t \frac{\partial}{\partial m} = -\rho_f(1 - \varepsilon)A \frac{\partial}{\partial m} \tag{38}$$

$$\frac{\partial}{\partial t} \rightarrow \left(\frac{\partial m}{\partial t}\right)_z \frac{\partial}{\partial m} + \frac{\partial}{\partial t} = \rho_f A \left[\frac{\partial}{\partial t} \int_o^L (1 - \varepsilon)dz - U_f + U_{f_o}\right] \frac{\partial}{\partial m} + \frac{\partial}{\partial t}. \tag{39}$$

An overall fiber balance on the mat is used to determine the quantities within the brackets of Equation (39).

The fiber consistency, s, is defined as the mass of fiber per unit mass of fluid in the suspension. The fiber flux in the suspension is

$$\rho_f U_f' = s\rho_w U_w'. \tag{40}$$

If it is assumed that the suspension flows without slip, the porosity in the suspension is given by

$$\varepsilon' = \frac{U_w'}{U_o} = 1 - \frac{U_f'}{U_o} = \frac{\rho_f}{\rho_f + s\rho_w} \tag{41}$$

and the fiber flux in the suspension is

$$\rho_f U_f' = \frac{s\rho_w \rho_f U_o}{\rho_f + s\rho_w} . \tag{42}$$

To be perfectly rigorous, the suspension fiber flux which should be used in the overall fiber balance is the flux relative to the surface of the mat. In that case, $\underline{U}_o$ is replaced in Equation (42) by $\underline{U}_o + (d\underline{L}/d\underline{t})$. However, $d\underline{L}/d\underline{t}$ cannot be determined without a detailed knowledge of the porosity in the mat. For any reasonable suspension consistency, $d\underline{L}/d\underline{t}$ will be very small compared to $\underline{U}_o$, and can thus be neglected.

The overall fiber balance on the mat is

$$\frac{s\rho_w\rho_f U_o}{\rho_f + s\rho_w} - \rho_f U_{f_o} = \frac{d}{dt}\int_o^L \rho_f(1-\varepsilon)dz. \tag{43}$$

Substituting (43) into Equation (39) yields

$$\frac{\partial}{\partial t} \rightarrow \rho_f A\left[\frac{s\rho_w U_o}{\rho_f + s\rho_w} - U_f\right]\frac{\partial}{\partial m} + \frac{\partial}{\partial t}. \tag{44}$$

Transforming Equations (33) and (34) gives

$$-\rho_f{}^2 U_f(1-\varepsilon)A\frac{\partial P'}{\partial m} = \rho_f{}^2(1-\varepsilon)A\left[\frac{s\rho_w U_o}{\rho_f+s\rho_w} - U_f\right]\frac{\partial P'}{\partial m} + \rho_f(1-\varepsilon)\frac{\partial P'}{\partial t} - \rho_f(1-\varepsilon)\phi \tag{45}$$

$$-\rho_w U_w \rho_f(1-\varepsilon)A\frac{\partial P}{\partial m} = \rho_w\varepsilon\rho_f A\left[\frac{s\rho_w U_o}{\rho_f+s\rho_w} - U_f\right]\frac{\partial P}{\partial m} + \rho_w\varepsilon\frac{\partial P}{\partial t} + \rho_f(1-\varepsilon)\phi. \tag{46}$$

Rearranging Equations (45) and (46) gives

$$-\rho_w A\left[U_o - \frac{U_f}{1-\varepsilon} + \frac{\varepsilon}{1-\varepsilon}\frac{s\rho_w U_o}{\rho_f+s\rho_w}\right]\frac{\partial P}{\partial m} = \frac{\rho_w\varepsilon}{\rho_f(1-\varepsilon)}\frac{\partial P}{\partial t} + \phi \tag{1}$$

$$\frac{s\rho_w\rho_f A U_o}{\rho_f + s\rho_w}\frac{\partial P'}{\partial m} + \frac{\partial P'}{\partial m} = \phi. \tag{2}$$

These last two equations are the retention equations.

## APPENDIX II

## APPLICATION OF THE RETENTION EQUATIONS TO A CONSTANT-RATE FILTRATION

The two retention equations are

$$-\rho_w A \left[ U_o - \frac{U_f}{1-\varepsilon} + \frac{\varepsilon}{1-\varepsilon} \frac{s\rho_w U_o}{\rho_f + s\rho_w} \right] \frac{\partial P}{\partial m} = \frac{\rho_w \varepsilon}{\rho_f (1-\varepsilon)} \frac{\partial P}{\partial t} + \phi \tag{1}$$

$$\frac{s\rho_w \rho_f A U_o}{\rho_f + s\rho_w} \frac{\partial P'}{\partial m} + \frac{\partial P'}{\partial t} = \phi. \tag{2}$$

In a constant-rate filtration ($U_o$ = constant), the mat-forming process occurs simultaneously with the retention process. The mat is formed from a suspension containing fluid, fibers, and particles. Thus, $s$ has some finite value. If $s$ is small compared to the consistency of the mat, then

$$U_f \ll U_o \tag{47}$$

$$\frac{\varepsilon s\rho_w U_o}{(1-\varepsilon)(\rho_f + s\rho_w)} \ll U_o \tag{48}$$

and

$$\frac{s\rho_w}{\rho_f + s\rho_w} \approx \frac{s\rho_w}{\rho_f}. \tag{49}$$

For this case, Equations (1) and (2) reduce to

$$-\rho_w A U_o \frac{\partial P}{\partial m} = \frac{\rho_w \varepsilon}{\rho_f (1-\varepsilon)} \frac{\partial P}{\partial t} + \phi \tag{50}$$

and

$$s\rho_w A U_o \frac{\partial P'}{\partial m} + \frac{\partial P'}{\partial t} = \phi \tag{51}$$

with the boundary conditions $P = P_o$ atm = 0, and $P' = P_o'$ atm = 0 for all times $t$. There is no initial condition since the mat does not exist until $t > 0$.

Since the suspension contains particles and fibers, retention by cofloculation can take place in suspension before the mat is formed. $\underline{P_o}$ and $\underline{P_o}'$ represent the free and bound particle concentrations, respectively, in the suspension. These are concentrations which exist at the surface of the mat.

If $\underline{P_o}$ and $\underline{P_o}'$ are constants and if the mat is considered to be in successive equilibrium states of compression, $\phi$ would be nearly independent of time at a given $\underline{m}$. For this case, Equations (51) and (50) simplify to

$$s\rho_w AU_o \frac{dP'}{dm} = \phi \tag{3}$$

and

$$-\rho_w AU_o \frac{dP}{dm} = \phi. \tag{4}$$

Combining Equations (3) and (4) gives

$$\frac{d}{dm}(P + sP') = 0. \tag{5}$$

Therefore,

$$P + sP' = sP_{oo} \tag{6}$$

which states at any $\underline{m}$, the sum of the free and bound particles concentration equals the initial concentration. At $\underline{m} = 0$,

$$P_o + sP_o' = sP_{oo}. \tag{52}$$

# APPENDIX III

## DETERMINATION OF TITANIUM DIOXIDE ON THE BECKMAN DB SPECTROPHOTOMETER

The following procedure was used to determine the amount of titanium dioxide in each layer split from the pulp pads. Titanium dioxide can be dissolved in a mixture of concentrated sulfuric acid and ammonium sulfate. Addition of hydrogen peroxide to this solution gives a yellow color which permits the concentration to be determined by measurement of the absorbance of the solutions. The details of this procedure and the preparation of the standards are given below.

One-half gram of titanium dioxide was accurately weighed into a 150-ml. beaker. Forty grams of ammonium sulfate and 50 ml. of concentrated sulfuric acid were added. The beaker was covered with a watch glass and heated on a hot plate until all solids dissolved. The contents were then quantitatively transferred to a 500-ml. volumetric flask and diluted to the mark with distilled water. Aliquots of this stock solution were placed in 50-ml. volumetric flasks and diluted to the 50 ml. with 10% sulfuric acid to form the working titanium dioxide standards. Nine standards were prepared, using 1, 2, 3, 4, 5, 7, 10, 12, and 15 ml., respectively, of the stock solution.

A blank solution was prepared by placing 5 ml. of the titanium dioxide stock solution in a 100-ml. volumetric flask and diluting it to the mark with 10% sulfuric acid. An acidic hydrogen peroxide solution was prepared by diluting 100 ml. of 35% hydrogen peroxide to 1 liter with 10% sulfuric acid. Ten ml. of each of the standards were pipeted into separate 25-ml. volumetric flasks and each filled to the mark with acidic hydrogen peroxide solution. The color intensity of each of the solutions was measured using the Beckman DB (25) at 407 nm. with the blank solution in the reference cell. A reference curve was

prepared by plotting the absorbance of each of the standards against its concentration in mg./liter.

The actual samples obtained from the pad splits were ashed and the ash dissolved in 2.5 ml. of sulfuric acid and 2 grams of ammonium sulfate. The dissolved titanium dioxide was transferred to a 25-ml. volumetric flask and diluted to the mark with distilled water. Five-ml. aliquots of each of the samples were placed in another 25-ml. volumetric flask and diluted to the mark with the acidic hydrogen peroxide solution. The absorbance of each of the samples was then read on the Beckman DB, using the same blank as was used on the standards. From the standard reference curve, the concentration of each of the samples could be obtained and the amount of titanium dioxide in each layer of the pad calculated.

# APPENDIX IV

## GENERATION OF BOUND PARTICLE DISTRIBUTION

Bound particle distributions are defined by determining $\underline{P}'$ as a function of $\underline{m}$, the accumulated mass of the pad. Experimentally, the quantities actually measured are the mass of particles plus pulp in a given layer, $\Delta\underline{W}_{\underline{i}}$, and the mass of particles in a given layer, $\Delta\underline{T}_{\underline{i}}$, where $\underline{i}$ denotes the $\underline{i}$th layer in the pad. The mass of pulp in a given layer was then given by

$$\Delta m_i = \Delta W_i - \Delta T_i . \tag{53}$$

It was then assumed that in each smaller layer the bound particle distribution was linear. The bound particle distribution could then be generated in the following manner.

$$P_i' = \Delta T_i / \Delta m_i \tag{54}$$

$$m_i = \sum_{i=1}^{i} \Delta m_{i-1} + \Delta m_i / 2. \tag{55}$$

# APPENDIX V

## BOUND PARTICLE DISTRIBUTION DATA

This appendix contains the details of the filtration for each pad, including the final bound particle distribution obtained.

TABLE I

FILTRATION CONDITIONS AND BOUND PARTICLE DISTRIBUTIONS FOR PADS P-1 THROUGH P-25

Data for Pads P-1, P-2, and P-5

Pads P-1, P-2, and P-5 were formed from the same suspension of $TiO_2$ and pulp. Details of the filtration are given below.

Pad P-1

Conditions:

Pulp Type = 3
Initial Ratio, $TiO_2$ to Pulp ($\underline{P}_{oo}$) = 0.050
pH of Suspension = 2.8
Mix Time of Suspension in Tank = 15 min.
Filtration Time = 850 sec.
Forming Velocity = 1 cm./sec.
Treatment of Pad After Formation = None

BOUND PARTICLE DISTRIBUTION PAD P-1

| Bound Particle Concentration, $\underline{P}'$, g. $TiO_2$/g. pulp | Mass Pulp Accumulated, $\underline{m}$, g. pulp |
|---|---|
| 0.0056 | 0.15 |
| 0.0124 | 0.40 |
| 0.0177 | 0.67 |
| 0.0236 | 0.99 |
| 0.0279 | 1.27 |
| 0.0300 | 1.50 |
| 0.0324 | 1.71 |
| 0.0333 | 1.98 |
| 0.0353 | 2.24 |
| 0.0356 | 2.48 |
| 0.0366 | 2.73 |
| 0.0374 | 3.12 |
| 0.0384 | 3.42 |

Pad P-2

Conditions:

Pulp Type = 3
Initial Ratio, $TiO_2$ to Pulp ($\underline{P}_{oo}$) = 0.050
pH of Suspension = 2.8
Mix Time of Suspension in Tank = 36 min.
Filtration Time = 530 sec.
Forming Velocity = 1 cm./sec.
Treatment of Pad After Formation = None

BOUND PARTICLE DISTRIBUTION PAD P-2

| Bound Particle Concentration, $\underline{P}'$, g. $TiO_2$/g. pulp | Mass Pulp Accumulated, $\underline{m}$, g. pulp |
|---|---|
| 0.0040 | 0.08 |
| 0.0085 | 0.25 |
| 0.0159 | 0.50 |
| 0.0224 | 0.79 |
| 0.0260 | 1.07 |
| 0.0301 | 1.44 |
| 0.0320 | 1.78 |
| 0.0332 | 2.05 |
| 0.0334 | 2.40 |

Pad P-5

Conditions:

Pulp Type = 3
Initial Ratio, $TiO_2$ to Pulp ($\underline{P}_{oo}$) = 0.050
pH of Suspension = 2.8
Mix Time of Suspension in Tank = 59 min.
Filtration Time = 750 sec.
Forming Velocity = 1 cm./sec.
Treatment of Pad After Formation = 10 min. of Permeation of the Pad at 1 cm./sec. pH of permeating fluid was the same as formation.

BOUND PARTICLE DISTRIBUTION PAD P-5

| Bound Particle Distribution, $\underline{P}'$, g. $TiO_2$/g. pulp | Mass Pulp Accumulated, $\underline{m}$, g. pulp |
|---|---|
| 0.0065 | 0.11 |
| 0.0142 | 0.40 |
| 0.0209 | 0.70 |
| 0.0259 | 0.97 |
| 0.0294 | 1.25 |
| 0.0317 | 1.55 |
| 0.0334 | 1.89 |
| 0.0346 | 2.21 |
| 0.0367 | 2.52 |
| 0.0364 | 2.86 |
| 0.0377 | 3.24 |
| 0.0394 | 3.55 |

Data for Pads P-3 and P-4

Pads P-3 and P-4 were formed from the same suspension of $TiO_2$ and pulp. Details of the filtration are given below.

Pad P-3

Conditions:

Pulp Type = 1
Initial Ratio, $TiO_2$ to Pulp ($\underline{P}_{oo}$) = 0.050
pH of Suspension = 2.8
Mix Time of Suspension in Tank = 15 min.
Filtration Time = 1050 sec.
Forming Velocity = 1 cm./sec.
Treatment of Pad After Formation = None

BOUND PARTICLE DISTRIBUTION PAD P-3

| Bound Particle Concentration, $\underline{P}'$, g. $TiO_2$/g. pulp | Mass Pulp Accumulated, $\underline{m}$, g. pulp |
|---|---|
| 0.0025 | 0.23 |
| 0.0057 | 0.62 |
| 0.0085 | 1.00 |
| 0.0109 | 1.42 |
| 0.0131 | 1.78 |
| 0.0149 | 2.12 |
| 0.0171 | 2.54 |
| 0.0191 | 2.95 |
| 0.0207 | 3.28 |
| 0.0224 | 3.54 |
| 0.0232 | 3.82 |
| 0.0245 | 4.10 |
| 0.0251 | 4.38 |
| 0.0264 | 4.79 |
| 0.0263 | 5.13 |

Pad P-4

Conditions:

Pulp Type = 1
Initial Ratio, $TiO_2$ to Pulp ($\underline{P}_{oo}$) = 0.050
pH of Suspension = 2.8
Mix Time in Tank = 38 min.
Filtration Time = 1010 sec.
Forming Velocity = 1 cm./sec.
Treatment of Pad After Formation = 10 min. of permeation of the pad at 1 cm./sec. pH of permeating fluid was the same as formation.

BOUND PARTICLE DISTRIBUTION PAD P-4

| Bound Particle Concentration, $\underline{P}'$ g. $TiO_2$/g. pulp | Mass Pulp Accumulated, $\underline{m}$, g. pulp |
|---|---|
| 0.0020 | 0.15 |
| 0.0042 | 0.45 |
| 0.0074 | 0.69 |
| 0.0074 | 0.93 |
| 0.0090 | 1.20 |
| 0.0118 | 1.56 |
| 0.0142 | 2.03 |
| 0.0164 | 2.42 |
| 0.0184 | 2.72 |
| 0.0197 | 3.03 |
| 0.0207 | 3.39 |
| 0.0219 | 3.76 |
| 0.0236 | 4.10 |
| 0.0246 | 4.36 |
| 0.0256 | 4.72 |
| 0.0253 | 5.03 |

Data for Pads P-6 and P-7

Pads P-6 and P-7 were formed from the same suspension of $TiO_2$ and pulp. Details of the filtration are given below.

Pad P-6

Conditions:

Pulp Type = 3
Initial Ratio, $TiO_2$ to Pulp = 0.050
pH of Suspension = 3.0
Mix Time of Suspension = 15 min.
Filtration Time - 825 sec.
Forming Velocity = 1 cm./sec.
Treatment of Pad After Formation = None

BOUND PARTICLE DISTRIBUTION PAD P-6

| Bound Particle Concentration, $\underline{P}'$, g. $TiO_2$/g. pulp | Mass Pulp Accumulated, $\underline{m}$, g. pulp |
|---|---|
| 0.0088 | 0.16 |
| 0.0197 | 0.50 |
| 0.0278 | 0.89 |
| 0.0337 | 1.28 |
| 0.0364 | 1.71 |
| 0.0399 | 2.11 |
| 0.0415 | 2.38 |
| 0.0411 | 2.68 |
| 0.0423 | 3.05 |
| 0.0415 | 3.46 |

Pad P-7

Conditions:

Pulp Type = 3
Initial Ratio, $TiO_2$ to Pulp = 0.050
pH of Suspension = 3.0
Mix Time of Suspension = 33 min.
Filtration Time = 825 sec.
Forming Velocity = 1 cm./sec.
Treatment of Pad After Formation = Permeation of the pad with suspension of nylon and pulp fibers at same velocity and pH as formation. Final pressure drop was 14.5 p.s.i. Permeation Time: 16 min.

BOUND PARTICLE DISTRIBUTION PAD P-7

| Bound Particle Distribution, $\underline{P}'$ g. $TiO_2$/g. pulp | Mass Pulp Accumulated, $\underline{m}$, g. pulp |
|---|---|
| 0.0018 | 0.16 |
| 0.0219 | 0.44 |
| 0.0284 | 0.75 |
| 0.0226 | 1.16 |
| 0.0374 | 1.55 |
| 0.0400 | 1.81 |
| 0.0409 | 2.12 |
| 0.0415 | 2.55 |
| 0.0424 | 2.99 |
| 0.0450 | 3.48 |

Data for Pads P-8 and P-9

Pads P-8 and P-9 were formed from the same suspension of $TiO_2$ and pulp. Details of the filtration are given below.

Pad P-8

Conditions:

Pulp Type = 3
Initial Ratio, $TiO_2$ to Pulp = 0.050
pH of Suspension = 2.8
Mix Time of Suspension = 15 min.
Filtration Time = 450 sec.
Forming Velocity = 1 cm./sec.
Treatment of Pad After Formation = None

BOUND PARTICLE DISTRIBUTION PAD P-8

| Bound Particle Concentration, P', g. $TiO_2$/g. pulp | Mass Pulp Accumulated, m, g. pulp |
|---|---|
| 0.0097 | 0.097 |
| 0.0157 | 0.233 |
| 0.0226 | 0.423 |
| 0.0295 | 0.673 |
| 0.0337 | 0.977 |
| 0.0380 | 1.280 |
| 0.0397 | 1.530 |
| 0.0410 | 1.780 |

Pad P-9

Conditions:

Pulp Type = 3
Initial Ratio, $TiO_2$ to Pulp = 0.050
pH of Suspension = 2.8
Mix Time of Suspension = 58 min.
Filtration Time = 450 sec.
Forming Velocity = 1 cm./sec.
Treatment of Pad After Formation = 6 min. of permeation of the pad at 2 cm./sec. pH of permeating fluid was the same as formation.

BOUND PARTICLE DISTRIBUTION PAD P-9

| Bound Particle Concentration, P' g. $TiO_2$/g. pulp | Mass Pulp Accumulated, m, g. pulp |
|---|---|
| 0.0119 | 0.12 |
| 0.0258 | 0.40 |
| 0.0322 | 0.63 |
| 0.0358 | 0.87 |
| 0.0394 | 1.21 |
| 0.0476 | 1.48 |
| 0.0419 | 1.66 |

Data for Pads P-10 and P-11

Pads P-10 and P-11 were formed from the same suspensions of $TiO_2$ and pulp. Details of the filtrations are given below.

## Pad P-10

Conditions:

Pulp Type = 1
Initial Ratio, $TiO_2$ to Pulp = 0.050
pH of Suspension = 2.8
Mix Time of Suspension = 15 min.
Filtration Time = 1100 sec.
Forming Velocity = 1 cm./sec.
Treatment of Pad After Formation = None

BOUND PARTICLE DISTRIBUTION PAD P-10

| Bound Particle Concentration, $\underline{P}'$ g. $TiO_2$/g. pulp | Mass Pulp Accumulated, $\underline{m}$, g. pulp |
|---|---|
| 0.0027 | 0.18 |
| 0.0071 | 0.50 |
| 0.0104 | 0.82 |
| 0.0145 | 1.22 |
| 0.0178 | 1.56 |
| 0.0198 | 1.86 |
| 0.0228 | 2.19 |
| 0.0243 | 2.45 |
| 0.0251 | 2.68 |
| 0.0274 | 3.00 |
| 0.0292 | 3.43 |
| 0.0320 | 3.78 |
| 0.0326 | 4.02 |
| 0.0338 | 4.36 |
| 0.0358 | 4.66 |
| 0.0352 | 5.01 |

## Pad P-11

Conditions:

Pulp Type = 1
Initial Ratio, $TiO_2$ to Pulp = 0.050
pH of Suspension = 2.8
Mix Time of Suspension = 41 min.
Filtration Time = 1000 sec.
Forming Velocity = 1 cm./sec.
Treatment of Pad After Formation = 10 min. of permeation of pad at 1 cm./sec. pH of permeating fluid was 6.8.

BOUND PARTICLE DISTRIBUTION PAD P-11

| Bound Particle Concentration, $\underline{P}'$, g. $TiO_2$/g. pulp | Mass Pulp Accumulated, $\underline{m}$, g. pulp |
|---|---|
| 0.0014 | 0.21 |
| 0.0024 | 0.55 |
| 0.0038 | 0.81 |
| 0.0048 | 1.15 |
| 0.0066 | 1.46 |
| 0.0063 | 1.73 |
| 0.0076 | 2.02 |
| 0.0089 | 2.40 |
| 0.0096 | 2.81 |
| 0.0109 | 3.17 |
| 0.0120 | 3.56 |
| 0.0125 | 3.91 |
| 0.0130 | 4.27 |
| 0.0124 | 4.62 |

Data for Pads P-12 and P-13

Pads P-12 and P-13 were formed from the same suspension of $TiO_2$ and pulp. Details of the filtration are given below.

| Conditions: | P-12 | P-13 |
|---|---|---|
| Pulp Type = | 2 | 2 |
| Initial Ratio, $TiO_2$ to Pulp = | 0.0475 | 0.0475 |
| pH of Suspension = | 11.4 | 11.4 |
| Mix Time of Suspension = | 29 min. | 15 min. |
| Filtration Time = | 1224 sec. | 537 sec. |
| Forming Velocity = | 1 cm./sec. | 2 cm./sec. |

BOUND PARTICLE DISTRIBUTIONS PAD P-12 AND PAD P-13

| Pad P-12 | | Pad P-13 | |
|---|---|---|---|
| Bound Particle Concn., $\underline{P}'$, g. $TiO_2$/g. pulp | Mass of Pulp Accum., $\underline{m}$, g. pulp | Bound Particle Concn., $\underline{P}'$, g. $TiO_2$/g. pulp | Mass Pulp Accum., $\underline{m}$, g. pulp |
| 0.0006 | 0.36 | 0.0008 | 0.48 |
| 0.0014 | 1.16 | 0.0022 | 1.20 |
| 0.0023 | 1.97 | 0.0029 | 1.83 |
| 0.0033 | 2.70 | 0.0043 | 2.59 |
| 0.0041 | 3.36 | 0.0052 | 3.21 |
| 0.0049 | 3.88 | 0.0064 | 3.75 |
| 0.0054 | 4.24 | 0.0076 | 4.30 |
| 0.0059 | 4.59 | | |
| 0.0059 | 4.94 | | |

Data for Pads P-14 and P-15

Pads P-14 and P-15 were formed from the same suspension of $TiO_2$ and pulp. Details of the filtration are given below.

| Conditions: | P-14 | P-15 |
|---|---|---|
| Pulp Type = | 2 | 2 |
| Initial Ratio, $TiO_2$ to Pulp = | 0.0475 | 0.0475 |
| pH of Suspension = | 10.1 | 10.1 |
| Mix Time of Suspension = | 27 min. | 15 min. |
| Filtration Time = | 1048 sec. | 542 sec. |
| Forming Velocity = | 1 cm./sec. | 1 cm./sec. |

BOUND PARTICLE DISTRIBUTIONS PAD P-14 AND PAD P-15

| Pad P-14 | | Pad P-15 | |
|---|---|---|---|
| Bound Particle Concn., $\underline{P}'$, g. $TiO_2$/g. pulp | Mass Pulp Accum., $\underline{m}$, g. pulp | Bound Particle Concn., $\underline{P}'$, g. $TiO_2$/g. pulp | Mass Pulp Accum., $\underline{m}$, g. pulp |
| 0.0010 | 0.27 | 0.0012 | 0.39 |
| 0.0017 | 0.88 | 0.0034 | 1.20 |
| 0.0029 | 1.54 | 0.0055 | 1.85 |
| 0.0040 | 2.16 | 0.0079 | 2.37 |
| 0.0050 | 2.73 | 0.0096 | 2.85 |
| 0.0062 | 3.40 | 0.0116 | 3.37 |
| 0.0076 | 4.00 | 0.0144 | 4.04 |
| 0.0083 | 4.43 | 0.0184 | 4.72 |

Data for Pads P-16 and P-17

Pads P-16 and P-17 were formed from the same suspension of $TiO_2$ and pulp. Details of the filtration are given below.

| Conditions: | P-16 | P-17 |
|---|---|---|
| Pulp Type = | 2 | 2 |
| Initial Ratio, $TiO_2$ to Pulp = | 0.0475 | 0.0475 |
| pH of Suspension = | 5.9 | 5.9 |
| Mix Time of Suspension = | 20 min. | 44 min. |
| Filtration Time = | 1100 sec. | 500 sec. |
| Forming Velocity = | 1 cm./sec. | 2 cm./sec. |

BOUND PARTICLE DISTRIBUTIONS PAD P-16 AND PAD P-17

| Pad P-16 | | Pad P-17 | |
|---|---|---|---|
| Bound Particle Concn., $\underline{P}'$, g. $TiO_2$/g. pulp | Mass of Pulp Accum., $\underline{m}$, g. pulp | Bound Particle Concn., $\underline{P}'$, g. $TiO_2$/g. pulp | Mass Pulp Accum., $\underline{m}$, g. pulp |
| 0.0008 | 0.17 | 0.0014 | 0.19 |
| 0.0008 | 0.44 | 0.0021 | 0.50 |
| 0.0014 | 0.73 | 0.0034 | 0.83 |
| 0.0021 | 1.31 | 0.0042 | 1.16 |
| 0.0021 | 1.44 | 0.0060 | 1.56 |
| 0.0029 | 1.80 | 0.0078 | 2.00 |
| 0.0037 | 2.24 | 0.0095 | 2.38 |

BOUND PARTICLE DISTRIBUTIONS PAD P-16 AND PAD P-17 (Cont'd)

| Pad P-16 | | Pad P-17 | |
|---|---|---|---|
| Bound Particle Concn., $\underline{P}$, g. $TiO_2$/g. pulp | Mass of Pulp Accum., $\underline{m}$, g. pulp | Bound Particle Concn., $\underline{P}'$, g. $TiO_2$/g. pulp | Mass Pulp Accum., $\underline{m}$, g. pulp |
| 0.0044 | 2.70 | 0.0111 | 2.77 |
| 0.0048 | 3.16 | 0.0128 | 3.13 |
| 0.0056 | 3.58 | 0.0148 | 4.47 |
| 0.0065 | 4.03 | 0.0167 | 3.83 |
| 0.0068 | 4.36 | 0.0178 | 4.23 |
| 0.0079 | 4.60 | | |
| 0.0085 | 4.96 | | |

Data for Pads P-18 and P-19

Pads P-18 and P-19 were formed from the same suspension of $TiO_2$ and pulp. Details of the filtrations are given below.

| Conditions: | P-18 | P-19 |
|---|---|---|
| Pulp Type = | 2 | 2 |
| Initial Ratio, $TiO_2$ to Pulp = | 0.0475 | 0.0475 |
| pH of Suspension = | 5.0 | 5.0 |
| Mix Time of Suspension = | 27 min. | 15 min. |
| Filtration Time = | 1135 sec. | 524 sec. |
| Forming Velocity = | 1 cm./sec. | 2 cm./sec. |

BOUND PARTICLE DISTRIBUTIONS PAD P-18 AND PAD P-19

| Pad P-18 | | Pad P-19 | |
|---|---|---|---|
| Bound Particle Concn., $\underline{P}'$, g. $TiO_2$/g. pulp | Mass Pulp Accum., $\underline{m}$, g. pulp | Bound Particle Concn., $\underline{P}'$, g. $TiO_2$/g. pulp | Mass Pulp Accum., $\underline{m}$, g. pulp |
| 0.0025 | 0.25 | 0.0017 | 0.11 |
| 0.0045 | 0.70 | 0.0021 | 0.32 |
| 0.0067 | 1.12 | 0.0046 | 0.61 |
| 0.0095 | 1.62 | 0.0079 | 0.96 |
| 0.0122 | 2.08 | 0.0108 | 1.31 |
| 0.0143 | 2.43 | 0.0138 | 1.72 |
| 0.0170 | 2.76 | 0.0168 | 2.15 |
| 0.0177 | 3.06 | 0.0191 | 2.46 |
| 0.0196 | 3.30 | 0.0212 | 2.70 |
| 0.0209 | 3.60 | 0.0222 | 2.97 |
| 0.0231 | 3.95 | 0.0238 | 3.23 |
| 0.0259 | 4.19 | 0.0264 | 3.47 |
| 0.0258 | 4.39 | 0.0280 | 3.72 |
| 0.0278 | 4.72 | 0.0292 | 3.93 |
| | | 0.0296 | 4.27 |

Data for Pads P-20 and P-21

Pads P-20 and P-21 were formed from the same suspension of $TiO_2$ and pulp. Details of the filtrations are given below.

| Conditions: | P-20 | P-21 |
|---|---|---|
| Pulp Type = | 2 | 2 |
| Initial Ratio, $TiO_2$ to Pulp = | 0.0475 | 0.0475 |
| pH of Suspension = | 4.5 | 4.5 |
| Mix Time of Suspension = | 33 min. | 15 min. |
| Filtration Time = | 1110 sec. | 541 sec. |
| Forming Velocity = | 1 cm./sec. | 1 cm./sec. |

BOUND PARTICLE DISTRIBUTIONS PAD P-20 AND P-21

| Pad P-20 | | Pad P-21 | |
|---|---|---|---|
| Bound Particle Concn., $\underline{P}'$, g. $TiO_2$/g. pulp | Mass Pulp Accum., $\underline{m}$, g. pulp | Bound Particle Concn., $\underline{P}'$, g. $TiO_2$/g. pulp | Mass Pulp Accum., $\underline{m}$, g. pulp |
| 0.0042 | 0.23 | 0.0029 | 0.27 |
| 0.0074 | 0.67 | 0.0063 | 0.68 |
| 0.0104 | 1.08 | 0.0099 | 1.05 |
| 0.0137 | 1.45 | 0.0138 | 1.48 |
| 0.0168 | 1.72 | 0.0171 | 1.89 |
| 0.0182 | 1.95 | 0.0218 | 2.30 |
| 0.0234 | 2.24 | 0.0204 | 2.60 |
| 0.0230 | 2.58 | 0.0249 | 2.84 |
| 0.0260 | 2.90 | 0.0248 | 2.84 |
| 0.0278 | 3.27 | 0.0265 | 3.13 |
| 0.0296 | 3.66 | 0.0284 | 3.42 |
| 0.0298 | 3.98 | 0.0300 | 3.72 |
| 0.0323 | 4.30 | 0.0316 | 4.06 |
| 0.0314 | 4.60 | 0.0329 | 4.38 |
| 0.0342 | 4.83 | 0.0347 | 4.62 |

Data for Pad P-22 and P-23

Pads P-22 and P-23 were formed from the same suspension of $TiO_2$ and pulp. Details of the filtrations are given below.

| Conditions: | P-22 | P-23 |
|---|---|---|
| Pulp Type = | 2 | 2 |
| Initial Ratio, $TiO_2$ to Pulp = | 0.0475 | 0.0475 |
| pH of Suspension = | 4.0 | 4.0 |
| Mix Time of Suspension = | 29 min. | 15 min. |
| Filtration Time = | 1070 sec. | 539 sec. |
| Forming Velocity = | 1 cm./sec. | 2 cm./sec. |

BOUND PARTICLE DISTRIBUTIONS PAD P-22 AND P-23

| Pad P-22 | | Pad P-23 | |
|---|---|---|---|
| Bound Particle Concn., $\underline{P}'$, g. $TiO_2$/g. pulp | Mass Pulp Accum., $\underline{m}$, g. pulp | Bound Particle Concn., $\underline{P}'$, g. $TiO_2$/g. pulp | Mass Pulp Accum., $\underline{m}$, g. pulp |
| 0.0041 | 0.14 | 0.0029 | 0.14 |
| 0.0078 | 0.52 | 0.0057 | 0.40 |
| 0.0137 | 0.97 | 0.0086 | 0.66 |
| 0.0184 | 1.35 | 0.0121 | 0.94 |

BOUND PARTICLE DISTRIBUTIONS PAD P-22 AND P-23 (Cont'd)

| Pad P-22 | | Pad P-23 | |
|---|---|---|---|
| Bound Particle Concn., $\underline{P}'$, g. $TiO_2$/g. pulp | Mass Pulp Accum., $\underline{m}$, g. pulp | Bound Particle Concn., $\underline{P}'$, g. $TiO_2$/g. pulp | Mass Pulp Accum., $\underline{m}$, g. pulp |
| 0.0223 | 1.79 | 0.0147 | 1.21 |
| 0.0260 | 2.21 | 0.0177 | 1.49 |
| 0.0296 | 2.50 | 0.0206 | 1.81 |
| 0.0305 | 2.77 | 0.0227 | 2.14 |
| 0.0323 | 3.10 | 0.0262 | 2.53 |
| 0.0348 | 3.42 | 0.0286 | 2.95 |
| 0.0362 | 3.69 | 0.0310 | 3.28 |
| 0.0373 | 3.99 | 0.0324 | 3.58 |
| 0.0384 | 4.32 | 0.0347 | 3.92 |
| 0.0394 | 4.64 | 0.0357 | 4.20 |

Data for Pad P-24 and P-25

Pads P-24 and P-25 were formed from the same suspension of $TiO_2$ and pulp. Details for the filtration are given below.

| Conditions: | P-24 | P-25 |
|---|---|---|
| Pulp Type = | 2 | 2 |
| Initial Ratio, $TiO_2$ to Pulp = | 0.0475 | 0.0475 |
| pH of Suspension = | 3.5 | 3.5 |
| Mix Time of Suspension = | 30 min. | 15 min. |
| Filtration Time = | 1034 sec. | 555 sec. |
| Forming Velocity = | 1 cm./sec. | 2 cm./sec. |

BOUND PARTICLE DISTRIBUTIONS PAD P-24 AND P-25

| Pad P-24 | | Pad P-25 | |
|---|---|---|---|
| Bound Particle Concn., $\underline{P}'$, g. $TiO_2$/g. pulp | Mass Pulp Accum., $\underline{m}$, g. pulp | Bound Particle Concn., $\underline{P}'$, g. $TiO_2$/g. pulp | Mass Pulp Accum., $\underline{m}$, g. pulp |
| 0.0075 | 0.28 | 0.0044 | 0.20 |
| 0.0145 | 0.72 | 0.0092 | 0.53 |
| 0.0183 | 1.03 | 0.0128 | 0.78 |
| 0.0230 | 1.32 | 0.0156 | 1.01 |
| 0.0276 | 1.70 | 0.0194 | 1.38 |
| 0.0315 | 2.13 | 0.0236 | 1.82 |
| 0.0352 | 2.58 | 0.0266 | 2.14 |
| 0.0381 | 3.02 | 0.0291 | 2.44 |
| 0.0400 | 3.39 | 0.0311 | 2.76 |
| 0.0410 | 3.82 | 0.0326 | 3.04 |
| 0.0434 | 4.17 | 0.0344 | 3.32 |
| | | 0.0357 | 3.70 |
| | | 0.0381 | 4.09 |
| | | 0.0396 | 4.39 |

# APPENDIX VI

## CALCULATIONS OF PSEUDO-COLLECTION EFFICIENCY

The collection efficiency of a compressible wood pulp pad is dependent on a number of variables. The changes in the collection efficiency within a pad may be determined by the following method.

The retention rate, $\phi$, can be expressed in terms of the collection efficiency as:

$$\phi = ES\rho_w AU_o s(P_{oo} - P'). \tag{23}$$

The retention rate is also given by:

$$\phi = s\rho_w AU_o \frac{dP'}{dm}. \tag{24}$$

Therefore,

$$s\rho_w AU_o \frac{dP'}{dm} = ES\rho_w U_o s(P_{oo} - P'). \tag{25}$$

Solving for $\underline{E}$ gives

$$\frac{ES}{A} = \frac{dP'/dm}{P_{oo} - P'}. \tag{27}$$

$\underline{A}$ is the cross-sectional area of the pad. $\underline{S}$ is the fiber specific surface. $\underline{S}$ is usually assumed to be equivalent to the retention area and is considered a constant. In this treatment, it is recognized that the retention area may not be constant. All area effects are lumped into the collection efficiency, and changes in area will be reflected as changes in the collection efficiency.

Using this method, a pseudocollection efficiency can be defined as:

$$E' = \frac{ES}{A} = \frac{dP'/dm}{P_{oo} - P'}. \tag{28}$$

This pseudocollection efficiency will reflect the changes in the local variables of pore size, velocity, and retention area within a given pad.

$d\underline{P}'/d\underline{m}$ is the slope of the bound particle distribution curve. It will be denoted as $\Psi$ for the remainder of this section. Thus,

$$E' = \frac{\Psi}{P_{oo} - P'} . \tag{56}$$

The error in $\underline{E}'$ due to errors in $\Psi$, $\underline{P}_{oo}$, and $\underline{P}'$ can be estimated by taking the differential of $\underline{E}'$. Thus,

$$dE' = \frac{d\Psi}{P_{oo} - P'} + \frac{\Psi d(P_{oo} - P')}{(P_{oo} - P')^2} . \tag{57}$$

Dividing Equation (56) by Equation (57) gives

$$\frac{dE'}{E'} = \frac{d\Psi}{\Psi} + \frac{dP_{oo} + dP'}{P_{oo} - P'} . \tag{58}$$

For small changes, this may be written as

$$\frac{\Delta E'}{E'} = \frac{\Delta \Psi}{\Psi} + \frac{\Delta P_{oo} + \Delta P'}{P_{oo} - P'} . \tag{59}$$

This equation was used to calculate the error involved in $\underline{E}'$.

To evaluate all of the quantities, a "best-fit" smooth curve was drawn through all of the data points of the bound particle distribution curves. From this "best-fit" curve, $\underline{P}'_{best}$ is read off at various $\underline{m}$'s. A "best" $\underline{P}_{oo}$ is known from the amount of pulp and titanium dioxide slurry added at the beginning of the filtration. $\underline{E}'$ is calculated at various $\underline{m}$'s by using $\Delta\underline{P}'_{best}/\Delta\underline{m}$ divided by $\underline{P}_{oo} - \underline{P}'_{best}$.

From the smoothed curves, values of $\underline{P}'_{Hi}$ and $\underline{P}'_{Lo}$ are estimated at various $\underline{m}$'s. $\underline{P}'_{Hi}$ is the estimated highest value of $\underline{P}'$, and $\underline{P}'_{Lo}$ is the estimated

lowest value of $\underline{P}'$ at a given $\underline{m}$. The average of the difference between these values gives a value of $\Delta\underline{P}'$ at each $\underline{m}$.

$\Delta\underline{P}_{\underline{o}\underline{o}}$ is a constant for each run. Its value is simply 5% of the best estimate of $\underline{P}_{\underline{o}\underline{o}}$ for the run. The 5% error in $\underline{P}_{\underline{o}\underline{o}}$ was arrived at by summing the errors involved in the pulp weight and the titanium dioxide weight.

$\Delta\Psi$ is determined by the average between a calculated $\Psi_{Hi}$ and $\Psi_{Lo}$. $\Psi_{Hi}$ is determined by taking the difference between the $\underline{P}'_{Lo}$'s and dividing by the difference between the $\underline{m}$'s from which the $\underline{P}'_{Lo}$'s were determined. $\Psi_{Lo}$ is determined in the same manner by using the $\underline{P}'_{Hi}$'s.

After the above calculations, $\Delta\underline{E}'/\underline{E}'$ may be determined by using the calculated $\underline{E}'$ times $\Delta\underline{E}'/\underline{E}$. Table II gives summaries of the results of using this method on Pad P-24.

TABLE II

SUMMARY OF CALCULATION OF $\underline{E}'$ FOR PAD P-24

($\underline{P}_{oo}$ = 0.0475 g. $TiO_2$/g. pulp]

| m. g. | $\underline{P}'_{Lo}$, g. $TiO_2$ / g. pulp | $\underline{P}'_{Hi}$, g. $TiO_2$ / g. pulp | $\Psi_{best}$, g. $TiO_2$ / g. pulp | $\Psi_{best}$, l/g. | $\underline{P}_{oo} - \underline{P}'_{best}$, g. $TiO_2$ / g. pulp | $\underline{E}'$ l/g. | $\Delta\underline{P}'$, g. $TiO_2$ / g. pulp | $\Psi_{Lo}$, l/g. | $\Psi_{Hi}$, l/g. | $\Delta\Psi$, l/g. | $\frac{\Delta\Psi}{\Psi_{best}}$ | $\underline{P}+\underline{P}_{oo}$, g. $TiO_2$ / g. pulp | $\frac{\Delta\underline{P}'+\underline{P}_{oo}}{\underline{P}_{oo}-\underline{P}_{best}}$ | $\Delta\underline{E}'/\underline{E}'$ | $\Delta\underline{E}'$, l/g. |
|---|---|---|---|---|---|---|---|---|---|---|---|---|---|---|---|
| 0.0 | 0.0020 | 0.0050 | 0.0030 | -- | 0.0445 | -- | 0.0015 | -- | -- | -- | -- | -- | -- | -- | -- |
| 0.5 | 0.0110 | 0.0125 | 0.0120 | 0.0160 | 0.0355 | 0.450 | 0.0007 | 0.0145 | 0.0160 | 0.0008 | 0.050 | 0.0031 | 0.0875 | 0.138 | 0.062 |
| 1.0 | 0.0180 | 0.0195 | 0.0190 | 0.0130 | 0.0285 | 0.407 | 0.0007 | 0.0130 | 0.0135 | 0.0003 | 0.023 | 0.0031 | 0.1090 | 0.132 | 0.054 |
| 1.5 | 0.0245 | 0.0255 | 0.0250 | 0.0110 | 0.0225 | 0.490 | 0.0005 | 0.0110 | 0.0115 | 0.0003 | 0.027 | 0.0029 | 0.1280 | 0.155 | 0.076 |
| 2.0 | 0.0295 | 0.0305 | 0.0300 | 0.0095 | 0.0175 | 0.544 | 0.0005 | 0.1095 | 0.0095 | 0 | 0 | 0.0029 | 0.1650 | 0.165 | 0.089 |
| 2.5 | 0.0340 | 0.0350 | 0.0345 | 0.0075 | 0.0130 | 0.577 | 0.0005 | 0.0075 | 0.0075 | 0 | 0 | 0.0029 | 0.2230 | 0.222 | 0.128 |
| 3.0 | 0.0370 | 0.0380 | 0.0375 | 0.0055 | 0.0100 | 0.550 | 0.0005 | 0.0055 | 0.0055 | 0 | 0 | 0.0029 | 0.2900 | 0.290 | 0.159 |
| 3.5 | 0.0395 | 0.0405 | 0.0400 | 0.0045 | 0.0075 | 0.600 | 0.0005 | 0.0045 | 0.0045 | 0 | 0 | 0.0029 | 0.3900 | 0.390 | 0.234 |
| 4.0 | 0.0415 | 0.0420 | 0.0420 | -- | 0.0055 | -- | 0.0005 | -- | -- | -- | -- | -- | -- | -- | -- |

## APPENDIX VII

## DETERMINATION OF STATES OF COMPRESSION

The following is the procedure for determining the states of compression of the pads during a constant-rate filtration.

Standard static compressibility tests as described by Ingmanson (23) were run on Type 2 and Type 4 pulps. The results are shown in Fig. 24.

The pressure drop across the pads was continuously recorded during each filtration. From these pressure-time plots, the pressure at any given time could be determined. This pressure reading could be converted into c, the state of compression by reading the pressure value from Fig. 24.

The total time of filtration and the total mass of pulp accumulated during that time were known experimental quantities. The mass of pulp accumulated at any time could be calculated from the mass balance equation,

$$m = \frac{M_T}{T_T} t, \tag{60}$$

where

$m$ = mass of pulp accumulated at time $t$, g.,

$M_T$ = total mass of pad, g.,

$T_T$ = total filtration time, min., and

$t$ = elapsed time from start of filtration.

The relationship between $c$ and $m$ could be established by picking an elapsed time, $t$. The mass of pulp accumulated, $m$, could then be calculated at the elapsed time, $t$, by Equation (60). At this same elapsed time, $t$, a pressure reading could be obtained from the pressure-time plots. Using this pressure reading, the state of compression of the pad could be determined from Fig. 24. The state

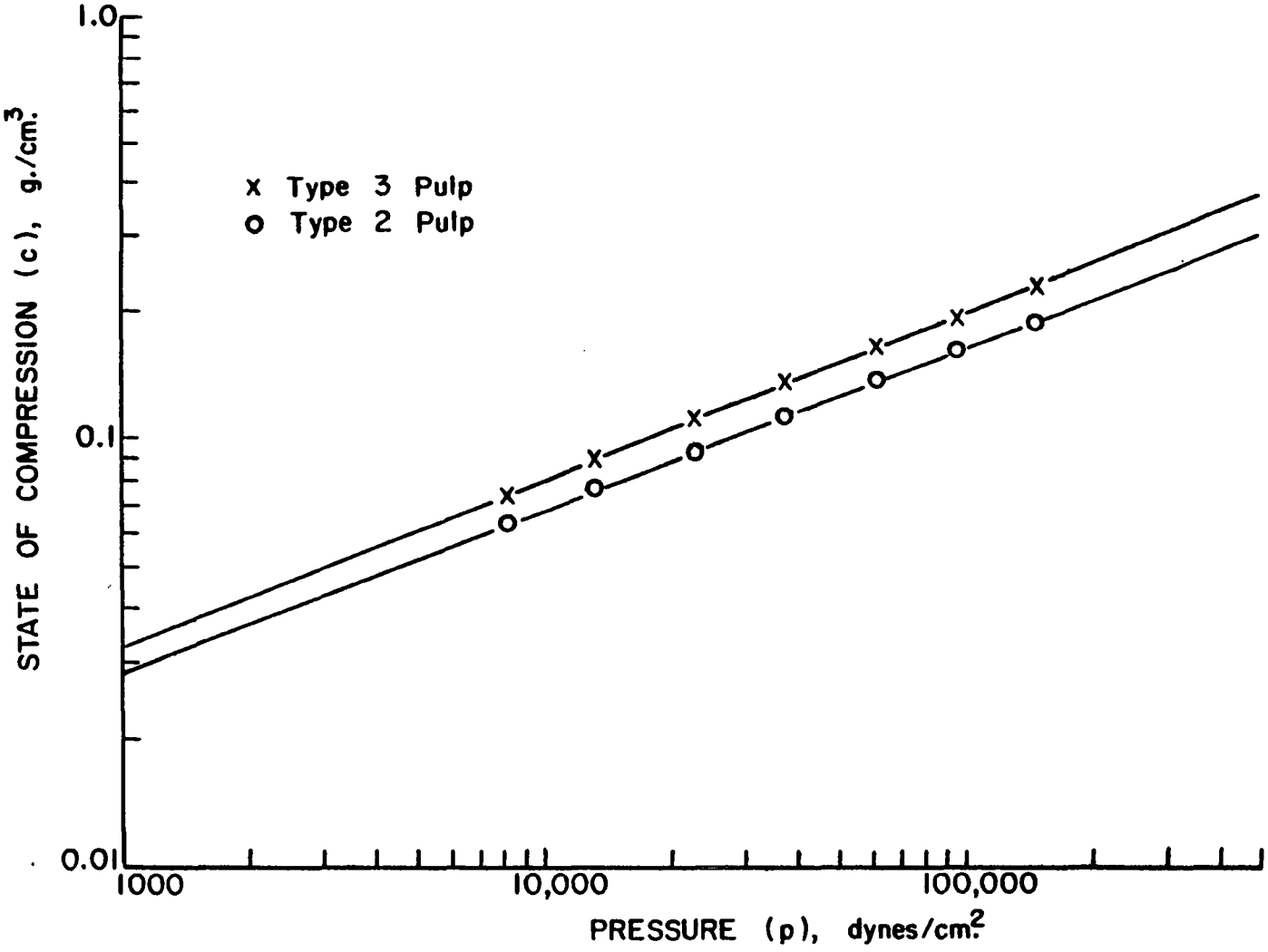


Figure 24. Relationship Between State of Compression and Applied Pressure

of compression at various values of pulp accumulated could be determined in this manner.

This procedure was used to obtain the relationship between $\underline{m}$ and $\underline{c}$ for the pH 4.5 pads at 1 and 2 cm./sec. forming velocity. These values were also used for the pads at pH's 5.0, 4.0, and 3.5. The pressure drop curves were changed slightly with the amount of particles retained. However, it was felt that the states of compression determined for the pH 4.5 pad were reasonable approximations of the states of compression for the other pads which were formed from the same pulp.

The same method was used for the pads formed from the Type 3 pulp.

# APPENDIX VIII

## FILTRATION EXPERIMENTS WITH HOLOPULP FIBERS

Holopulp fibers, as described in the experimental section, were used in a series of removal experiments. The details of the experiments and results are given below.

Microscopic observations were made on these fibers. There appeared to be a large percentage of primary wall still associated with the fibers. This primary wall appeared as gelatinous areas on the fibers. The primary wall is composed primarily of hemicelluloses and pectin. The presence of these substances is believed responsible for the results observed in these filtration experiments.

The first holopulp experiment utilized fibers that had received 30 min. of classification on the Bauer-McNett classifier. Only the fraction retained on the 14-mesh screen was used in the filtration. Two pads were formed from a suspension at pH 3.0 and at a forming velocity of 1 cm./sec. The second pad formed (P-27) received an additional 10 minutes of permeation with distilled water at 1 cm./sec. The details of the filtrations are given in Table III and the results are shown in Fig. 25. As can be seen in Fig. 25, the overall retention was very low. Removal with water was achieved. The removal is fairly uniform at approximately 50%.

The next holopulp experiment utilized fibers which had been stirred 30 min. in the British disintegrator and then classified using the same procedure as before. Again, only the fraction retained on the 14-mesh screen was used for the filtration. Two pads were formed from a suspension at pH 2.9 and at a forming velocity of 1 cm./sec. The second pad formed (P-29) received an additional 10 min. of permeation with distilled water at 1 cm./sec. The details

TABLE III

FILTRATION CONDITIONS AND BOUND PARTICLE DISTRIBUTIONS FOR PADS P-26 THROUGH P-35

Data for Pads P-26 and P-27

Pads P-26 and P-27 were formed from the same suspension of $TiO_2$ and holopulp. The holopulp was classified for 30 minutes and the fraction retained on 14-mesh screens was used in the filtration experiment. Details of the filtration are given below.

| Conditions: | P-26 | P-27 |
|---|---|---|
| Pulp type = | Holopulp | Holopulp |
| Initial Ratio, $TiO_2$ to Pulp ($\underline{P}_{oo}$) = | 0.050 | 0.050 |
| pH of Suspension = | 3.0 | 3.0 |
| Mix Time of Suspension in Tank = | 15 min. | 38 min. |
| Filtration Time = | 1100 sec. | 1000 sec. |
| Forming Velocity = | 1 cm./sec. | 1 cm./sec. |
| Treatment of Pad After Formation = | None | Permeated 10 min. with distilled water at 1 cm./sec. |

BOUND PARTICLE DISTRIBUTIONS PADS P-26 AND P-27

| Pad P-26 | | Pad P-27 | |
|---|---|---|---|
| Bound Particle Concn., $\underline{P}'$, g. $TiO_2$/g. pulp | Mass Pulp Accum., $\underline{m}$, g. pulp | Bound Particle Concn., $\underline{P}'$, g. $TiO_2$/g. pulp | Mass Pulp Accum., $\underline{m}$, g. pulp |
| 0.0010 | 0.10 | 0.0012 | 0.21 |
| 0.0013 | 0.33 | 0.0016 | 0.61 |
| 0.0019 | 0.53 | 0.0025 | 1.01 |
| 0.0026 | 0.71 | 0.0031 | 1.39 |
| 0.0031 | 0.91 | 0.0041 | 1.78 |
| 0.0044 | 1.16 | 0.0051 | 2.08 |
| 0.0059 | 1.56 | 0.0051 | 2.32 |
| 0.0069 | 1.91 | 0.0055 | 2.57 |
| 0.0081 | 2.14 | 0.0060 | 2.84 |
| 0.0090 | 2.36 | 0.0072 | 3.24 |
| 0.0102 | 2.66 | 0.0080 | 3.59 |
| 0.0116 | 2.97 | 0.0091 | 3.82 |
| 0.0125 | 3.25 | 0.0102 | 3.99 |
| 0.0134 | 3.53 | | |
| 0.0153 | 3.79 | | |
| 0.0164 | 4.02 | | |
| 0.0169 | 4.27 | | |

Data for Pads P-28 and P-29

Pads P-28 and P-29 were formed from the same suspension of $TiO_2$ and holopulp. The holopulp was stirred 30 minutes in the British Disintegrator and then classified for 30 minutes. The fraction retained on 14-mesh screen was used in the filtration experiments. Details of the filtrations are given below.

| Conditions: | P-28 | P-29 |
|---|---|---|
| Pulp Type = | Holopulp | Holopulp |
| Initial Ratio, $TiO_2$ to Pulp ($\underline{P}_{oo}$) = | 0.050 | 0.050 |
| pH of Suspension = | 2.9 | 2.9 |
| Mix Time of Suspension in Tank = | 15 min. | 41 min. |
| Filtration Time = | 1100 sec. | 1000 sec. |
| Forming Velocity | 1 cm./sec. | 1 cm./sec. |
| Treatment of Pad After Formation = | None | Permeated 10 min. with distilled water at 1 cm./sec. |

BOUND PARTICLE DISTRIBUTIONS PADS P-28 AND P-29

| Pad P-28 | | Pad P-29 | |
|---|---|---|---|
| Bound Particle Concn., $\underline{P}'$, g. $TiO_2$/g. pulp | Mass Pulp Accum., $\underline{m}$, g. pulp | Bound Particle Concn., $\underline{P}'$, g. $TiO_2$/g. pulp | Mass Pulp Accum., $\underline{m}$, g. pulp |
| 0.0014 | 0.15 | 0.0029 | 0.09 |
| 0.0023 | 0.44 | 0.0031 | 0.25 |
| 0.0032 | 0.75 | 0.0013 | 0.49 |
| 0.0043 | 0.99 | 0.0022 | 0.86 |
| 0.0048 | 1.26 | 0.0032 | 1.22 |
| 0.0063 | 1.56 | 0.0027 | 1.55 |
| 0.0069 | 1.84 | 0.0033 | 1.85 |
| 0.0088 | 2.36 | 0.0040 | 2.12 |
| 0.0104 | 2.83 | 0.0052 | 2.45 |
| 0.0096 | 3.08 | 0.0049 | 2.81 |
| 0.0127 | 3.38 | 0.0059 | 3.10 |
| 0.0143 | 3.80 | 0.0064 | 3.30 |
| 0.0155 | 4.16 | 0.0063 | 3.62 |
| 0.0162 | 4.46 | 0.0070 | 3.95 |
| 0.0176 | 4.71 | 0.0079 | 4.29 |
| | | 0.0087 | 4.67 |

Data for Pads P-30 and P-31

Pads P-30 and P-31 were formed from the same suspension of $TiO_2$ and holopulp. The holopulp was stirred 1 hour in the British Disintegrator and then classified for 30 minutes. The fraction retained on 14-mesh screen was used in the filtration experiments. Details of the filtration are given below.

| Conditions: | P-30 | P-31 |
|---|---|---|
| Pulp Type = | Holopulp | Holopulp |
| Initial Ratio, $TiO_2$ to Pulp ($\underline{P}_{oo}$) = | 0.050 | 0.050 |
| pH of Suspension = | 3.1 | 3.1 |
| Mix Time of Suspension in Tank = | 15 min. | 40 min. |
| Filtration Time = | 1100 sec. | 1090 sec. |
| Forming Velocity = | 1 cm./sec. | 1 cm./sec. |
| Treatment of Pad After Formation = | None | Permeated 10 min. with distilled water at 1 cm./sec. |

BOUND PARTICLE DISTRIBUTIONS PADS P-30 AND P-31

| Pad P-30 | | Pad P-31 | |
|---|---|---|---|
| Bound Particle Concn., $\underline{P}'$, g. $TiO_2$/g. pulp | Mass Pulp Accum., $\underline{m}$, g. pulp | Bound Particle Concn., $\underline{P}'$, g. $TiO_2$/g. pulp | Mass Pulp Accum., $\underline{m}$, g. pulp |
| 0.0008 | 0.14 | 0.0012 | 0.17 |
| 0.0018 | 0.49 | 0.0010 | 0.51 |
| 0.0030 | 0.89 | 0.0021 | 0.84 |
| 0.0044 | 1.19 | 0.0029 | 1.15 |
| 0.0076 | 1.39 | 0.0030 | 1.40 |
| 0.0061 | 1.64 | 0.0037 | 1.67 |
| 0.0069 | 1.95 | 0.0046 | 2.03 |
| 0.0086 | 2.30 | 0.0057 | 2.35 |
| 0.0093 | 2.61 | 0.0062 | 2.68 |
| 0.0100 | 2.82 | 0.0068 | 2.97 |
| 0.0124 | 3.17 | 0.0073 | 3.25 |
| 0.0142 | 3.54 | 0.0085 | 3.54 |
| 0.0153 | 3.80 | 0.0090 | 3.80 |
| 0.0163 | 4.09 | 0.0103 | 4.11 |
| 0.0182 | 4.43 | 0.0108 | 4.46 |

Data for Pads P-32 and P-33

Pads P-32 and P-33 were formed from the same suspension of $TiO_2$ and holopulp. The holopulp was stirred 2 hours in the British Disintegrator and then classified for 30 minutes. The fraction retained on 14-mesh screen wire was used in the filtration experiments. Details of the filtration are given below.

| Conditions: | P-32 | P-33 |
|---|---|---|
| Pulp Type = | Holopulp | Holopulp |
| Initial Ratio, $TiO_2$ to Pulp ($\underline{P}_{oo}$) = | 0.050 | 0.050 |
| pH of Suspension = | 2.9 | 2.9 |
| Mix Time of Suspension in Tank = | 15 min. | 38 min. |
| Filtration Time = | 1100 sec. | 1020 sec. |
| Forming Velocity = | 1 cm./sec. | 1 cm./sec. |
| Treatment of Pad After Formation = | None | Permeated 10 min. with distilled water at 1 cm./sec. |

BOUND PARTICLE DISTRIBUTIONS PADS P-32 AND P-33

| Pad P-32 | | P-33 | |
|---|---|---|---|
| Bound Particle Concn., $\underline{P}'$, g. $TiO_2$/g. pulp | Mass Pulp Accum., $\underline{m}$, g. pulp | Bound Particle Concn., $\underline{P}'$, g. $TiO_2$/g. pulp | Mass Pulp Accum., $\underline{m}$, g. pulp |
| 0.0017 | 0.17 | 0.0020 | 0.14 |
| 0.0033 | 0.44 | 0.0027 | 0.37 |
| 0.0045 | 0.66 | 0.0031 | 0.66 |
| 0.0057 | 0.95 | 0.0039 | 0.97 |
| 0.0076 | 1.28 | 0.0044 | 1.23 |
| 0.0093 | 1.60 | 0.0050 | 1.49 |
| 0.0113 | 1.87 | 0.0056 | 1.72 |
| 0.0124 | 2.10 | 0.0063 | 1.97 |

BOUND PARTICLE DISTRIBUTIONS PADS P-32 AND P-33 (Cont'd)

| Pad P-32 | | Pad P-33 | |
|---|---|---|---|
| Bound Particle Concn., $\underline{P}'$, g. $TiO_2$/g. pulp | Mass Pulp Accum., $\underline{m}$, g. pulp | Bound Particle Concn., $\underline{P}'$, g. $TiO_2$/g. pulp | Mass Pulp Accum., $\underline{m}$, g. pulp |
| 0.0140 | 2.45 | 0.0071 | 2.29 |
| 0.0157 | 2.77 | 0.0079 | 2.60 |
| 0.0172 | 2.98 | 0.0088 | 2.80 |
| 0.0182 | 3.24 | 0.0094 | 3.02 |
| 0.0197 | 3.55 | 0.0103 | 3.30 |
| 0.0204 | 3.83 | 0.0106 | 3.60 |
| 0.0216 | 4.06 | 0.0129 | 3.84 |
| 0.0242 | 4.36 | 0.0132 | 4.12 |
| | | 0.0134 | 4.50 |

Data for Pads P-34 and P-35

Pads P-34 and P-35 were formed from the same suspension of $TiO_2$ and holopulp. This holopulp was caustic extracted and then classified for 30 minutes. The fraction retained on 14-mesh screen was used in the filtration experiments. Details of the filtration are given below.

| Conditions: | P-34 | P-35 |
|---|---|---|
| Pulp Type = | Caustic Extracted Holopulp | Caustic Extracted Holopulp |
| Initial Ratio, $TiO_2$/Pulp ($\underline{P}_{oo}$) = | 0.050 | 0.050 |
| pH of Suspension = | 2.9 | 2.9 |
| Mix Time of Suspension in Tank = | 15 min. | 38 min. |
| Filtration Time = | 1100 sec. | 1020 sec. |
| Forming Velocity = | 1 cm./sec. | 1 cm./sec. |
| Treatment of Pad After Formation = | None | Permeated 10 min. with distilled water at 1 cm./sec. |

BOUND PARTICLE DISTRIBUTIONS PADS P-34 AND P-35

| P-34 | | P-35 | |
|---|---|---|---|
| Bound Particle Concn., $\underline{P}'$, g. $TiO_2$/g. pulp | Mass Pulp Accum., $\underline{m}$, g. pulp | Bound Particle Concn., $\underline{P}'$, g. $TiO_2$/g. pulp | Mass Pulp Accum., $\underline{m}$, g. pulp |
| 0.0021 | 0.12 | 0.0047 | 0.12 |
| 0.0038 | 0.34 | 0.0061 | 0.49 |
| 0.0053 | 0.59 | 0.0077 | 0.86 |
| 0.0080 | 0.99 | 0.0080 | 1.18 |
| 0.0106 | 1.34 | 0.0106 | 1.49 |
| 0.0120 | 1.55 | 0.0117 | 1.75 |
| 0.0136 | 1.78 | 0.0126 | 2.13 |
| 0.0152 | 2.06 | 0.0142 | 2.51 |
| 0.0172 | 2.36 | 0.0155 | 2.81 |
| 0.0189 | 2.65 | 0.0170 | 3.07 |
| 0.0199 | 2.95 | 0.0173 | 3.33 |
| 0.0215 | 3.27 | 0.0202 | 3.56 |
| 0.0235 | 3.53 | 0.0191 | 3.72 |
| 0.0247 | 3.87 | 0.0193 | 3.94 |
| 0.0266 | 4.25 | | |
| 0.0284 | 4.52 | | |

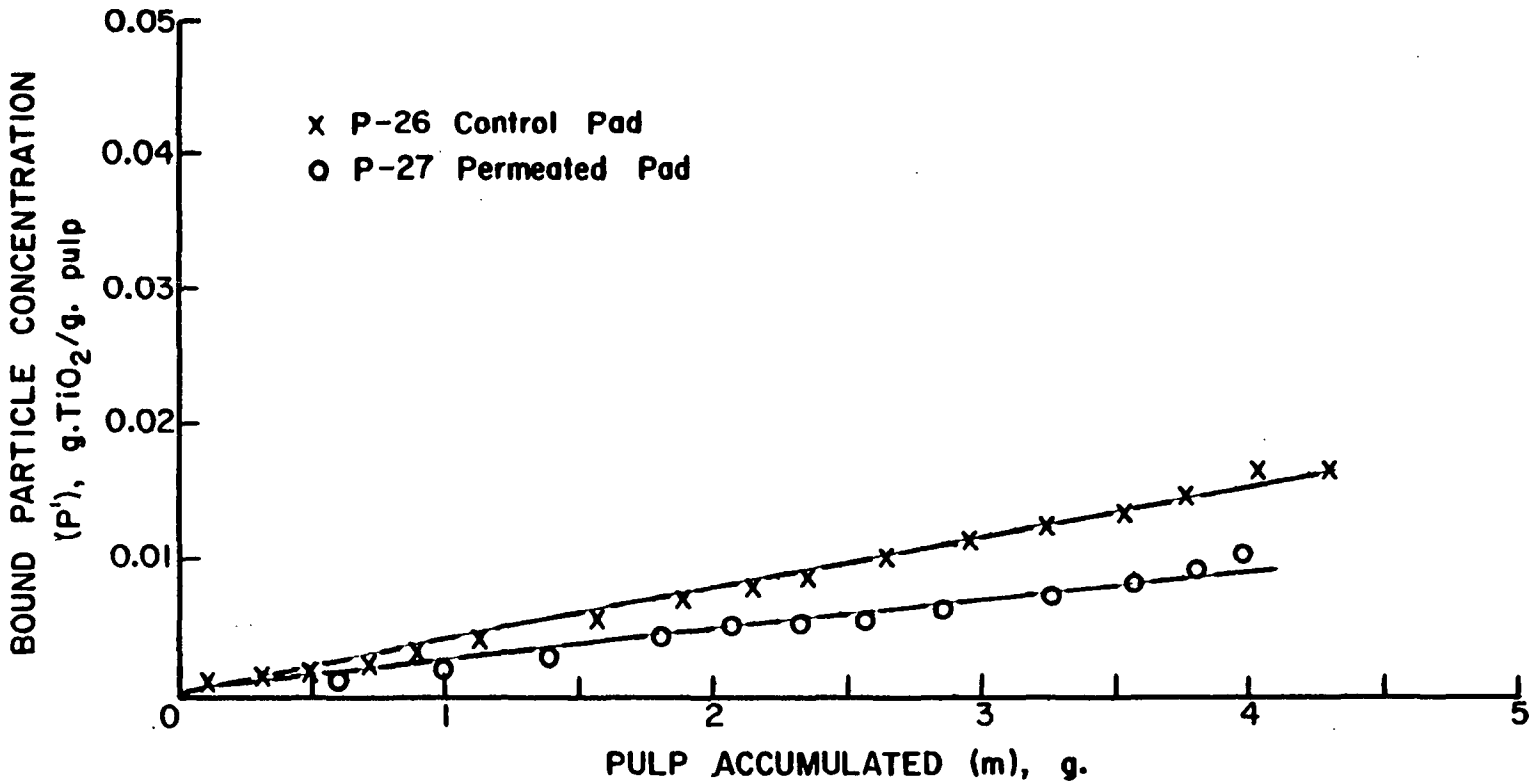


Figure 25. Bound Particle Distributions for Pulp Pads. P-27 was Additionally Permeated with Distilled Water at the Same Velocity as Formation

of the filtration are given in Table III and the results are shown in Fig. 26. The results of this experiment are approximately the same as the previous results. The pulp treatment had little effect on its retention behavior.

The holopulp fibers were then stirred for 1 hr. in the British Disintegrator, followed by classification as before. Using only the fraction retained on the 14-mesh screen, two pads were formed at pH 3.1 and at a forming velocity of 1 cm./sec. The second pad formed (P-31) received an additional 10 min. of permeation with distilled water at 1 cm./sec. permeating velocity. The details of the filtration are given in Table III and the results are shown in Fig. 27. The results of this experiment are also approximately the same as the other two experiments.

The recorded pressure drop data for these three filtrations was approximately the same. This indicated that the pulp had not been appreciably affected by the beating and classifying treatment.

The holopulp fibers were next subjected to 2 hr. of stirring in the British Disintegrator followed by classification. Two pads were formed from the fraction retained on the 14-mesh screen. The pH of the suspension was set at 2.9 and the forming velocity was 1 cm./sec. The second pad formed (P-33) received an additional 10 min. of permeation with distilled water at 1 cm./sec. permeating velocity. The details of the filtrations are given in Table III and the results are shown in Fig. 28. As seen in this figure, the retention has improved slightly.

The pressure drop across these pads was approximately double the pressure drop of the three previous experiments. This indicates an increase in surface area and may explain the increase in retention for these pads.

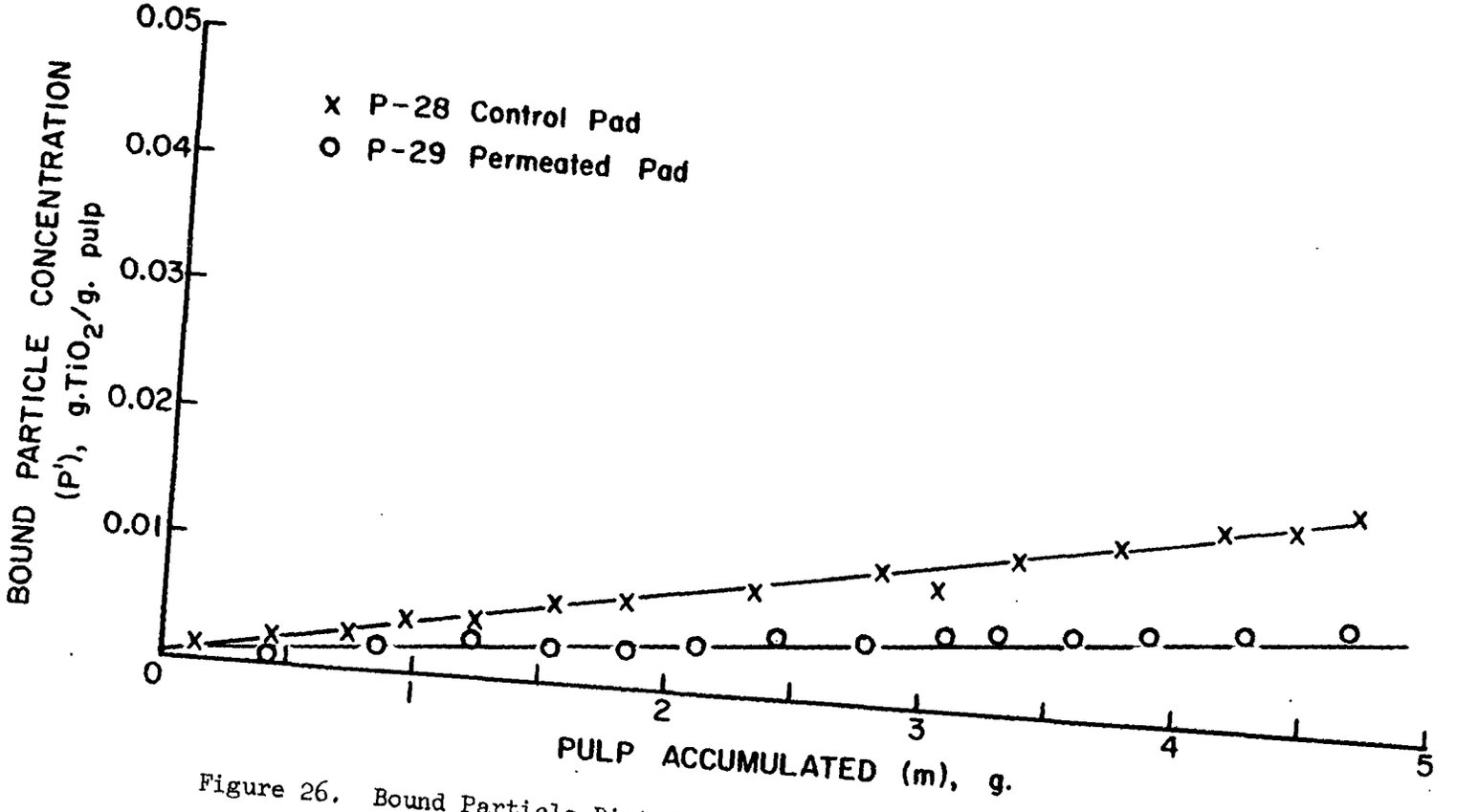


Figure 26. Bound Particle Distributions for Pulp Pads. P-29 was Additionally Permeated with Distilled Water at the Same Velocity as Formation

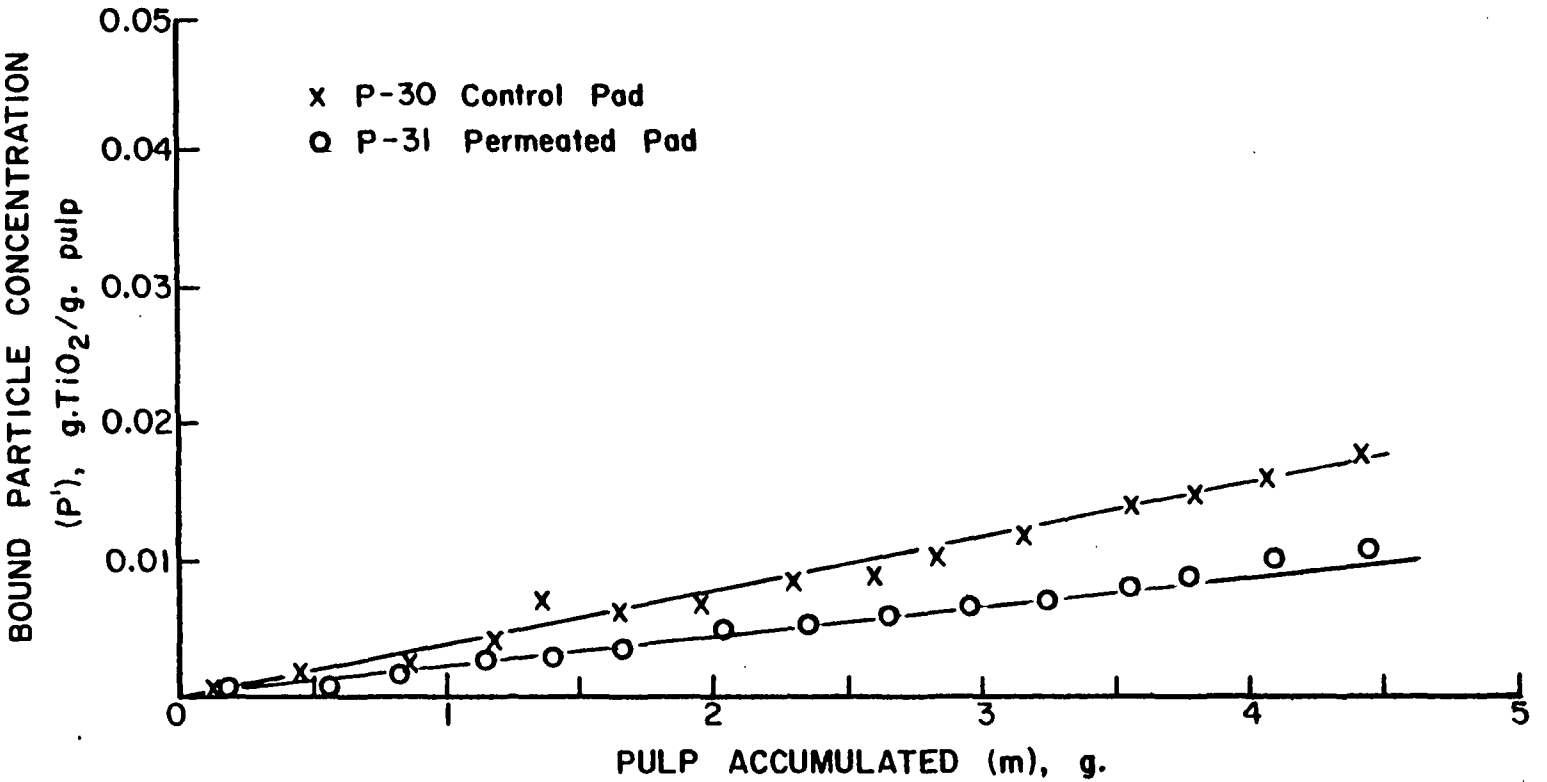


Figure 27. Bound Particle Distributions for Pulp Pads. P-31 was Additionally Permeated with Distilled Water at the Same Velocity as Formation

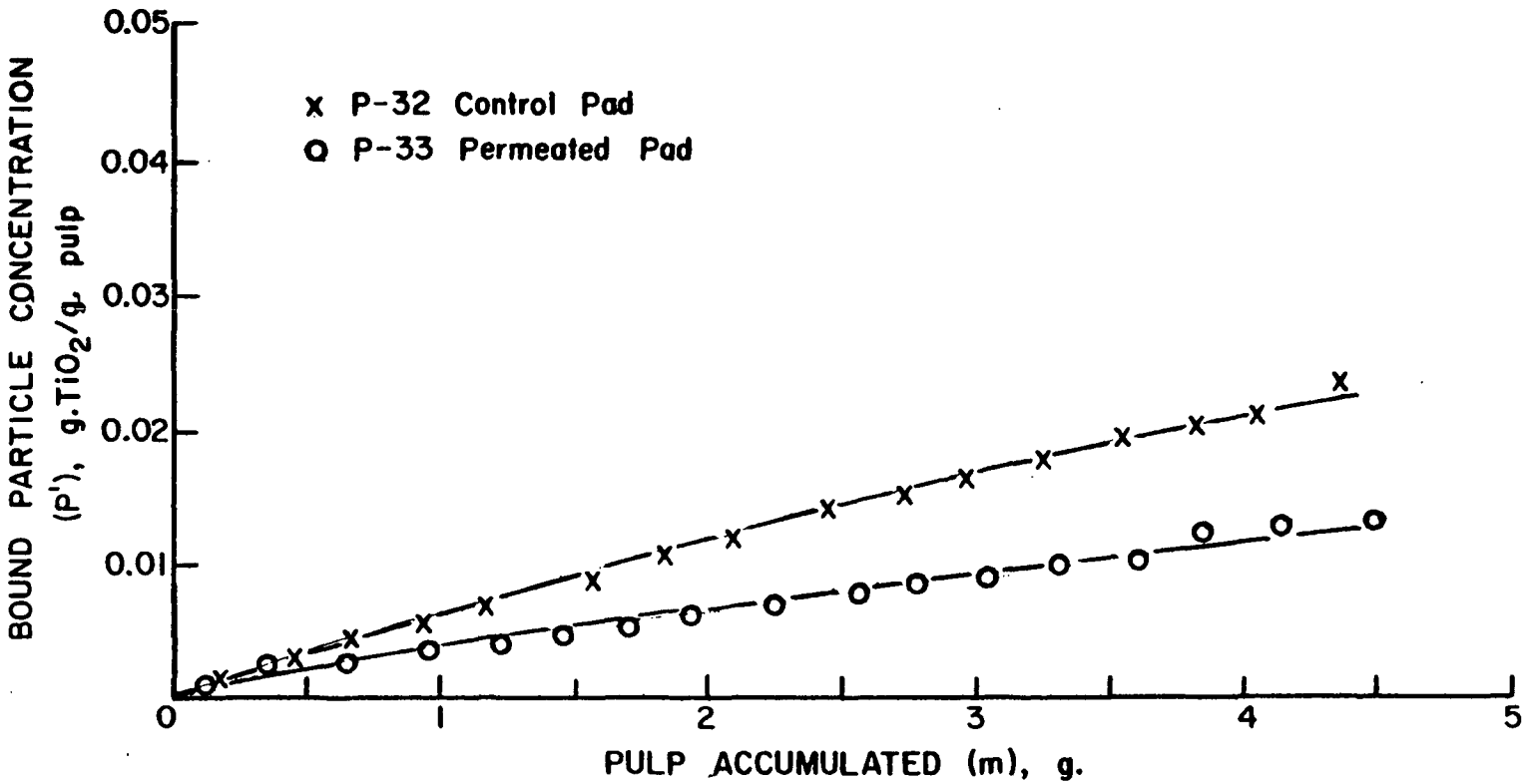


Figure 28. Bound Particle Distributions for Pulp Pads. P-33 was Additionally Permeated with Distilled Water at the Same Velocity as Formation

The reason for the low retention observed in all of these filtrations with holopulp fibers is believed to be due to the presence of the hemicellulose and pectin on the fibers and no doubt also in solution. It is known that the presence of polymeric materials can have marked effects on flocculation behavior of hydrophobic colloids (18). Hydrophilic polymers can act as both flocculating and dispersing agents on hydrophobic colloids. The mechanism is visualized as follows: The polymers absorb on the hydrophobic colloid surfaces. At some optimum concentration, single polymer molecules are adsorbed on two or more particles simultaneously and form bridges. This action leads to flocculation of the hydrophobic colloid even against an opposing electrical double layer barrier. At higher polymer concentrations or under conditions of long-continued or more intense agitation, polymer molecules tend to adsorb on single particles with little or no bridging. This leads to stabilization of the particle dispersion due to the entropy barrier which develops as particles approach one another.

The presence of the hemicellulose and pectin on the fibers and most probably in the solution could lead to a stabilization of the system as described above. Adsorption of the materials on the titanium dioxide particles could result in a large entropy barrier, making the particles difficult to retain.

With this mechanism in mind, it was decided to do a caustic extraction on the holopulp and see if there was any difference in the retention behavior of the fibers. The purpose of the caustic extraction was to remove the hemicellulosic material.

Two hundred grams of the holopulp were mixed with a 6% sodium hydroxide solution. The suspension was stirred for 30 min. at room temperature. The caustic was then filtered off and the above procedure repeated.

After filtering the second time, the pulp was washed with dilute acetic acid (4%). It was then washed with distilled water until a neutral pH was achieved.

The caustic-extracted pulp was then classified and the 14-mesh fraction was used in a filtration experiment. Two pads were formed from a suspension at pH 2.9. The forming velocity was 1 cm./sec. The second pad formed (P-35) was permeated with distilled water at 1 cm./sec. permeation velocity. The details of the filtration are given in Table III and the results are shown in Fig. 29. As seen in the figure, the level of retention has been improved by the caustic extraction.

The results of this experiment give support to the proposed idea of the adsorption of the hemicelluloselike polymers leading to entropy stabilization of the titanium dioxide particles. However, it is by no means conclusive proof. This area needs further investigation.

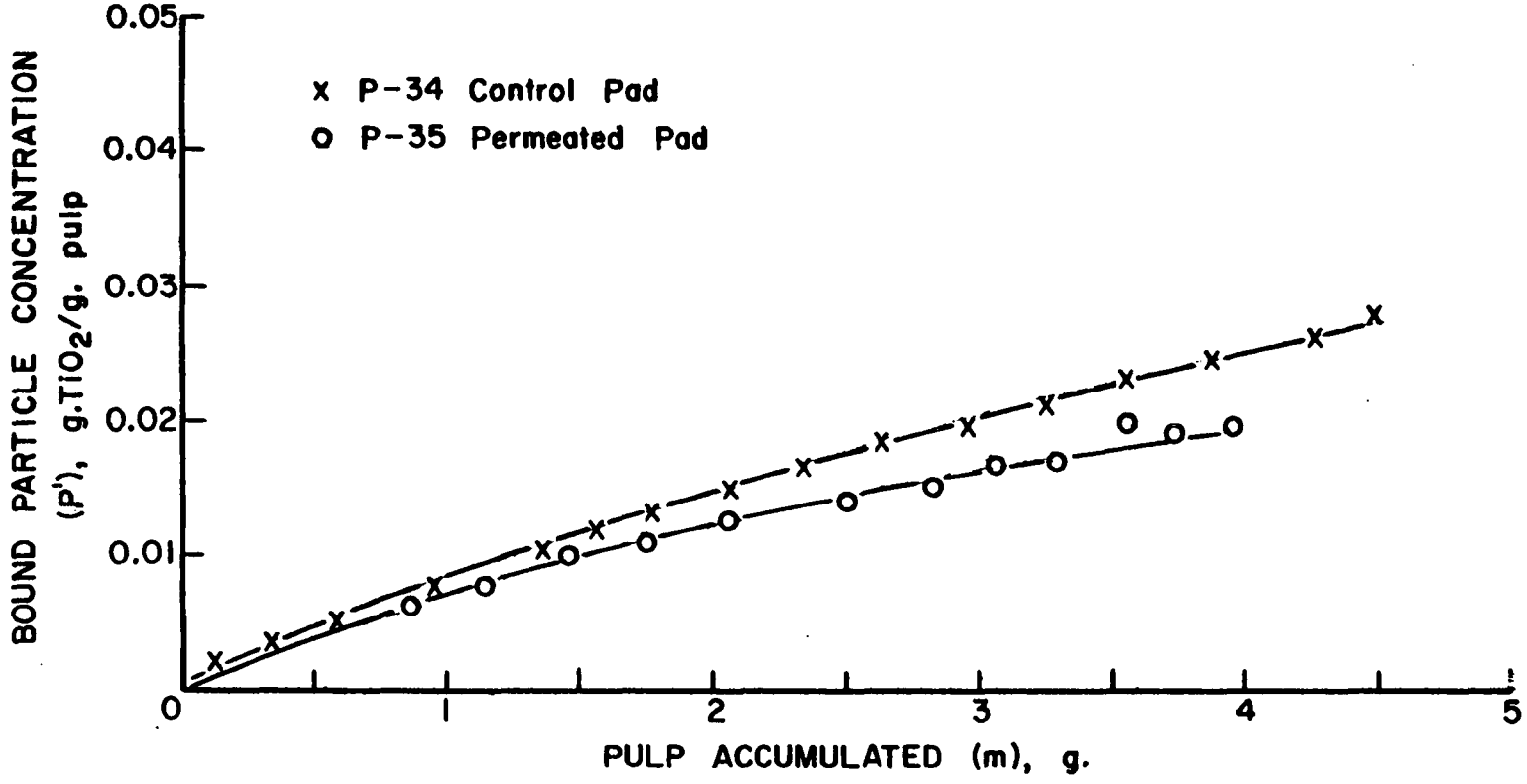


Figure 29. Bound Particle Distributions for Pulp Pads. P-35 was Additionally Permeated with Distilled Water at the Same Velocity as Formation

# APPENDIX IX

## REMOVAL EXPERIMENT USING RAYON FIBER

Duplicate pads of rayon fibers were formed at 1 cm./sec. forming velocity. The pH of the suspension was set at 3.1. After formation of the second pad and without interruption of the flow, this pad was permeated an additional 10 min. with distilled water at pH 6.3. Details of the experiment are given in Table IV and the results are shown in Fig. 30. As can be seen in the figure, little or no removal was observed.

The results of this experiment can be contrasted with the results shown in Fig. 9. The results of Fig. 9 were interpreted as being due to repeptization. No dispersion was observed in the rayon experiment. A possible explanation for this behavior could be that it is due to occluded impurities which might have been introduced into the rayon fibers during manufacture. However, a satisfactory explanation of this result cannot be given. A detailed study of the rayon fiber under a variety of colloidal conditions was not performed. This result serves as another example of the complexity of the retention process and points out the problems encountered in attempting to generalize the results of one retention system to another.

TABLE IV

FILTRATION CONDITIONS AND BOUND PARTICLE DISTRIBUTIONS FOR PADS P-36 AND P-37

Data for Pads P-36 and P-37

Pads P-36 and P-37 were formed from the same suspension of $TiO_2$ and rayon fiber. Details of the filtrations are given below.

| Conditions: | P-36 | P-37 |
|---|---|---|
| Pulp Type = | Rayon Fibers | Rayon Fibers |
| Initial Ratio, $TiO_2$ to Pulp ($\underline{P}_{oo}$) = | 0.050 | 0.050 |
| pH of Suspension = | 3.1 | 3.1 |
| Mix Time of Suspension = | 15 min. | 39 min. |
| Filtration Time = | 1100 sec. | 1050 sec. |
| Forming Velocity = | 1 cm./sec. | 1 cm./sec. |
| Treatment of Pad After Formation = | None | Permeated 10 min. with distilled water at 1 cm./sec. |

BOUND PARTICLE DISTRIBUTIONS PADS P-36 AND P-37

| Pad P-36 | | Pad P-37 | |
|---|---|---|---|
| Bound Particle Concn., $\underline{P}'$, g. $TiO_2$/g. pulp | Mass Pulp Accum., $\underline{m}$, g. pulp | Bound Particle Concn., $\underline{P}'$, g. $TiO_2$/g. pulp | Mass Pulp Accum., $\underline{m}$, g. pulp |
| 0.0036 | 0.07 | 0.0056 | 0.18 |
| 0.0069 | 0.30 | 0.0108 | 0.54 |
| 0.0114 | 0.56 | 0.0146 | 0.97 |
| 0.0138 | 0.72 | 0.0197 | 1.16 |
| 0.0170 | 0.82 | 0.0219 | 1.30 |
| 0.0170 | 0.98 | 0.0229 | 1.50 |
| 0.0200 | 1.15 | 0.0250 | 1.79 |
| 0.0218 | 1.28 | 0.0270 | 2.09 |
| 0.0222 | 1.51 | 0.0296 | 2.48 |
| 0.0252 | 1.78 | 0.0324 | 2.84 |
| 0.0292 | 1.93 | 0.0345 | 3.06 |
| 0.0270 | 2.06 | 0.0350 | 3.30 |
| 0.0315 | 2.26 | 0.0378 | 3.61 |
| 0.0325 | 2.44 | 0.0382 | 3.85 |
| 0.0329 | 2.66 | 0.0404 | 4.07 |
| 0.0359 | 2.92 | 0.0417 | 4.32 |
| 0.0394 | 3.05 | 0.0422 | 4.50 |
| 0.0378 | 3.22 | | |
| 0.0390 | 3.46 | | |
| 0.0398 | 3.77 | | |
| 0.0446 | 4.02 | | |
| 0.0435 | 4.23 | | |
| 0.0420 | 4.54 | | |

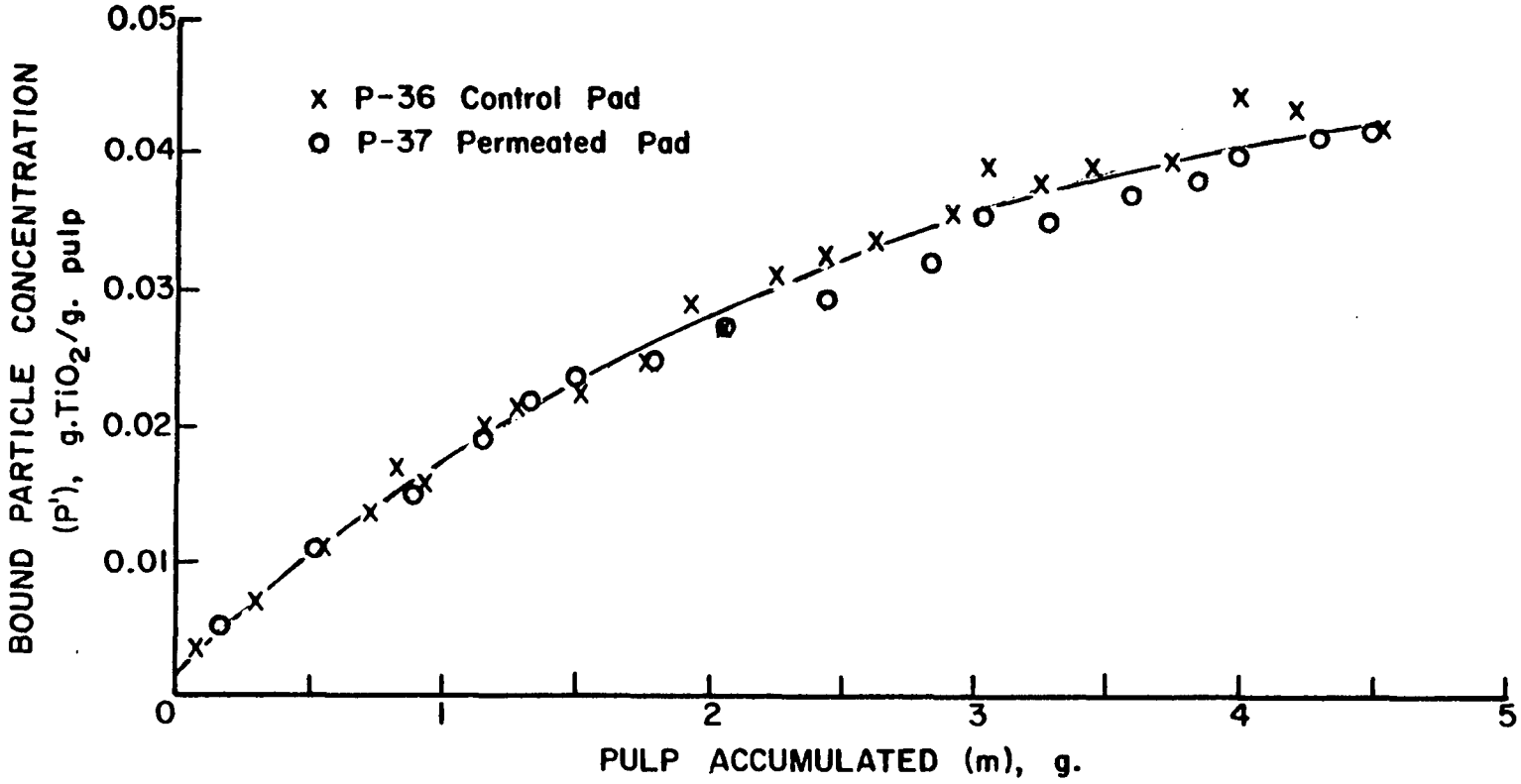


Figure 30. Bound Particle Distributions for Pulp Pads. P-37 was Additionally Permeated with Distilled Water at the Same Velocity as Formation

# APPENDIX X

## FILTRATION EXPERIMENTS AT pH'S 2.1, 2.6, AND 12.0

Filtration experiments performed at extremely high and low pH's gave anomalous results. These experiments are presented here with probable explanations for the observed results.

The experiments were carried out by making up suspensions containing enough fiber and particle to form 2 pads. The pH of the suspension was then adjusted with either HCl or NaOH. Constant-rate filtrations were then carried out at forming velocities of both 1 and 2 cm./sec.

Table V and Fig. 31 and 32 summarize the results of the filtrations performed at pH 2.1 and pH 2.6. As seen in Fig. 31 and 32, the amount of retention at 1 cm./sec. forming velocity is significantly higher than at 2 cm./sec. This is in keeping with the expected results of retention under good flocculating conditions. However, the overall level of retention for these pads is below that obtained for Pads P-24 and P-25 which were formed at pH 3.5.

It is believed that the reason for this result is due to fiber-fiber flocculation occurring at these low pH's. During these experiments, extensive fiber-fiber flocculation was observed. As the fibers flowed down the filtration tube, they tended to form into small clumps. The result was poorly formed pads with abnormal porosity variations. This probably caused preferential areas of flow in the pads, and, in effect, reduced the fiber area available for retention.

Table V and Fig. 33 summarize the results of a filtration carried out at pH 12. This is the highest level of retention observed for any filtration in this series of experiments. At this high pH, the sodium ion content is quite

TABLE V

FILTRATION CONDITIONS AND BOUND PARTICLE DISTRIBUTIONS FOR PADS P-38 THROUGH P-43

Data for Pads P-38 and P-39

Pads P-38 and P-39 were formed from the same suspension of $TiO_2$ and pulp. Details of the filtrations are given below.

| Conditions: | P-38 | P-39 |
|---|---|---|
| Pulp Type = | 2 | 2 |
| Initial Ratio, $TiO_2$ to Pulp ($\underline{P}_{oo}$) = | 0.0475 | 0.0475 |
| pH of Suspension = | 2.1 | 2.1 |
| Mix Time of Suspension in Tank = | 28 min. | 15 min. |
| Filtration Time = | 1122 sec. | 552 sec. |
| Forming Velocity = | 1 cm./sec. | 2 cm./sec. |

BOUND PARTICLE DISTRIBUTIONS PADS P-38 AND P-39

| Pad P-38 | | Pad P-39 | |
|---|---|---|---|
| Bound Particle Concn., $\underline{P}'$, g. $TiO_2$/g. pulp | Mass Pulp Accum., $\underline{m}$, g. pulp | Bound Particle Concn., $\underline{P}'$, g. $TiO_2$/g. pulp | Mass Pulp Accum., $\underline{m}$, g. pulp |
| 0.0062 | 0.25 | 0.0045 | 0.29 |
| 0.0119 | 0.75 | 0.0095 | 0.82 |
| 0.0164 | 1.17 | 0.0132 | 1.22 |
| 0.0192 | 1.48 | 0.0170 | 1.51 |
| 0.0223 | 1.76 | 0.0186 | 1.90 |
| 0.0251 | 2.12 | 0.0227 | 2.48 |
| 0.0290 | 2.60 | 0.0263 | 2.99 |
| 0.0319 | 3.03 | 0.0283 | 3.43 |
| 0.0324 | 3.31 | 0.0309 | 3.86 |
| 0.0360 | 3.67 | 0.0332 | 4.13 |
| 0.0384 | 4.05 | | |

Data for Pads P-40 and P-41

Pads P-40 and P-41 were formed from the same suspension of $TiO_2$ and pulp. Details of the filtrations are given below.

| Conditions: | P-40 | P-41 |
|---|---|---|
| Pulp Type = | 2 | 2 |
| Initial Ratio, $TiO_2$ to Pulp ($\underline{P}_{oo}$) = | 0.0475 | 0.0475 |
| pH of Suspension = | 2.6 | 2.6 |
| Mix Time of Suspension = | 31 min. | 15 min. |
| Filtration Time = | 897 sec. | 552 sec. |
| Forming Velocity = | 1 cm./sec. | 2 cm./sec. |

BOUND PARTICLE DISTRIBUTIONS PADS P-40 AND P-41

| Pad P-40 | | Pad P-41 | |
|---|---|---|---|
| Bound Particle Concn., $\underline{P}'$, g. $TiO_2$/g. pulp | Mass Pulp Accum., $\underline{m}$, g. pulp | Bound Particle Concn., $\underline{P}'$, g. $TiO_2$/g. pulp | Mass Pulp Accum., $\underline{m}$, g. pulp |
| 0.0054 | 0.20 | 0.0049 | 0.29 |
| 0.0096 | 0.57 | 0.0098 | 0.80 |
| 0.0131 | 0.93 | 0.0131 | 1.19 |
| 0.0185 | 1.43 | 0.1580 | 1.58 |
| 0.0217 | 1.92 | 0.1860 | 1.98 |
| 0.0243 | 2.23 | 0.0207 | 2.34 |
| 0.0267 | 2.62 | 0.0229 | 2.69 |
| 0.0298 | 3.08 | 0.0248 | 3.10 |
| 0.0316 | 3.40 | 0.0366 | 3.50 |
| 0.0319 | 3.73 | 0.0285 | 3.86 |
| | | 0.0296 | 4.22 |
| | | 0.0313 | 4.60 |

Data for Pads P-42 and P-43

Pads P-42 and P-43 were formed from the same suspension of $TiO_2$ and pulp. Details of the filtrations are given below.

| Conditions: | P-42 | P-43 |
|---|---|---|
| Pulp Type = | 2 | 2 |
| Initial Ratio, $TiO_2$ to Pulp ($\underline{P}_{oo}$) = | 0.0475 | 0.0475 |
| pH of Suspension = | 12.0 | 12.0 |
| Mix Time of Suspension in Tank = | 33 min. | 18 min. |
| Filtration Time = | 962 sec. | 570 sec. |
| Forming Velocity = | 1 cm./sec. | 2 cm./sec. |

BOUND PARTICLE DISTRIBUTIONS PADS P-42 AND P-43

| Pad P-42 | | Pad P-43 | |
|---|---|---|---|
| Bound Particle Concn., $\underline{P}'$, g. $TiO_2$/g. pulp | Mass Pulp Accum., $\underline{m}$, g. pulp | Bound Particle Concn., $\underline{P}'$, g. $TiO_2$/g. pulp | Mass Pulp Accum., $\underline{m}$, g. pulp |
| 0.0161 | 0.18 | 0.0105 | 0.25 |
| 0.0234 | 0.54 | 0.0213 | 0.71 |
| 0.0289 | 0.96 | 0.0276 | 1.18 |
| 0.0344 | 1.40 | 0.0329 | 1.64 |
| 0.0378 | 1.72 | 0.0356 | 2.00 |
| 0.0377 | 2.15 | 0.0373 | 2.32 |
| 0.0421 | 3.70 | 0.0379 | 2.74 |
| 0.0441 | 3.16 | 0.0380 | 3.23 |
| 0.0463 | 3.54 | 0.0385 | 3.59 |
| 0.0478 | 3.94 | 0.0414 | 3.91 |

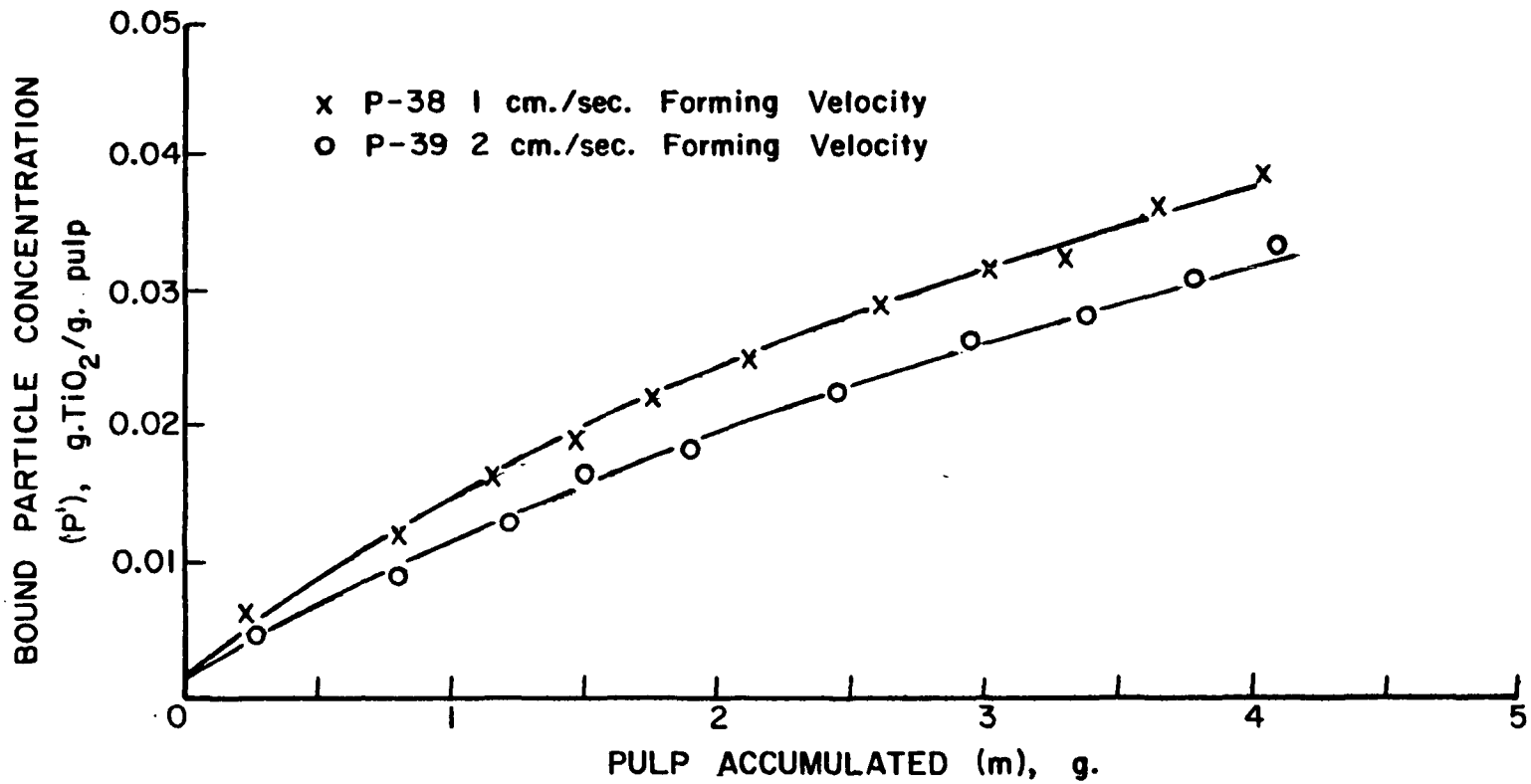


Figure 31. Bound Particle Distributions for Pulp Pads. Pads Formed from Suspension at pH 2.1

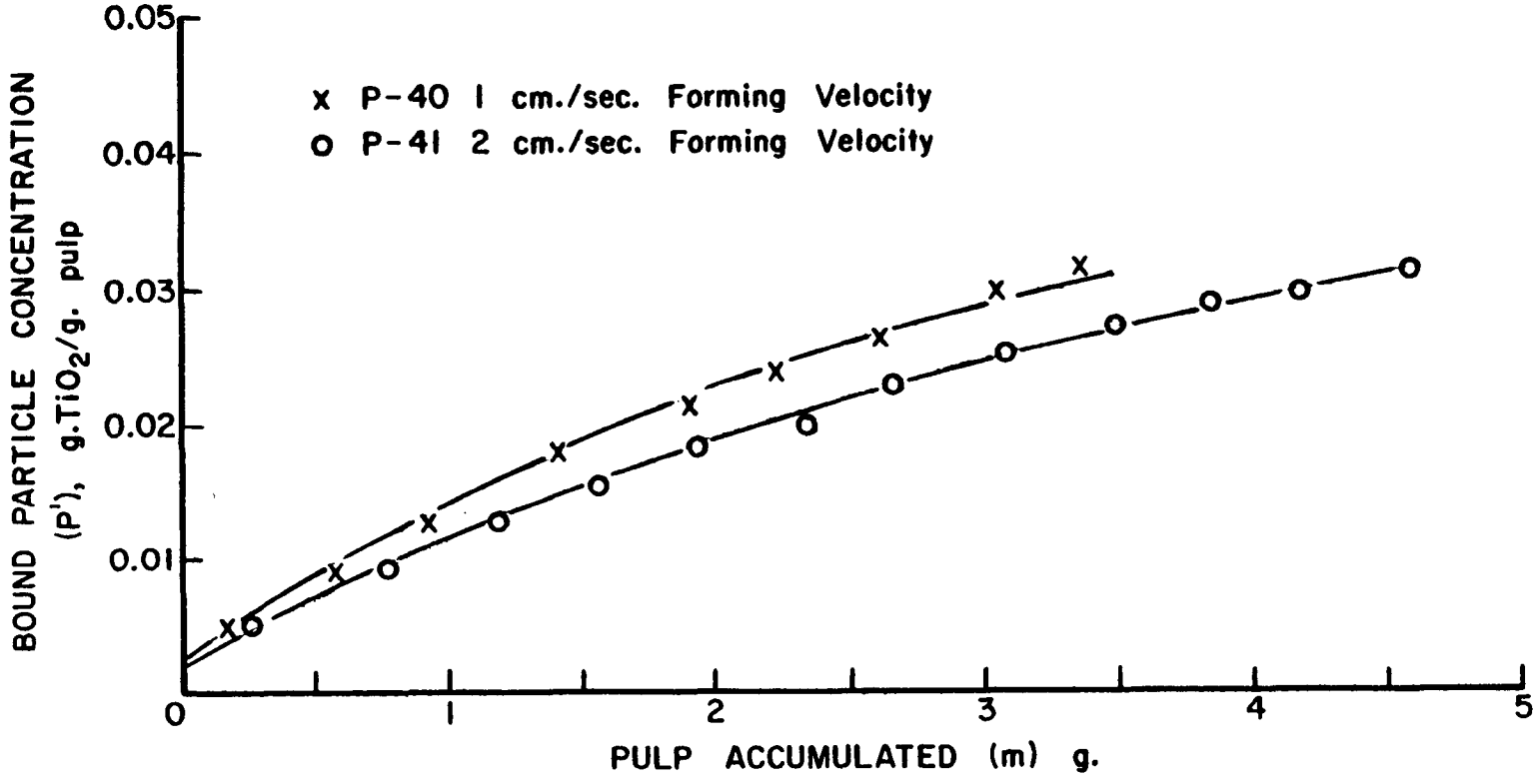


Figure 32. Bound Particle Distributions for Pulp Pads. Pads Formed from Suspension at pH 2.6

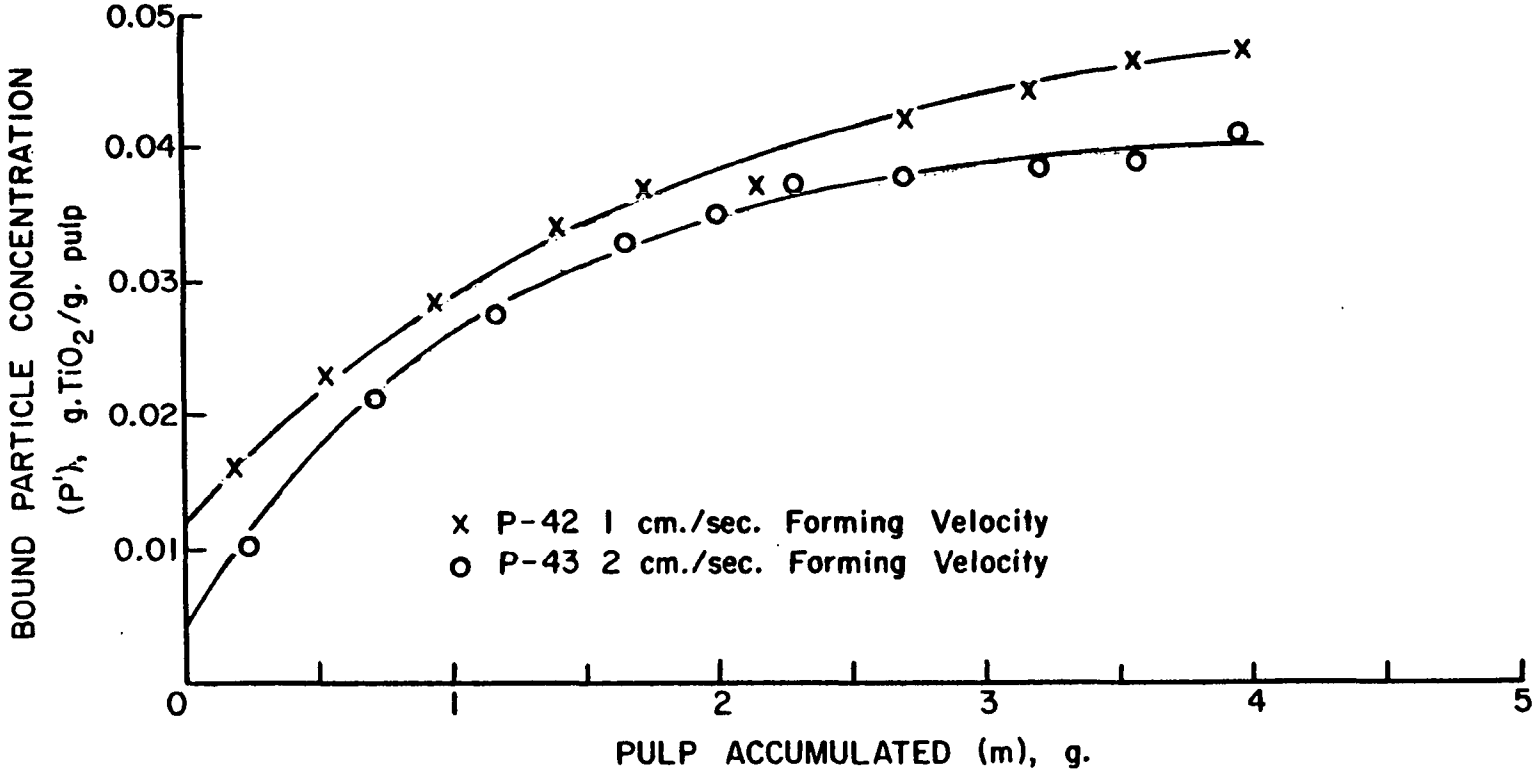


Figure 33. Bound Particle Distributions for Pulp Pads. Pads Formed from Suspension at pH 12.0

high. There may have been enough sodium ion to lead to coflocculation between the fibers and titanium dioxide particles. At this pH, the pulp became highly swollen and gelatinous. In this condition, the particles could easily become imbedded in the fiber wall. To test this explanation, another filtration was performed at the same pH. A pad was formed at 1 cm./sec. and then the flow was changed to distilled water. The pad was permeated for an additional 24 min. with distilled water. The effluent below the septum did not become turbid, indicating little or no removal. The particles did not redisperse as previously observed with the Type 1 pulp. This retention independent of colloidal environment is an indication of mechanical entrapment of the particles.